

**POLY(DIMETHYL SILOXANE) – BASED COMPOSITE
NANOFILTRATION MEMBRANES FOR NON-AQUEOUS
APPLICATIONS**

DISSERTATION

To obtain
The doctor's degree at the University of Twente,
On the authority of the rector magnificus,
prof. dr. F.A. van Vught,
on account of the decision of the graduation committee,
to be publicly defended
on Wednesday 24 November 2004 at 15.00

by

Nela Stafie

Born on 28 November 1970
in Adjud, Romania

This dissertation has been approved by:

Promotor: Prof. dr. -Ing. M. Wessling

Assistant promotor: Dr. D. Stamatialis

Celor dragi care sunt si au fost alaturi de mine...

This research was financially supported by the Netherlands Organisation for Scientific
Research (NWO).

Poly (dimethyl siloxane) - based composite nanofiltration membranes for non-aqueous
applications

Nela Stafie

Ph.D. thesis, University of Twente, Enschede, The Netherlands

ISBN 90-365-2112-2

© 2004 Nela Stafie

Printed by Print Partners Ipskamp, Enschede.

Contents

Chapter 1	1
Introduction	
1.1 Structure of this thesis	1
1.2 Literature review of the transport models of organic systems through SRNF membranes	3
1.3 Selected literature results for the transport of non-aqueous systems through NF membranes	7
1.4 Applications of NF	9
1.5 References	11
Chapter 2	15
Preparation and characterization of composite membranes with PDMS as the selective layer	
2.1 Introduction	16
2.2 Theoretical background	17
2.2.1 Chemical and physical properties of PDMS	17
2.2.2 NF membrane preparation and the pore intrusion phenomena	18
2.2.3 Mass transport through porous and non porous membranes	19
2.3 Experimental	22
2.3.1 Materials	22
2.3.2 PAN/PDMS composite preparation	23
2.3.3 Membrane characterization	24
2.3.4 Liquid permeation set-up and procedure	24
2.4 Results and discussion	27
2.4.1 Characterization of the PAN support	27
2.4.2 Preparation of PAN/PDMS composite membranes	30
2.4.3 Reproducibility of the dip-coating method	31
2.4.4 Liquid permeation	33
2.4.5 Comparison with other silicone type membranes	35
2.5 Conclusions	41
2.6 List of symbols	41
2.7 References	43
Appendix I: Effect of stirring rate on the membrane performance	45
Appendix II: Influence of the PDMS thickness on the membrane performance	48
Chapter 3	55
Insight into the transport of hexane – solute systems through tailor-made composite membranes	
3.1 Introduction	56
3.2 Theoretical background	57
3.3 Experimental	59
3.3.1 Materials	59
3.3.2 Membrane preparation	60

3.3.3	Permeation set-up and procedure	61
3.3.4	Swelling experiments	62
3.4	Results and discussion	63
3.4.1	Characterization of the PAN/PDMS composite membranes	63
3.4.2	Swelling measurements	64
3.4.3	Permeation performance	67
3.4.4	Retention performance	77
3.5	Conclusions	79
3.6	List of symbols	80
3.7	Acknowledgements	81
3.8	References	82
 Chapter 4		 85
Effect of cross-linking degree of PDMS on the permeation performance of PAN/PDMS composite membranes		
4.1	Introduction	87
4.2	Theoretical background	88
4.3	Experimental	92
4.3.1	Materials	92
4.3.2	Membrane preparation and characterization	93
4.4	Results and discussion	96
4.4.1	Pre-polymer and cross-linker characterization	96
4.4.2	ATR-FTIR and mechanical analysis of the dense PDMS membrane	97
4.4.3	Swelling experiments of dense PDMS membrane in hexane	100
4.4.4	Swelling of dense PDMS membranes in PIB 550 /hexane solutions	102
4.4.5	Permeation experiments	105
4.4.6	Retention performance	114
4.5	Conclusions	116
4.6	List of symbols	117
4.7	Acknowledgements	118
4.8	References	119
 Chapter 5		 125
The permeation performance of the PAN/PDMS composite membranes at high-pressure		
5.1	Introduction	126
5.2	The effect of approximations in the solution-diffusion model at high pressure and large penetrants	127
5.3	Experimental	129
5.3.1	Materials	129
5.3.2	Permeation set-ups	130
5.3.3	Analytical methods	132
5.4	Results and discussion	132
5.4.1	Permeation experiments with the PAN/PDMS composite membrane	132
5.4.2	Permeation experiments with the GKSS membrane	145
5.5	Conclusions	150
5.6	List of symbols	151

5.7	References	152
Chapter 6		155
Effect of solvent and solute type on the mass transport through the PAN/PDMS composite membrane		
6.1	Introduction	156
6.2	Experimental	157
	6.2.1 Materials	157
	6.2.2 Permeation set-up and analytical methods	158
	6.2.3 Swelling experiments	158
6.3	Results and discussion	159
	6.3.1 Viscosity of the feed solutions	159
	6.3.2 The influence of the solvent on separation performance	160
	6.3.2.1 Swelling measurements with dense PDMS membrane	160
	6.3.2.2 Permeation performance	162
	6.3.3 The influence of the solute on separation performance	171
6.4	Conclusions	176
6.5	List of symbols	177
6.6	References	178
Chapter 7		181
Preparation and characterization of a composite membrane with PEO-PDMS-PEO as selective layer		
7.1	Introduction	182
7.2	Experimental	184
	7.2.1 Materials	184
	7.2.2 Acylation of PEO-PDMS-PEO	184
	7.2.3 Membrane preparation	185
	7.2.4 Membrane characterization	186
7.3	Results and discussion	187
	7.3.1 Characterization of the PEO-PDMS-PEO dense membrane	187
	7.3.2 Gas permeation properties of the PAN/PEO-PDMS-PEO composite	192
	7.3.3 Solvent permeation characteristics of the PAN/PEO-PDMS and PAN/PDMS composites	194
7.4	Conclusions	197
7.5	List of symbols	198
7.6	Acknowledgements	198
7.7	References	199
Chapter 8		203
Conclusions and outlook		
Summary		207
Samenvatting		211
Aknowledgements		215

Introduction

1.1. Structure of this thesis

Most of the published studies on the solvent resistant nanofiltration (SRNF) membrane have been performed on the commercially available membranes and their exact physico-chemical properties are not completely known. In this thesis, we will prepare and thoroughly characterize a tailor-made composite membrane and will correlate its transport characteristics with the properties of the selective top-layer.

Figure 1 shows the diagram of the investigation covered in this thesis.

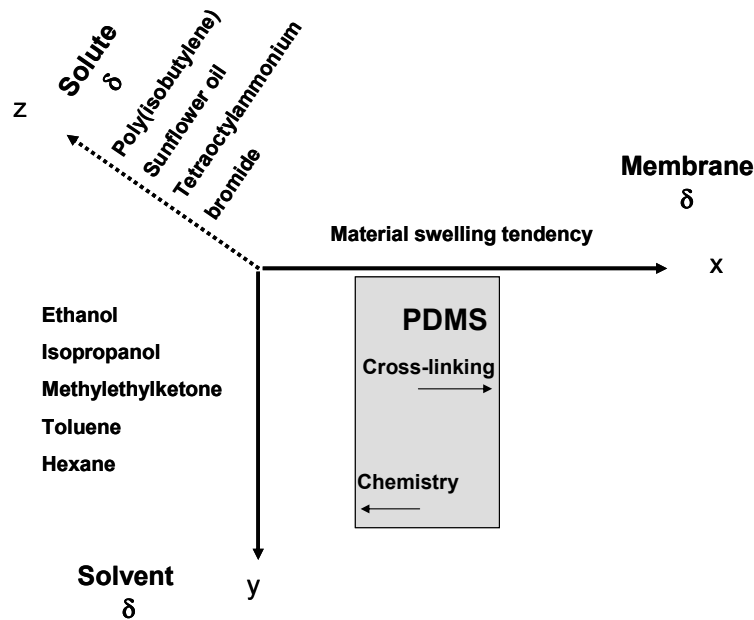


Figure 1: Diagram of the investigation covered in this thesis.

Chapter 2 describes the preparation of the PAN/PDMS tailor-made composite membrane. The gas and liquid permeation are performed to select the most suitable coating parameters for the oil/hexane application. Furthermore, the performance of PAN/PDMS membrane is compared with the other silicone type nanofiltration membranes. **Appendix I** presents the effect of stirring rate on the membrane performance. The influence of the PDMS thickness on the transport properties of PAN/PDMS composite membrane is studied in **Appendix II**.

Chapter 3 gives an insight into the transport of hexane-solute systems through the PAN/PDMS tailor-made composite membrane. The important parameters which control the transport of hexane and oil/poly(isobutylene)PIB are identified (y and z axis of *Figure 1*). The flux of hexane is found to be dependent on the apparent viscosity and membrane swelling. For solute transport, a systematic study on the flux coupling and solvent-induced dragging as a function of molecular weight of the solute and feed concentration is given. Besides that, osmotic phenomena similar to those reported in aqueous systems are reported.

Chapter 4 describes the effect of the cross-linking degree of PDMS on the mass transport through the dense PDMS and the PAN/PDMS composite membranes (x axis of *Figure 1*). Besides, the effect of PDMS cross-linking degree on the membrane swelling and partition coefficient is investigated. This allows us to obtain PAN/PDMS composite membrane with high permeation characteristics (large fluxes and good retention) by further improving the balance between cross-linking degree and pore-penetration.

Chapter 5 focuses on the performances of PAN/PDMS tailor-made membrane at high pressure (up to 30 bar). No membrane compaction and no significant difference between the membrane performance at high and low pressure are depicted. The results of experiments performed in a cross-flow configuration set up at various flow rates are similar to the data obtained with the dead-end set up, indicating that no concentration polarization phenomenon occurs for the studied systems.

Chapter 6 shows the influence of the solvent type (toluene and hexane) and solute type (oil and tetraoctylammonium bromide, TOABr) on the performance of the PAN/PDMS composite membrane (y and z axis of *Figure 1*). By

following the permeation behavior of these solutions through PAN/PDMS composite membrane, we obtain valuable information concerning the osmotic phenomena and the solvent-induced dragging effect. This effect is more significant for toluene/oil than for hexane/oil system.

Chapter 7 describes the preparation of a hydrophilized PDMS-based composite membrane using PEO-PDMS-PEO triblock copolymer as the selective top layer (x axis of *Figure 1*). In fact, in this chapter we aim to investigate if the same parameters concerning the mass transport described in the earlier chapters can describe the fundamental aspects of transport phenomena in the hydrophilized PDMS-based membrane. For this investigation, the flux of various solvents through the new membrane is studied.

Chapter 8 summarizes the main conclusions of the work described in this thesis and gives an outlook and suggestions for future work.

1.2. Literature review of the transport models of organic systems through SRNF membranes

Several transport models have been proposed in the solvent resistant nanofiltration membrane literature, most of them being extension of the existing models from aqueous to the non-aqueous NF systems. This extension, however, is not always straightforward because the organic solvents have a wide range of polarity, viscosity and surface tension [1]. The prediction of the separation characteristics of organic systems is much more challenging since physico-chemical properties of solute and its interactions with membrane and solvent significantly affect the mass transport through the NF membrane. Generally, three models have been used to describe mass transport through SRNF membranes:

1. Solution-diffusion model

The basic premise of the solution-diffusion model is that the permeating species dissolve in the membrane material and molecularly diffuse through it as a consequence of a concentration gradient. In Chapter 2, the solution-diffusion model will be discussed more. Nevertheless, we will give a brief discussion below. The classic theory developed by Lonsdale et al. [2] considers the transport of solute and solvent to be independent without any effect of one to the other. The flux of a species i , J_i , through the membrane is given by:

$$J_i = \frac{D_i K_i}{\ell} [c_{if} - c_{ip} \exp(\frac{-\nu_i (p_f - p_p)}{R_g T})] \quad \text{Equation 1}$$

where D_i is the diffusion coefficient of i through the membrane, K_i is the partition coefficient, ℓ is the membrane thickness, c_{if} , c_{ip} is the feed and permeate concentrations of species i , respectively, ν_i is the partial molar volume of species i , p_f , p_p is the feed and permeate sides pressures, respectively, R_g is the gas constant and T is the temperature.

The prediction of the membrane performance (flux and retention) with this model is limited to the organic systems where experimental data (diffusion and/or sorption) are available. In addition, the model assumes that no solvent-solute coupling exists. However, several experimental findings have reported the coupling of the solvent-solute transport [3, 4]. The effect of solvent transport on the solute transport is taken into consideration in a recent reformulation of the solution-diffusion theory for reverse osmosis [5].

Solution-diffusion model was applied for the silicone and polyimide-based NF [4, 6] and the combination of solution-diffusion model with concentration polarization and thermodynamic activities was used by Peeva et al. [7] to predict the fluxes. Paul et al. [8] developed a solution-diffusion model for the swollen membranes by using polymer volume fractions as the driving force for the solvent transport through lightly cross-linked natural rubber membranes.

Bhanushali et al. [9] used a solution-diffusion based approach to model the permeation of organic solvents through various hydrophobic and hydrophilic membranes. This approach uses physical properties of the solvent such as the solvent viscosity and its molar volume for predicting the flux.

2. Spiegler-Kedem model.

Transport of a binary solution through a RO/NF membrane can be described by phenomenological equations derived by Spiegler-Kedem [10]:

$$J_i = P(\Delta p - \sigma \Delta \pi) \quad \text{Equation 2}$$

$$J_j = B \Delta \pi + (1 - \sigma) J_i \Delta c \quad \text{Equation 3}$$

where J_i is the solvent flux, $\Delta \pi$ is the transmembrane osmotic pressure, and P is the pure solvent permeability coefficient (a function of the solubility and the diffusion coefficient of the solvent in the membrane material), Δp is the transmembrane pressure, σ the reflection coefficient, J_j is the solute flux, B is the solute permeability coefficient, and Δc is the average of solute concentrations across the membrane. The flux of the solvent/solute depends on its solubility and diffusivity and also on the convective flow. The denser the membrane, the higher the contribution of the solution-diffusion mechanism [3]. The drawback of this model is that the membrane is considered to be a “black box”. The transport of solvent and solute through a membrane considers only the driving forces and their resulting fluxes [11]. In addition, the various coefficients (i.e. P , B and σ) are not easy to determine, especially in the transport of multi-component systems through the membrane.

The Spiegler-Kedem model was used to model some of the experimental results reported in literature [3, 12].

3. Pore-flow model

The pore flow model assumes that the mass transport occurs by pressure driven convective flow through the pores of the membranes. In contrast to the solution-diffusion model, the membrane material is not an active participant at the molecular level in the pore flow mechanism.

For liquids, the flux through a porous membrane can be described by the Hagen-Poiseuille equation for viscous flow:

$$J = \frac{n\pi r_p^4 \Delta p}{8\eta A \tau l} \quad \text{Equation 4}$$

where J is the liquid flux, n the number of pores, r_p the pore radius, Δp the pressure difference across the membrane, η is the liquid viscosity, A is the membrane area, τ the membrane tortuosity, l the membrane thickness.

Gibbins et al. [13] and Robinson et al. [14] used the pore flow model to describe the mass transport membrane through some polyimide and silicone-based NF.

Machado et al. [15] proposed a resistance-in-series model to describe the flux of organic solvents through the silicone-based NF membranes. Three significant resistances to mass transport were identified as viscous flow in the membrane top layer, viscous flow in the porous support and hydrophilic/hydrophobic resistances.

Our experimental results using the poly (acrylonitrile) PAN /poly (dimethylsiloxane) (PDMS)-based tailor-made composite membranes showed the importance of the membrane-solvent/solute interaction. The solution-diffusion model was used to describe the aspects of the solvent transport. In addition, the coupling between the solute and solvent fluxes was found to be important (see Chapters 3, 5 and 6).

1.3. Selected literature results for the transport of non-aqueous systems through NF membranes

Traditionally, NF processes have been applied to aqueous systems primarily for the purposes of water purification and other water-related applications. However, for a non-aqueous system, membrane-solute, membrane-solvent and solute-solvent interactions can not be neglected. An additional complexity arises from the stability of membrane material in the non-aqueous system combined with good level of performance, i.e. high flux and retention, for a long time period.

Pure solvent transport

When extending the principles from water to organic solvents, affinity of the solvent for the membrane material becomes very important. For a typical NF membrane, the water permeability is in the order of $7.2 \text{ lm}^{-2}\text{h}^{-1}\text{bar}^{-1}$ [16]. However, for the same membrane (assuming that it is solvent resistant), the permeability to solvents such as hexane is reduced to 1/10 to 1/100 of the water value [16]. Paul et al. [8] studied pure solvent permeation through lightly cross-linked natural rubber membranes, indicating the relation between the membrane swelling and the flux. Machado et al. [15] studied the permeation of several organic solvents (polar and non-polar) through the hydrophobic silicone-based commercial membranes (MPF series, purchased from Koch). They reported higher fluxes of non-polar solvents (pentane to octane) than of the polar solvents (methanol and ethanol). Similar results were found by Robinson et al. [14] for a developmental silicone-based membrane, indicating the importance of the solvent-membrane interactions. Bhanushali et al. [9] studied the permeation of organic solvent (polar and non polar) through various hydrophobic and hydrophilic NF membranes. They reported that the surface energy of the membrane and physical properties of the solvent (such as the solvent viscosity and its molar volume) are important for predicting the solvent flux. For example, for a silicone-based NF, at 23°C, the hexane permeability was $1.62 \text{ lm}^{-2}\text{h}^{-1}\text{bar}^{-1}$ as

opposed to ethanol permeability of $0.9 \text{ lm}^{-2}\text{h}^{-1}\text{bar}^{-1}$. On the contrary, for a hydrophilic-based membrane, the methanol flux at 13 bar was $18 \text{ lm}^{-2}\text{h}^{-1}$ as opposed to the hexane flux through the same membrane being $2.5 \text{ lm}^{-2}\text{h}^{-1}$ at similar pressure. Vankelecom et al. [1] reported low permeability of methanol compared to that toluene (about 0.06 and $1.2 \text{ lm}^{-2}\text{h}^{-1}\text{bar}^{-1}$, respectively) through a laboratory-made PDMS NF membrane. They concluded that the affinity of the various solvents used (polar and non-polar) for the membrane and their viscosity determined the solvent flux.

Solvent-solute transport

For a binary solute/solvent system, experimental observations in non-aqueous media have shown that the solute affinity towards the solvent as well as towards the membrane material become important for the transport.

Paul et al. [17] studied the diffusion characteristics of Sudan IV (384 MW organic dye) in various solvents through a lightly cross-linked natural rubber membrane (no pressure was applied). The results revealed the importance of the solvent for the solute transport. For example, the diffusivity of Sudan IV with hexane as solvent was 200 times higher than that observed when ethanol was used. Bhanushali et al. [3] studied the mass transport (under pressure) through hydrophilic and hydrophobic NF membranes using Sudan IV and triglycerides in organic solvents (polar and non-polar). The observed rejection of Sudan IV was about 25% in n-hexane and negligible in methanol (at about 15 bar) by a silicone-based membrane. However, for a hydrophilic polyamide based membrane, the rejection was 43% in n-hexane and 86% in methanol (at 15 bar). The separation behavior of various dyes have been reported [18, 19] for various hydrophilic (MPF 44 and Desal-5) and hydrophobic (MPF-50 and MPF-60) commercial membranes. Several solutes were used, among which positively charged safranin O (350 MW) and solvent blue 35 (350 MW, neutral solute). Various solvents were studied including water, methanol, ethyl acetate, and toluene. The separation behavior was found to be strongly dependent on the membrane type and on the charge of the solute. For example, the rejection of

0.01% w/w safranin O in methanol was 68% and 6% for the MPF-44 and MPF-50 membranes, respectively. The retention of MPF-60 membrane for solvent blue was higher in methanol than in ethyl acetate (81% and 66%), indicating the importance of the solute charge for the rejection mechanism.

Subramanian et al. [20] reviewed recently the permeation behavior of nonporous, dense, silicone-based composite membranes (supplied by Nitto-Denko, Japan) for edible oil refining. They reported membrane retention of 60% for lutein and only 18% for β -carotene due to the lower affinity of lutein for the membrane. Koops et al. [12] performed permeation experiments of several solutes in ethanol and n-hexane through a laboratory-made cellulose acetate membrane. They concluded that the competition between solute-membrane-solvent interactions is important for the mass transport. For example, the rejection of docosanoic acid in hexane, was very low (-35%) while its rejection in ethanol was 90%. White et al. [6] reported a strong preference to transport of the aromatic solute dissolved in toluene through a polyimide-based NF membrane.

Despite the above mentioned research studies attempting to relate membrane performances to the transport mechanism through the SRNF membranes, a systematic and comprehensive work is still needed in order to identify key parameters that could affect the membrane transport characteristics, flux and retention.

1.4. Applications of NF

Solvent resistant nanofiltration membranes have a strong potential for a variety of applications ranging from pharmaceutical to chemical and food industries. One of the applications is the separation and purification of edible oil. In recent years, several papers have been published on the membrane applications in the edible oil industry [20-22] for the solvent recovery (hexane, acetone, isopropanol, and ethanol) and oil refining processes. The solvent recovery by membrane processes is environmentally friendly and safer with respect to health

and explosion hazards compared to the evaporation. Subramanian et al. [20] reported that nonporous membranes were effective in reducing the color of the oil, while Zwijnenberg et al. [22] reported triglyceride retention of 80-95%, depending on the type of the membrane used.

In the pharmaceutical industry, drugs with MW higher than 300 MW in solvents such as ethanol, isopropanol, ethyl acetate etc could be recovered at room temperature by NF-based processes. For example, Sheth et al. [23] reported for MPF-60 membrane a rejection of around 96% erythromycin in ethyl acetate.

NF membranes can also be used in the recovery of homogeneous catalyst in chemical/pharmaceutical industries [24-266], lowering the costs of catalyst and enabling wide use of homogeneous catalysis to eliminate mass-transfer limitations for the reaction rate. Nair et al. [25], for example, studied the reaction of styrene and iodobenzene to form *trans*-stilbene with a palladium-based Heck catalyst in three different organic solvents. They used the MPF-series (purchased from Koch, USA) and polyimide membranes (purchased from Grace and Co.) and reported better separation and permeation characteristics of the polyimide-based membrane compared to the MPF-membranes. Luthra et al [26] used a similar approach but for a phase-transfer catalyst (PTC) system involving the reaction of bromoheptane and potassium iodide to form iodoheptane. In this reaction, tetraoctylammonium bromide was used as the PTC and toluene as the organic solvent. Again a polyimide-based membrane was able to concentrate the catalyst in the retentate. De Smet et al. [27] reported on a hybrid process that combines NF with homogeneous and heterogeneous catalysis (transition metal complexes).

Solvent lube oil dewaxing processes are commonly used in refinery operations. Current recovery processes employ dissolution in solvent blends followed by precipitation of the wax by cooling. Exxon Mobil in conjunction with W.R. Grace Company have developed a membrane-based process that allows faster processing of the solvent [6]. The membrane used in this process was a developmental asymmetric polyimide-based membrane, with a reported rejection for the lube oil higher than 95%.

1.5. References

1. I. F. J. Vankelecom, K. De Smet, L. E. M. Gevers, A. Livingston, D. Nair, S. Aerts, S. Kuypers, P. A. Jacobs, Physico-chemical interpretation of the SRNF transport mechanism for solvents through dense silicone membranes, *Journal of Membrane Science* 231 (2004) p99-108.
2. H. Lonsdale, U. Merten, and R. Riley, Transport of cellulose acetate osmotic membranes, *Journal of Applied Polymer Science*, 9 (1965) 1341.
3. D. Bhanushali, S. Kloos, D. Bhattacharyya, Solute transport in solvent-resistant nanofiltration membranes for non-aqueous systems: experimental results and the role of solute-solvent coupling, *Journal of Membrane Science* 208 (2002) p 343-359.
4. N. Stafie, D. F. Stamatialis, M. Wessling, Insight into the transport of hexane-solute systems through tailor-made composite membranes, *Journal of Membrane Science* 228 (2004) p103-116.
5. D. R. Paul, Reformulation of the solution-diffusion theory of reverse osmosis, *Journal of Membrane Science* 241 (2004) p371-386.
6. White, Transport properties of a polyimide solvent resistant nanofiltration membrane, *Journal of Membrane Science* 205 (2002) p191-202.
7. L. G. Peeva, E. Gibbins, S. S. Luthra, L. S. White, R. P. Stateva, A. G. Livingston, Effect of concentration polarisation and osmotic pressure on flux in organic solvent nanofiltration, *Journal of Membrane Science* 236 (2004) p121-136.
8. D. R. Paul, O. M. Ebra-Lima, Pressure-induced diffusion of organic liquids through highly swollen polymer membranes, *Journal of Applied Polymer Science* 14 (1970) p2201-2224.
9. K. S. Bhanushali D, Kurth C, Bhattacharyya D, Performance of solvent-resistant membranes for non-aqueous systems: solvent permeation results and modeling, *Journal of Membrane Science* 189 (2001) p1-21.
10. K.S. Spiegler, O. Kedem, Thermodynamics of hyperfiltration (reverse osmosis), criteria for efficient membranes, *Desalination* 1 (1966) 311.

11. M. Mulder, Basic principles of membrane technology, Kluwer Academic Publishers, Dordrecht, The Netherlands, 1997.
12. G. H. Koops, S. Yamada, S.-I. Nakao, Separation of linear hydrocarbons and carboxylic acids from ethanol and hexane solutions by reverse osmosis, *Journal of Membrane Science* 189 (2001) 241-254.
13. E. Gibbins, M. D' Antonio, D. Nair, L. S. White, L. M. Freitas dos Santos, I. F. J. Vankelecom, A. G. Livingston, Observations on solvent flux and solute rejection across solvent resistant nanofiltration membranes, *Desalination* 147 (2002) p307-313.
14. J. P. Robinson, E. S. Tarleton, C. R. Millington, A. Nijmeijer, Solvent flux through dense polymeric nanofiltration membranes, *Journal of Membrane Science* 230 (2004) p29-37.
15. D.R. Machado, D. Hasson, R. Semiat, Effect of solvent properties on permeate flow through nanofiltration membranes. Part I: investigation of parameters affecting solvent flux, *Journal of Membrane Science* 163 (1999) p93-102.
16. D. Bhanushali, D. Bhattacharyya, Advances in solvent-resistant nanofiltration membranes - experimental observations and applications, *Advanced membrane technology annals of the New York Academy of sciences* 984 (2003) p159-177.
17. D. R. Paul, M. Garcin, W. E. Garmon, Solute diffusion through swollen polymer membranes, *Journal of Applied Polymer Science* 20 (1976) p609-625.
18. J. Whu, B. Baltzis, K. Sirkar, Nanofiltration studies of larger organic microsolute in methanol solutions, *Journal of Membrane Science* 170 (2000) p159-172.
19. X.J. Yang, A. G. Livingston, L.M. Freitas dos Santos, Experimental observations of nanofiltration with organic solvents, *Journal of Membrane Science* 190 (2001) p45-55.
20. R. Subramanian, M. Nakajima, K. S. M. S. Raghavarao, T. Kimura, Processing vegetable oils using nonporous denser polymeric composite

- membranes, *Journal of American Oil Chemists Society* 81 (2004) p313-322.
21. K. Ebert, F. P. Cuperus, Solvent resistant nanofiltration membranes in edible oil processing, *Membrane Technology* 107 (1999) p5-8.
 22. H. J. Zwijnenberg, A. M. Krosse, K. Ebert, K.-V. Peinemann, F. P. Cuperus, Acetone-stable nanofiltration membranes in deacidifying vegetable oil, *Journal of American Oil Chemists Society* 76 (1999) p83-87.
 23. J. P. Sheth, Y. Qin, K. K. Sirkar, B. C. Baltzis, Nanofiltration-based diafiltration process for solvent exchange in pharmaceutical manufacturing, *Journal of Membrane Science* 211 (2003) p251-261.
 24. A. Datta, K. Ebert, H. Plenio, Nanofiltration for homogeneous catalysis separation: Soluble polymer-supported palladium catalysts for Heck, Sonogashira, and Suzuki coupling of aryl halides, *Organometallics* 22 (2003) p4685-4691.
 25. L. S. Nair D, Scarpello JT, White LS, dos Santos LMF, Livingston AG, Homogeneous catalyst separation and re-use through nanofiltration of organic solvents, *Desalination* 147 (2002) p301-306.
 26. Y. X. Luthra SS, dos Santos LMF, White LS, Livingston AG, Homogeneous phase transfer catalyst recovery and re-use using solvent resistant membranes, *Journal of Membrane Science* 201 (2002) p65-75.
 27. K. De Smet, S. Aerts, E. Ceulemans, I. F. J. Vankelecom, P. A. Jacobs, Nanofiltration-coupled catalysis to combine the advantages of homogeneous and heterogeneous catalysis, *Chemical Communications* 7 (2001) p597-598

Preparation and characterization of composite membranes with PDMS as the selective layer

Abstract

This chapter describes the preparation and characterization of the solvent resistant nanofiltration (SRNF) composite membranes used for the oil/hexane separation. The tailor-made composite membranes consist of poly(acrylonitrile) (PAN) ultrafiltration support membrane and polydimethylsiloxane (PDMS) as the selective top layer. The influence of the coating solution concentration upon the membrane performance is studied. A composite membrane with good quality of the PDMS top layer is obtained when the 7 % (w/w) PDMS/hexane coating solution is applied. The composite membrane is stable under the tested conditions and no membrane compaction occurs in the feed pressure range of 1-7 bar. The results show that the PAN/PDMS composite membrane presents good permeation performance, high hexane permeability (around $3 \text{ lm}^{-2}\text{h}^{-1}\text{bar}^{-1}$) and good oil retention (about 90%). Finally, its performance is compared with the commercially available silicone type membrane, MPF-50, and a silicone membrane supplied by GKSS Forschungszentrum, Germany.

2.1. Introduction

Nanofiltration (NF) research has been mainly focused on aqueous systems; however, a lot of pharmaceutical and fine chemical conversions as well as extraction applications are carried out in organic, non-aqueous media. For example, in the vegetable oil industry, the oil extraction from different seeds is mostly performed using n-hexane as solvent. Hexane recovery by membrane processes is environmentally more friendly and safer with respect to health and explosion hazards compared to distillation [1]. Silicone-based membranes were used earlier in the vegetable oil industry by some researchers [2-5] but the exact chemical composition and morphology of the membrane was not clearly revealed. Therefore, the conclusions concerning transport phenomena could not be related to the nature and properties of the membranes.

The goal of this work is to prepare and characterize tailor-made composite membranes with controlled composition and separation characteristics. The membrane consists of poly(acrylonitrile) (PAN) as the support and polydimethylsiloxane (PDMS) as the selective top layer. The PAN support combines sufficient chemical stability with good membrane performance and is used in a wide range of applications [6]. Its morphology is stable in the dry state, without requiring impregnation with substances like glycerol to prevent pore collapse. In addition, PDMS has high chemical and thermal stability, combined with low toxicity [7, 8] that makes it suitable for the edible oil industry.

First, our work describes a systematic investigation of the parameters that are important to prepare a stable, defect-free PAN/PDMS composite membrane. The optimum concentration of the PDMS coating solution, the number of coating steps in combination with the support pore size are defined. Then, the composites are tested in filtration experiments with pure hexane and oil/hexane solutions. The results are compared with the commercially available silicone type membrane, MPF-50, and a silicone membrane supplied by GKSS Forschungszentrum, Germany.

2.2. Theoretical background

2.2.1. Chemical and physical properties of PDMS

Polydimethylsiloxanes, frequently referred to by the generic name silicones, are polymers with a unique combination of properties, due to the presence of an inorganic siloxane backbone and organic methyl groups attached to the silicon. PDMS is extensively used in various applications due to some fundamental structural properties:

- low intermolecular forces between the methyl groups;
- unique flexibility of the siloxane backbone;
- high bonding energy of the siloxane bond.

These properties result in a low glass transition temperature ($T_g = -123^\circ\text{C}$), as well as a good thermal, chemical, and oxidative stability. In order to prepare silicone membrane, the PDMS should be cross-linked. In this work, PDMS 615 supplied by General Electric is used. It is a two-component system: (a) RTV A that contains a dimethylvinyl terminated pre-polymer and the Pt-catalyst, and (b) RTV B that contains the cross-linker with several hydride groups. The hydrosilylation (addition reaction) relies on the ability of the hydrosilane bond of the cross-linker ($\equiv\text{SiH}$) to add across a carbon-carbon double bond belonging to the pre-polymer in the presence of the Pt catalyst – see *Figure 1*.

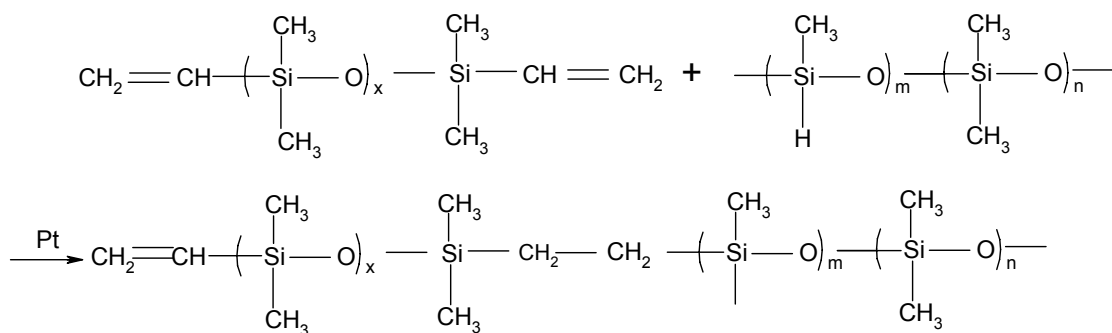


Figure 1: Scheme of the cross-linking reaction for the silicone network formation.

2.2.2. NF membrane preparation and the pore intrusion phenomena

Bearing in mind the inverse relation between transmembrane flux and membrane thickness, the preparation of thin, selective membranes is important. However, thin freestanding PDMS films are usually not strong enough to withstand high pressures. Therefore, a porous support is required that will ensure mechanical stability. Composite membranes can be prepared by a coating procedure. This method is suitable for preparation of thin composite membranes and can be easily scaled-up for industrial production [9]. Generally, the surface of the support membrane is briefly contacted with the polymer coating solution. After subsequent solvent evaporation, a thin polymer film is formed onto the support. The thickness of the coating layer basically depends on the concentration of the polymer solution and on the pore size of the support. The support should have relatively high porosity in order to avoid additional mass transfer resistance for the permeating compounds. However, wide pores in the support may lead to pore intrusion of the coating solution. Moreover, the duration of contact between the support and polymer coating solution is a process parameter which can influence the quality of the resulting coating layer. Therefore, a closer look at the important parameters related to the composite membrane preparation is crucial in order to obtain the optimum membrane characteristics – i.e. good adhesion to the support layer, low pore intrusion, etc. Generally, the top-layer thickness depends on the balance between the viscous forces, the capillary forces and the inertial forces [9].

When the support has large pores and/or when the viscosity of the coating solution is too low, pore intrusion phenomena may occur. This significantly influences the membrane performance and has been in fact the foundation of industrial gas separation using membranes [10]. Confinement of the top layer material in the porous support restricts the swelling of the polymer immobilized inside the pore due to the rigidity of the support matrix. In literature, several methods to reduce pore intrusion have been reported [11]. One suggests the use of polymer solutions in which the dimensions of the polymer chains are bigger than the pore size of the support. The polymer chain dimension depends on the interaction between the polymer chain and the solvent: a good solvent leads to more extended polymer chains. Another way to prevent pore penetration is to use a coating solution with high viscosity due to the increased concentration and/or increased molecular weight of the polymer prior to

coating, for instance, by pre-cross-linking, as it will be discussed later in this chapter. Another approach is by filling the support pores with a liquid that is not miscible with the coating solution. Water, however, as the pore filling liquid, should be avoided for the type of pre-polymer/cross-linker PDMS used in this work due to a competitive process of hydrolysis of the SiH groups. The sensitivity of the PDMS cross-linker towards moisture has already been reported in literature [7, 8, 12, 13]: the SiH groups may be consumed by an undesired side reaction involving water.

2.2.3. Mass transport through porous and non porous membranes

Below, we summarize briefly the transport mechanism of liquids and gases through the porous and dense membranes:

1. convective flow;
2. diffusion through porous membrane;
3. solution-diffusion through dense membrane.

1. For liquids, the flux through a porous membrane can be described by the Hagen-Poiseuille equation for viscous flow:

$$J = \frac{n\pi r_p^4 \Delta p}{8\eta A \tau l} \quad \text{Equation 1}$$

where J is the liquid flux, n the number of pores, r_p the pore radius, Δp the pressure difference across the membrane, η is the liquid viscosity, A is the membrane area, τ the membrane tortuosity, l the membrane thickness.

2. The gas transport through a porous membrane depends on the pore size: when relative large pores or defects are present (>10 nm), the gas flux is mainly determined by the viscous flow in which gas molecules collide exclusively with each other [9, 14]. At smaller pore sizes, the gas flux is mainly determined by Knudsen diffusion: diffusing gas molecules collide more with the pore walls than with the other gas molecules. The gas flow is described by:

$$J_{k,g} = \frac{P_{k,g} \Delta p}{l} = \frac{n \pi r_p^2 D_{k,g} \Delta p}{A R_g T \tau l} \quad \text{Equation 2}$$

where $J_{k,g}$ is the gas flux, $P_{k,g}$ is the gas permeability coefficient, R_g the gas constant, T the temperature, and $D_{k,g}$ is the Knudsen diffusion coefficient. This diffusion coefficient can be calculated using:

$$D_{k,g} = 0.66 r_p \sqrt{\frac{8 R_g T}{\pi M W}} \quad \text{Equation 3}$$

where MW is the molecular weight of the gas.

Equation 3 shows that the gas flow is inversely proportional to the square root of the molecular weight. Therefore, the separation of two gases by the Knudsen mechanism depends on the square root of their corresponding molecular weight.

3. According to the solution-diffusion model which was developed by Lonsdale et al. [15] and recently reviewed by Wijmans and Baker [16], the flux of a species i through a non porous, dense membrane is given by:

$$J_i = \frac{D_i K_i}{l} [c_{if} - c_{ip} \exp(\frac{-\nu_i (p_f - p_p)}{R_g T})] \quad \text{Equation 4}$$

where D_i is the diffusion coefficient of i through the membrane, K_i is the sorption coefficient, c_{if} , c_{ip} is the feed and permeate concentrations of species i , respectively, ν_i is the partial molar volume of species i , p_f , p_p is the feed and permeate sides pressures, respectively. The primary assumption made in the model is that the flux of the solute and solvent are independent. For the pure solvent and by incorporation of the osmotic pressure, *Equation 4* becomes:

$$J_i = \frac{D_i K_i c_{if}}{l} [1 - \exp(\frac{-\nu_i (\Delta p - \Delta \pi)}{R_g T})] \quad \text{Equation 5}$$

where $\Delta\pi$ is the difference in osmotic pressure across the membrane. When the exponential term is small (low pressure range and solvent with small partial molar volume) then the *Equation 5* can be written to a very good approximation as:

$$J_i = \frac{D_i K_i c_{if} v_i}{l R_g T} (\Delta p - \Delta\pi) \quad \text{Equation 6 a}$$

or

$$J_i = P(\Delta p - \Delta\pi) \quad \text{Equation 6 b}$$

where P is a constant equal to the term $\frac{D_i K_i c_{if} v_i}{l R_g T}$ and is called the solvent permeability.

Similarly, the flux of the solute *j* is:

$$J_j = \frac{D_j K_j}{l} [c_{jf} - c_{jp} \exp(\frac{-v_j (p_f - p_p)}{R_g T})] \quad \text{Equation 7a}$$

At low pressure range and for solutes of small partial molar volume, the exponential term is small and the *Equation 7a* can be written to a very good approximation as:

$$J_j = B(c_{jf} - c_{jp}) \quad \text{Equation 7b}$$

where $B = \frac{D_j K_j}{l}$ is usually constant and is called the solute permeability. *Equation 6b*

indicates a linear increase of solvent flux with increasing transmembrane pressure difference, whereas *Equation 7b* indicates that the solute flux remains unaffected by the pressure difference.

2.3. Experimental

2.3.1. Materials

The PAN ultrafiltration membranes (with MWCO of 30 and 50 kDa) were provided by GKSS - Germany. These membranes were delivered in the dry state and used without further treatment. *Table 1* presents the PAN specifications given by the manufacturer.

Table 1: Manufacturer data of PAN support.

PAN Type	d_{50}^a (nm)	MWCO ^b (kDa)
HVII	11.6	50
HVIII	6.7	30

^a d_{50} mean pore size

^b MWCO – molecular weight cut-off, measured with an aqueous Dextran solution

The selective top layer of the composite was PDMS (RTV 615 type, kindly supplied by General Electric, The Netherlands). The silicone kit was a two-component system, consisting of a vinyl-terminated pre-polymer (RTV A) and a cross-linker containing several hydride groups (RTV B). Curing of the PDMS-membrane occurs via a Pt-catalysed hydrosilylation reaction to form a densely cross-linked polymer network (see *Figure 1*).

The n-hexane (Merck, The Netherlands) and the sunflower oil (Fluka, The Netherlands) were used as supplied, without further purification. The refined sunflower oil consisted of a mixture of triglycerides (mostly C18 with traces of C16-C20 fatty acids), with molecular weight around 900. Linoleic acid was the major component with unsaturated bonds.

The MPF-50 (silicone type composite membrane) was purchased from Koch - USA. This membrane was supplied in the wet state, soaked in 50 % ethanol/water solution. The GKSS membrane was also a silicone based composite, PAN-PDMS, kindly

provided by GKSS Forschungszentrum, Germany. This membrane was delivered in the dry state and used without further treatment.

2.3.2. PAN/PDMS composite preparation

The PAN/PDMS tailor-made composite membranes were prepared in a two-step coating procedure:

- Dip coating of the PAN support membrane in a 1 % (w/w) PDMS/hexane solution and placing in a N₂ oven at 65 °C for 4 h.
- Dip coating of the membranes with pre-cross-linked PDMS/hexane solutions of various concentrations. (Initially, 15 % (w/w) PDMS/hexane solution is pre-cross-linked at 60°C for 3 h, and then diluted at various concentrations). The composites were then placed in a N₂ oven at 65 °C for 4 h to complete the cross-linking.

Before the coating process, the PAN support was glued on a glass plate with PVC tape and was slowly immersed in a vessel containing the coating solution. The gluing of the support membrane guaranteed the coating solution to only contact the skin layer of the UF-support membrane. The angle of immersion was 90° - see *Figure 2*.

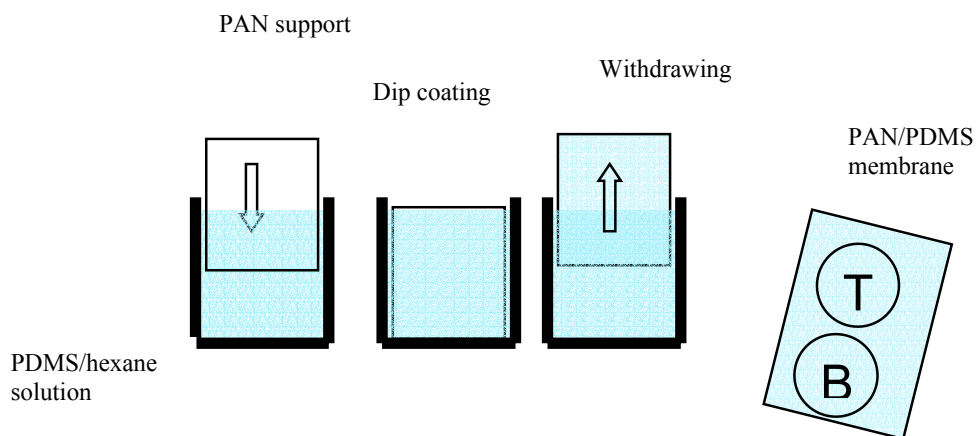


Figure 2: Schematic drawing of the dip coating process (T and B indicates the top and bottom side, respectively, of the PAN/PDMS composite membrane).

The prepared membrane composites are coded Mx-y, where x is the PDMS concentration and y is the MWCO of the PAN support.

2.3.3. Membrane characterization

The viscosities of the PDMS/hexane solutions were measured using an Ubbelohde viscometer (model OC with an instrument coefficient of 0.0143 cSt/s) obtained from Tomson, The Netherlands. The densities of the solutions were measured using Digital Density Meter DMA 50, purchased from Anton Paar, The Netherlands. Both the viscosity and density measurements were performed in triplicate at 25°C.

Scanning Electron Microscopy (SEM) was used for investigation of the PAN/PDMS composites morphology. The microscopic studies were performed using a Scanning Electron Microscope Jeol JSM-5600LV, at 5 kV. The cross-sectioned samples were prepared by breaking the specimens in liquid nitrogen. After drying for at least 4 hours in a vacuum oven at 30° C, the samples were sputtered with gold (with a sputtering device, model SCD 040, Balzers Union) under vacuum for 300 s at a current intensity of 15 mA.

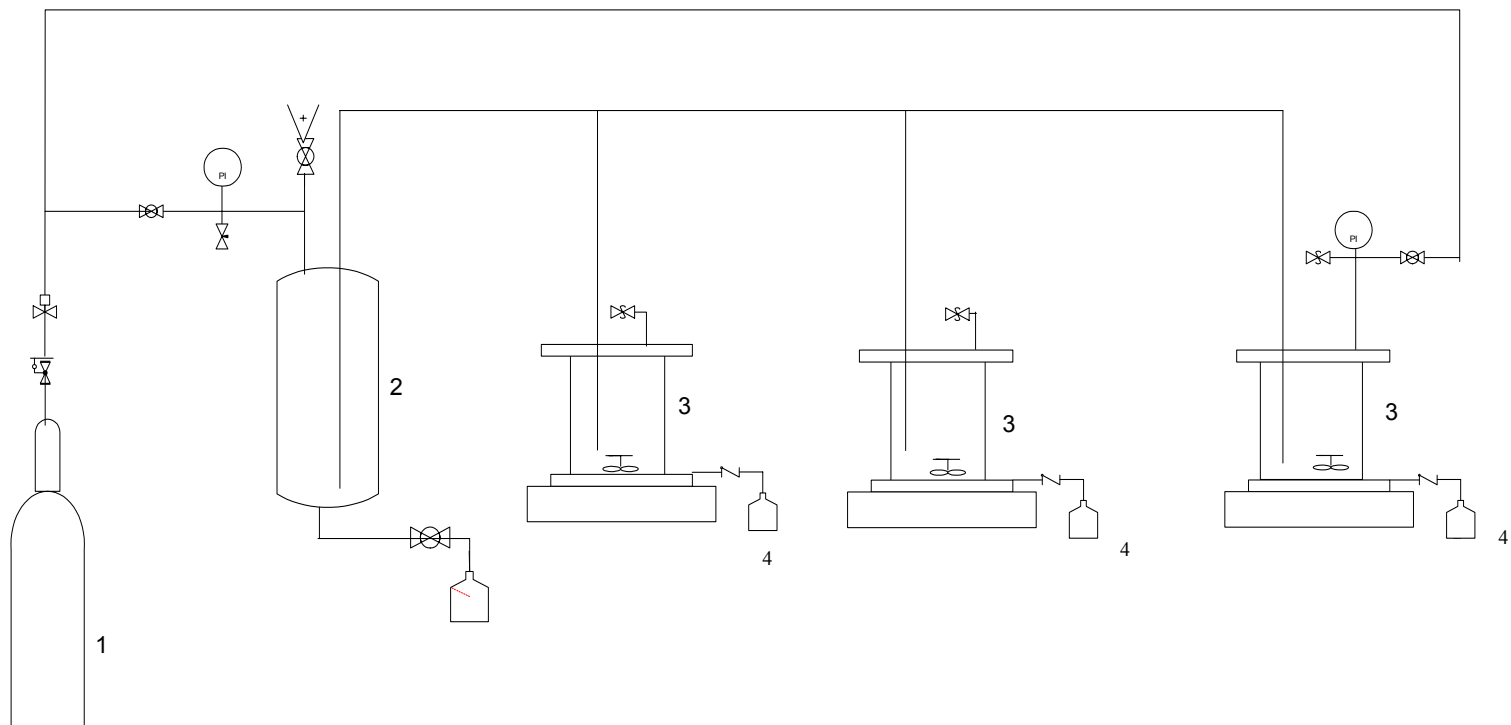
The quality of the composite membrane was assessed by performing single gas permeation measurements with N₂ and CO₂, using the set-up and procedure described in [10]. The gas fluxes through the membrane were measured by a soap-bubble meter (feed pressure in the range of 1 - 2.5 bar and downstream pressure of 1 bar). The selectivity of CO₂ over N₂ (α_{CO_2/N_2}) of the membranes was calculated by:

$$\alpha_{CO_2/N_2} = \frac{P_{CO_2}}{P_{N_2}} \quad \text{Equation 8}$$

where P_{CO_2} and P_{N_2} is the CO₂ and N₂ gas permeability (note that the intrinsic PDMS selectivity, for CO₂ over N₂, is $\alpha_{CO_2/N_2} = 11.6$).

2.3.4. Liquid permeation set-up and procedure

All the liquid permeation experiments were performed in a dead-end filtration set-up with 3 test cells (*Figure 3*).



1 = gas cylinder, 2 = feed reservoir, 3 = stirred permeation cells, 4 = permeate vessels

Figure 3: Schematic diagram of the liquid permeation set-up.

Each cell had a capacity of 350 cm³ and an effective membrane area of 12.6 cm². A porous stainless steel disc supported the tested membrane. For the permeation experiments, the feed solution was placed in a feed tank and N₂ gas was used to apply pressures up to 7 bar. A magnetic bar suspended from the top provided continuous stirring above the membrane surface. The bar was driven by an external explosion proof magnetic stirrer (Variomag[®], H+P Labortechnik GmbH, Germany).

All the permeation experiments were performed at room temperature (24 ± 3 °C). For oil/hexane solution the following protocol was used: the membranes were placed in the test cells and a pre-conditioning step with pure hexane at 7 bar for 1 h was performed. The system was then slowly depressurised, the hexane was removed, the oil/hexane solution was placed in the reservoir and new pressure was applied. After each measurement, the system was slowly depressurised, the permeate was collected and analysed and then returned to the feed reservoir. The sunflower oil concentration in the feed and permeate solutions (c_{jf} , c_{jp} , respectively) was analysed by refractive index measurements at 25 °C using a Abbe-3 refractometer, from Carl Zeiss, Germany. The sunflower oil retention was calculated using the equation:

$$R = \left(1 - \frac{c_{jp}}{c_{jf}} \right) \times 100 \quad \text{Equation 9}$$

The flux through the membrane was calculated by dividing the permeate volume (in l) by the membrane area (in m²) and the collecting time (h). The permeate volume was determined by dividing the collected weight by the permeate density.

Values and error bars reported in the tables and figures are based on the measurements with at least three different membranes.

2.4. Results and discussion

2.4.1. Characterization of the PAN support

The gas transport through the PAN support is expected to be of the Knudsen type: the ratio of the CO₂ and N₂ fluxes should be equal to the reciprocal ratio of the square root of the gas molecular weight.

$$\alpha_{CO_2/N_2} = \frac{J_{CO_2,g}}{J_{N_2,g}} = \sqrt{\frac{M_{N_2}}{M_{CO_2}}} = 0.79 \quad \text{Equation 10}$$

The selectivity of CO₂ over N₂ for the PAN support is found to be 0.80, very close to the ratio of the square root of the N₂ over CO₂ molecular weight, 0.79, showing that the gas transport mechanism is indeed Knudsen.

SEM pictures (cross-section and surface) of the PAN support membrane are shown in *Figure 4*. The cross-section picture shows a homogeneous pore structure. A uniform surface is observed and no pore-like features are depicted at this SEM magnification, as expected from the pore size reported by the supplier (maximum 12 nm - see *Table I*).

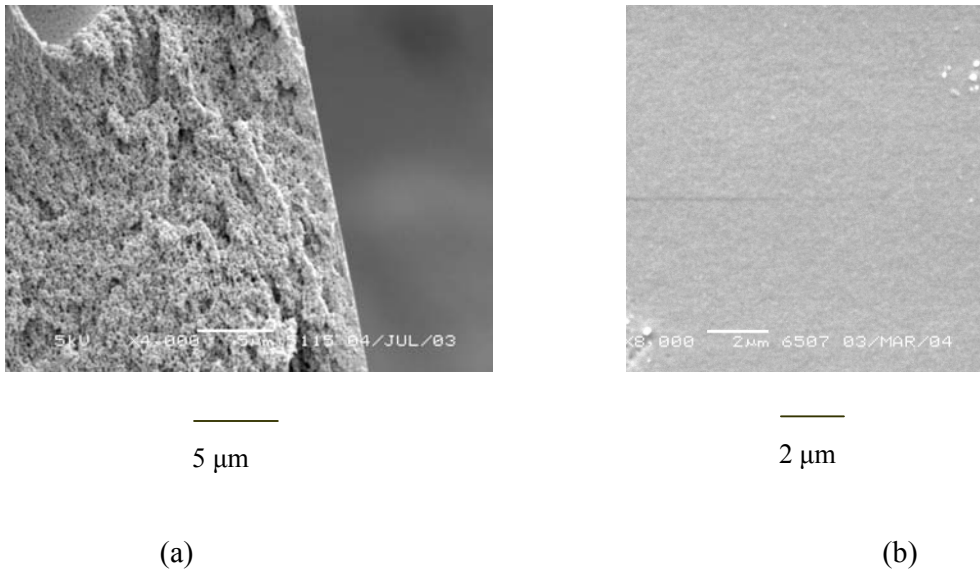


Figure 4: SEM pictures of PAN support (a) cross section (magnification 4000x) and (b) surface (magnification 8000x).

To check if PAN is a suitable support for the composite membrane preparation, its thermal and chemical stability under the membrane preparation conditions were studied. First, the influence of the thermal treatment at 65°C in a N₂ oven on the membrane structure was evaluated by performing gas and liquid (water and hexane) permeation experiments before and after the thermal treatment: no difference was noticed, showing that the PAN morphology was stable under the studied conditions.

Figure 5 presents typical results of the fluxes of various solvents through the PAN support versus time, at a transmembrane pressure of 1 bar. In all cases, the solvent fluxes are constant in time.

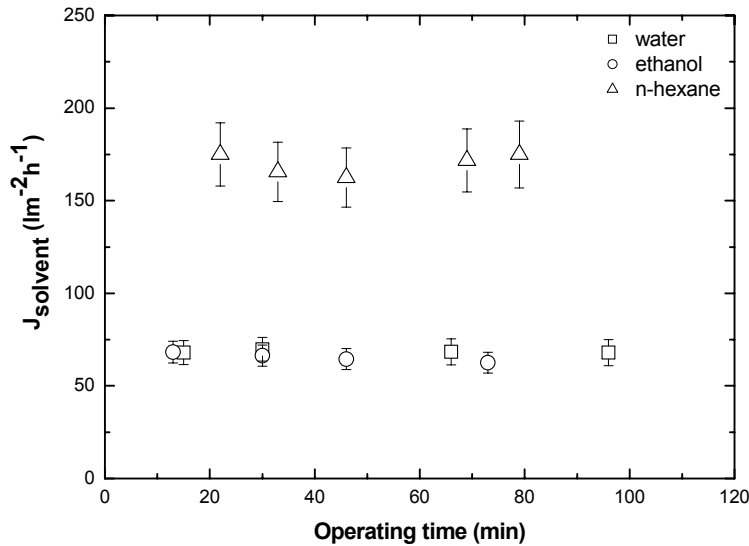


Figure 5: Solvent flux as a function of operating time through PAN support. Experimental conditions: transmembrane pressure of 1 bar, at 24 ± 3 °C.

The effect of the transmembrane pressure on the solvent flux was also studied in the range of 1-7 bar. The results are plotted in *Figure 6*. The presented data are steady-state values, collected after 1 h of permeation.

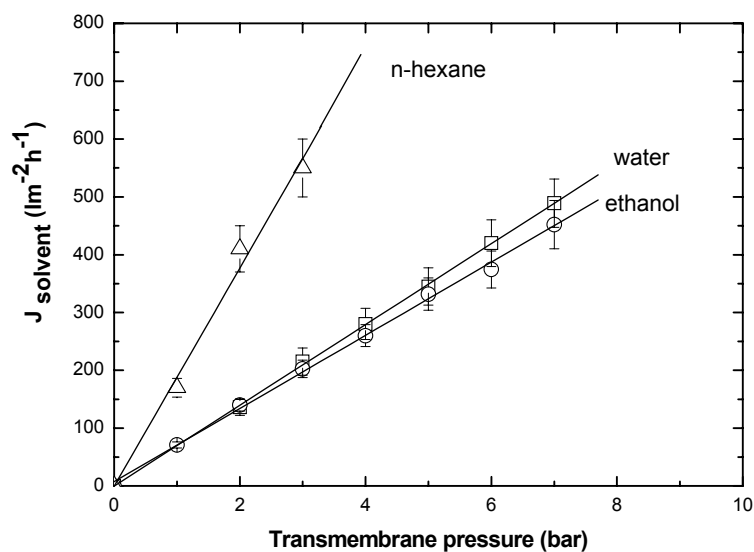


Figure 6: Solvent flux as a function of transmembrane pressure, at 24 ± 3 °C.

The solvent flux increases linearly with the applied pressure, showing no appreciable membrane compaction at this pressure range. *Table 2* presents the solvent permeability (calculated from the slopes of *Figure 6*).

Table 2: Solvent permeability of PAN support and its normalization by solvent viscosity.

Solvent	η^a (cP)	P (l m ⁻² h ⁻¹ bar ⁻¹)	$P_{\text{norm}}=P\eta$ (cP l m ⁻² h ⁻¹ bar ⁻¹)
Water	1.00	69 ± 7	69 ± 7
Ethanol	1.08	62 ± 5	67 ± 5
n-hexane	0.32	188 ± 20	60 ± 6

^a viscosity data taken from [17], at 25°C

The solvent permeability normalized by solvent viscosity is statistically not different (in the range of 60-69 cPlm⁻²h⁻¹bar⁻¹), showing that liquid flow through the PAN depends on the solvent viscosity, according to the Hagen-Poiseuille equation (see *Equation 1*).

The stability of the membranes under the permeation conditions was investigated, too. After the liquid permeation experiments were performed, the membranes were allowed to dry and the liquid permeation experiments were performed again. The results were consistent with those of *Figure 5* and *Figure 6*. Moreover, the examination of the PAN support after permeation experiments by SEM did not reveal any changes in membrane morphology.

All the above results show that PAN membrane has the required stability for the tested solvents and conditions, indicating its stability for the preparation of the PAN/PDMS composites.

2.4.2. Preparation of PAN/PDMS composite membranes

The influence of the PDMS concentration on the quality of the prepared PAN/PDMS composite membranes was systematically studied. For this test, the PAN support with MWCO of 30 kDa was used. To identify the optimum coating conditions, gas permeation experiments were used.

For the gas permeation data, the CO₂ permeability was taken as the quality indicator, assuming that the selectivity of a dense, defect-free coating is determined only by the top-layer. Note that this assumption is only correct for a support which does not contribute to the total mass transport resistance. In any other case, the model of Henis and Tripodi should be applied [10]. *Figure 7* shows that the normalized CO₂ permeability from *Equation 2*, (P_{CO_2}/l), decreases systematically with increasing polymer coating solution concentration, as expected. The gas selectivity, α_{CO_2/N_2} , increases, approaching the intrinsic gas selectivity of PDMS, for the 7 % (w/w) PDMS/hexane coating solution.

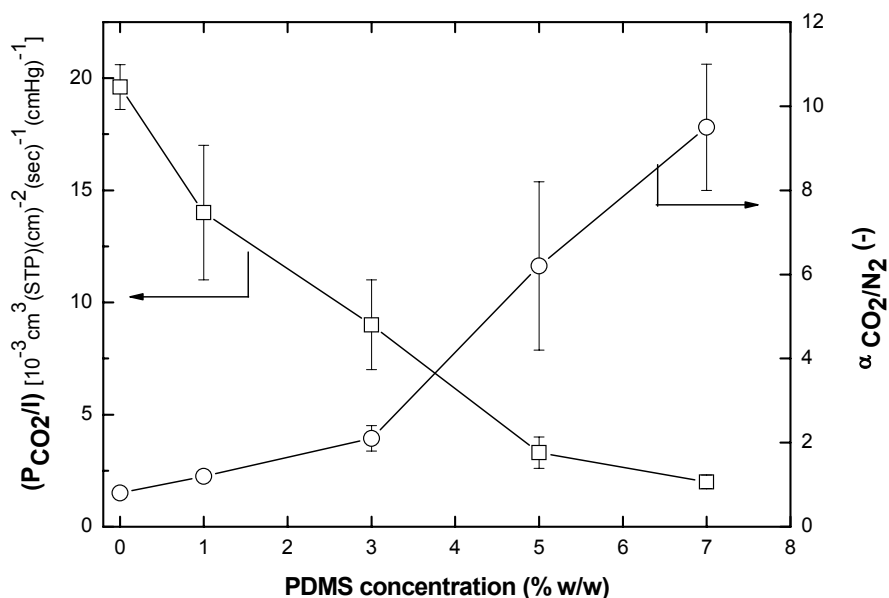


Figure 7: The normalized CO_2 permeability ($P_{CO_2/l}$) and α_{CO_2/N_2} of the composite membranes as a function of the PDMS concentration in the coating solution. Experiments performed with pure gas at 24 ± 3 °C.

For PDMS concentration in the range of 1 - 5 % (w/w), low gas selectivity is obtained in comparison with the PDMS intrinsic selectivity (11.6), indicating that the coating layer has defects. The results of *Figure 7* show that it is important to use concentration of PDMS solution of 7 % w/w in order to obtain a defect-free membrane. The good quality of the top layer can be directly correlated to the viscosity of the coating solution: the kinematic viscosity of the solution increases from 0.49 to 0.99 cSt when the concentration increases from 0 to 7% w/w. At relatively high viscosity, the composite has a defect-free coating layer.

Based on the initial screening experiments, the PAN/PDMS composites prepared with 7 % (w/w) PDMS coating solutions are selected for further studies.

2.4.3. Reproducibility of the dip-coating method

The uniformity of the PDMS top layer thickness was studied too. A difference in the top-layer thickness dependent on the flat sheet position relative to the dip-coating

vessel might be expected. Therefore, the quality of the membrane at the top (T) or at the bottom (B) side of the prepared PAN/PDMS membranes was evaluated (see *Figure 2* defining the top as the upper part of the support, which probably has shorter contact time with the coating solution). The MWCO of the support was varied, using PAN with a MWCO of 30 and 50 kDa. *Table 3* shows the performance characteristics of PAN/PDMS composite membranes, as a function of the top-bottom position and of the MWCO of the PAN support. The $l_{\text{eff.CO}_2}$ is the PDMS thickness determined from the CO₂ permeation experiments and l_{SEM} is the PDMS top-layer visualized by SEM.

Table 3: Performance characteristics of the PAN/PDMS composite membranes. Experiments performed with pure gas at 24 ± 3 °C.

Membrane	PDMS conc. (w/w)	MWCO _{PAN} (kDa)	Membrane position	$\alpha_{\text{CO}_2/\text{N}_2}$ (-)	$l_{\text{eff.CO}_2}$ (μm)	l_{SEM} (μm)
M7-30	7	30	T	9.6 ± 1.8	1.9 ± 0.2	0.7 ± 0.2
			B	9.8 ± 1.4	2.0 ± 0.3	0.8 ± 0.2
M7-50	7	50	T	9.5 ± 2.1	2.1 ± 0.5	0.8 ± 0.2
			B	9.2 ± 2.3	2.3 ± 0.4	0.9 ± 0.2

Typical SEM image of the cross-section is shown in *Figure 8*.

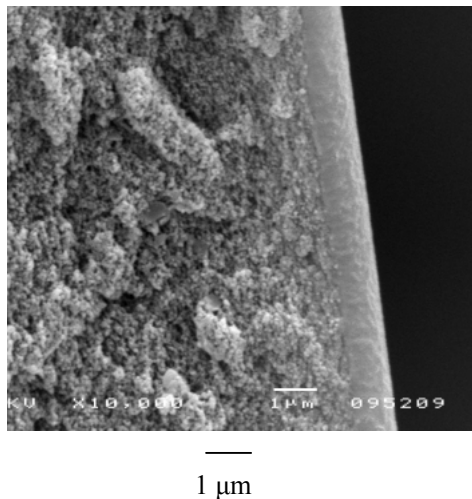


Figure 8: SEM picture of the cross-section of the M7-30 (magnification 10000x).

The selectivity of CO₂ over N₂ is close to the intrinsic PDMS selectivity. No significant difference in the PDMS top-layer performance (gas selectivity and PDMS effective and visualized thickness) at different position of the membrane or of the MWCO of the PAN is observed. It seems that the viscous forces of the coating solution are the dominant parameters compared to the capillary forces of the PAN support.

The effective thickness of the PDMS layer is larger than the thickness visualized by SEM. It seems that in between the support and the dense top layer exists an intermediate layer where the PDMS penetrates into the pores of the support.

2.4.4. Liquid permeation

The liquid permeation performance of the M7-30 composite membrane in hexane and oil/hexane solutions is systematically investigated, including the longer-term permeation experiments too. The use of the PAN/PDMS membrane in subsequent experiments was evaluated by permeating hexane for 2 days (run 1 and 2, filtration of about 6 h per day), showing that the hexane flux through the membrane is constant over the operating time - *Figure 9*.

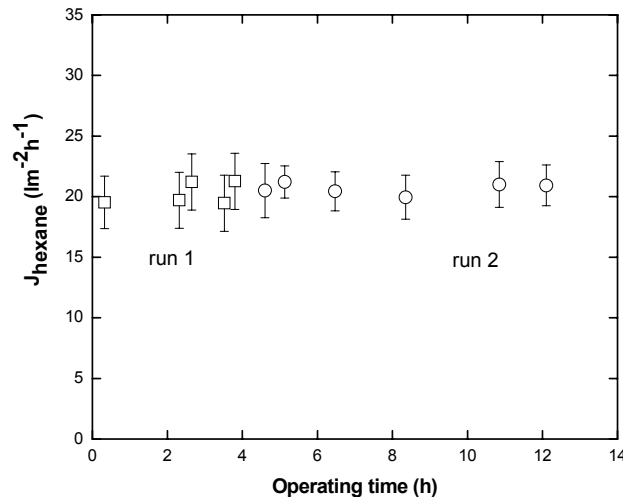


Figure 9: Hexane flux through the M7-30 composite membranes as a function of operating time. Experimental conditions: 7 bar, 24 ± 3 °C.

The stability of the composite membrane is further confirmed by SEM examination of the membrane surface and cross-section before and after liquid permeation. There is no change in the PAN/PDMS membrane morphology.

In addition, the long-term permeation through the membrane is studied, using a 8 % (w/w) oil/hexane feed solution, at transmembrane pressure of 7 bar. *Figure 10* presents the results after three consecutive days (runs) of oil/hexane permeation for about 6 h per day. No significant changes in membrane performances are found.

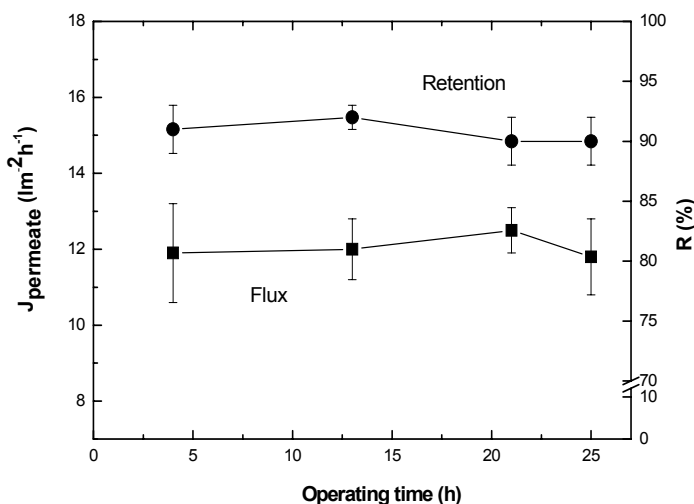


Figure 10: Permeate flux and oil retention of the M7-30. Experimental conditions: 7 bar, at 24 ± 3 °C.

The influence of drying on the performance for the composites was also investigated. First, the flux and retention of a 8 % (w/w) oil/hexane feed solution, at 7 bar, 24 ± 3 °C was measured. Subsequently, the membranes were dried and then a new permeation experiment under the same experimental conditions was performed. No significant difference between the flux and retention values of virgin and used membranes was observed.

From all the above results, we conclude that the tailor-made PAN/PDMS membranes are stable under the tested conditions.

2.4.5. Comparison with other silicone type membranes

The commercially available NF membrane MPF-50 and a GKSS silicone membrane were also characterized in order to compare their separation performances with those of the PAN/PDMS tailor-made membranes.

The MPF-50 is a silicone type membrane of which the exact chemical composition is not known. Its structure was characterized by SEM and ATR-FTIR and its separation performance by liquid permeation experiments (hexane and oil/hexane solutions).

Figure 11 shows the SEM pictures of the cross-section of the MPF-50 membrane, confirming the composite nature of the MPF-50, with a selective top-layer and a porous support.

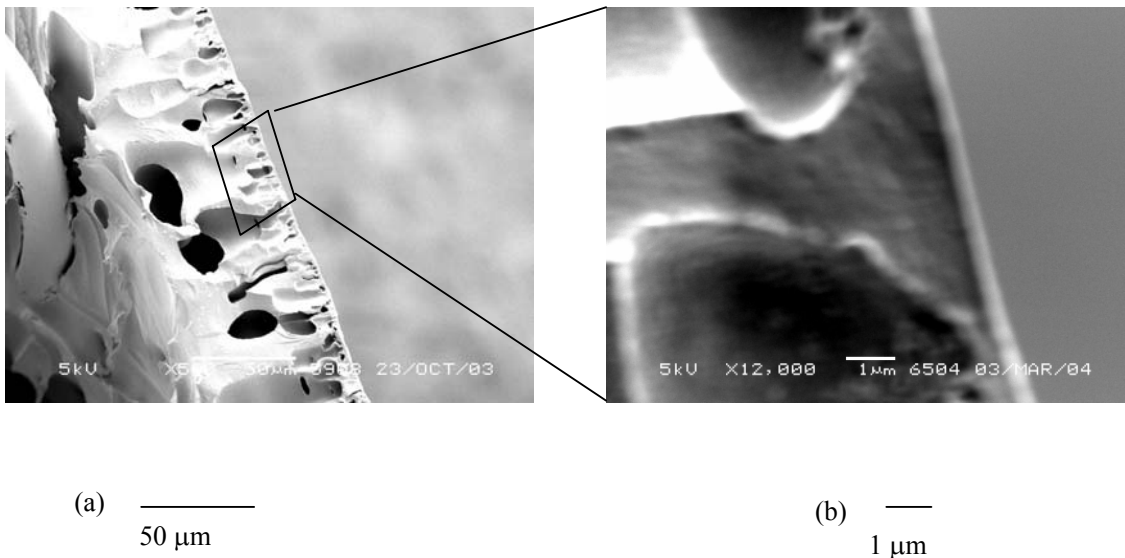


Figure 11: SEM pictures of the cross-section of MPF-50 membrane, (a) magnification of 500x and (b) zooming in (magnification 12000x) on details of the surface region.

The top view of the MPF 50 (presented in *Figure 12*) shows a relatively smooth surface. Similar observations were reported by Machado et al. [18] and Vankelecom et al. [19].

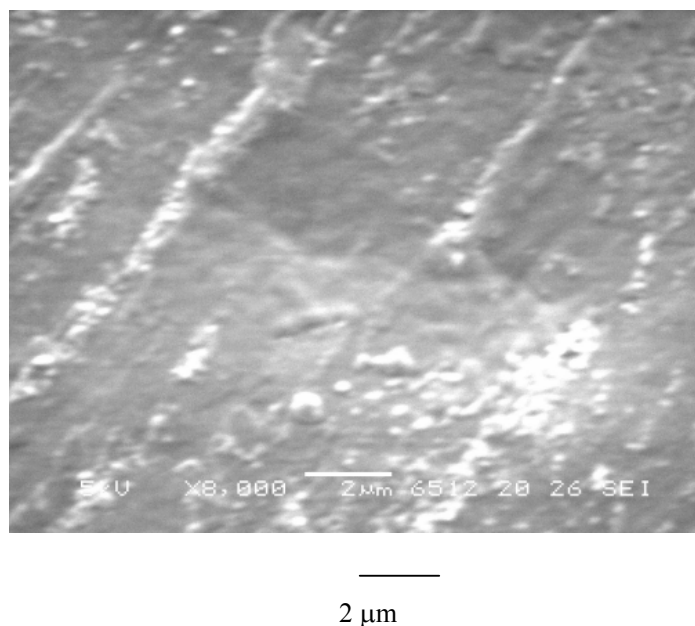


Figure 12: SEM picture of the surface of the MPF-50 (magnification 8000x).

Figure 13 shows the ATR-FTIR spectrum of the MPF-50 membrane. In the region from 3100 cm^{-1} to 1100 cm^{-1} some pronounced peaks characteristic of the Si-O-Si in siloxanes [17] are observed, suggesting a silicone-type coating layer, in agreement with the results reported by others [18, 19].

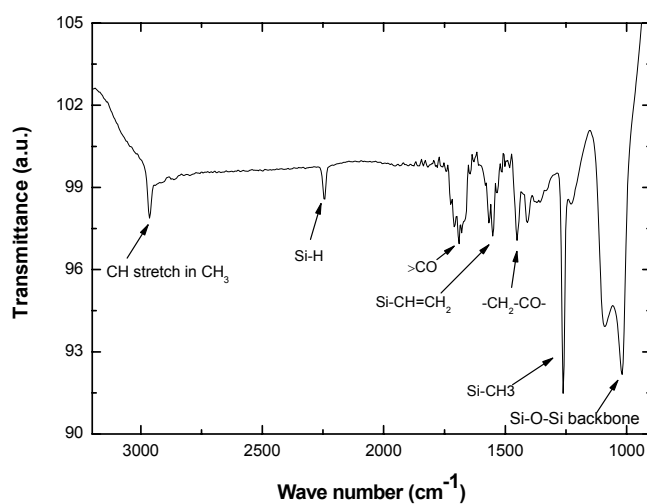


Figure 13: ATR- FTIR spectrum of the MPF-50 membrane.

The gas permeation experiments showed that the membrane selectivity, α_{CO_2/N_2} , was around 1.2, indicating that the gas transport mechanism through the MPF-50 dried membrane is of viscous type. By examining the membrane after the gas permeation measurement, large cracks on the membrane surface (membrane top layer) could be observed. It seems that the selective top-layer becomes brittle upon drying (the supplier recommends the use of the membrane in the wet state only), indicating that the measured gas selectivity corresponds to the support layer of the MPF-50 composite rather than to the silicone type top-layer.

The GKSS membrane used in the current study is a radiation cross-linked PAN/PDMS composite [20]. The gas permeation experiments show that the membrane selectivity α_{CO_2/N_2} is 10.3 ± 0.4 , confirming a defect-free PDMS top-layer. SEM pictures of the membrane cross-section and surface are shown in *Figure 14*. They reveal a relatively uniform surface which is characteristic for a PDMS dense layer.

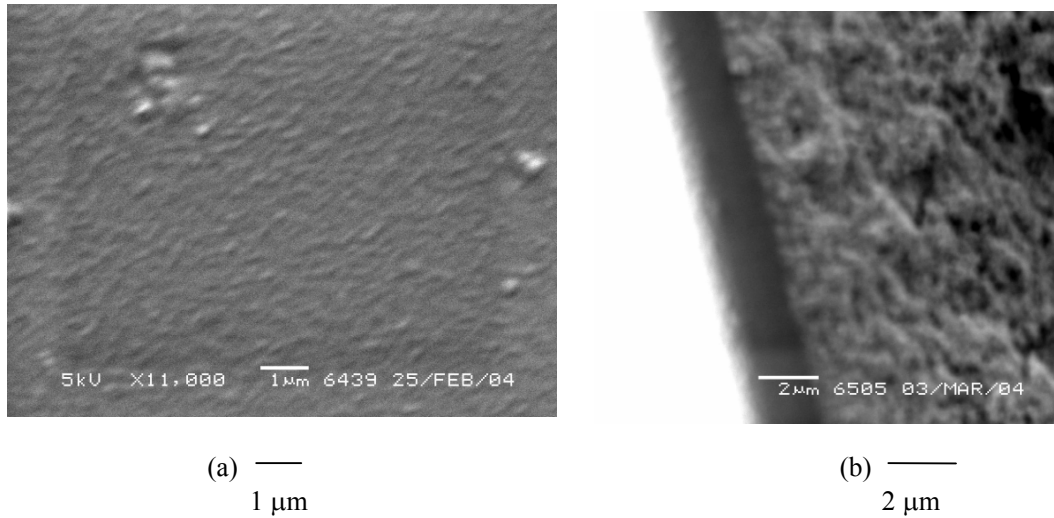


Figure 14: SEM pictures of (a) the top-surface and (b) the cross-section of the GKSS membrane.

The effective thickness, calculated from the gas permeation experiments is around 2.2 μm , in good agreement with the visualized top-layer thickness by SEM (l_{SEM} of about 2 μm), indicating that there might be no pore intrusion in the support.

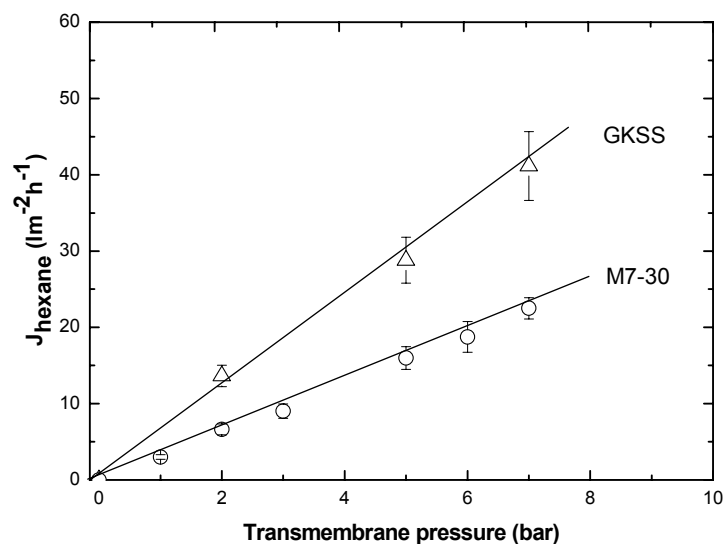


Figure 15: Hexane flux as a function of the transmembrane pressure, at 24 ± 3 °C.

Figure 15 presents the effect of transmembrane pressure on the hexane flux for M7-30 and GKSS membranes. We do not have data for the hexane flux through the MPF-50 membrane due to the difficulty to position the membrane in the permeation set-up. As received from the supplier, the membrane is rather curled, which makes the membrane handling difficult for the configuration of our permeation cell (however, we managed to perform one permeation experiment with 8% (w/w) oil/hexane, data shown later). In addition, the membrane should always be kept in a wet state to avoid irreversible changes of the membrane morphology (manufacturer's data sheet information). On the contrary, the GKSS and our PAN/PDMS tailor-made membranes were easy to handle and they could be used in the dry state without further treatment.

At the same experimental conditions, the hexane permeability through the GKSS membrane is about two times higher than through M7-30 (5.9 and $3.1 \text{ lm}^{-2}\text{h}^{-1}\text{bar}^{-1}$, respectively). The difference might be due to the restricted swelling caused by the confinement of PDMS within the porous support (for the M7-30) or/and due to the difference in the cross-linking degree of the PDMS network.

In both cases, the hexane flux increases linearly with the applied pressure. Hence, for the hexane transport through the membrane, the Equation 6 b can be used (this

equation gives a reasonable prediction of the hexane flux, due to the relative low molar volume of hexane and low pressure range applied). Other studies reported also on the linearity of the flux of various solvents (polar and non-polar) with applied pressure through hydrophobic and hydrophilic NF membranes [18, 21-23].

Figure 16 presents the effect of the feed pressure on the hexane flux for a 8 % w/w oil/hexane feed solution.

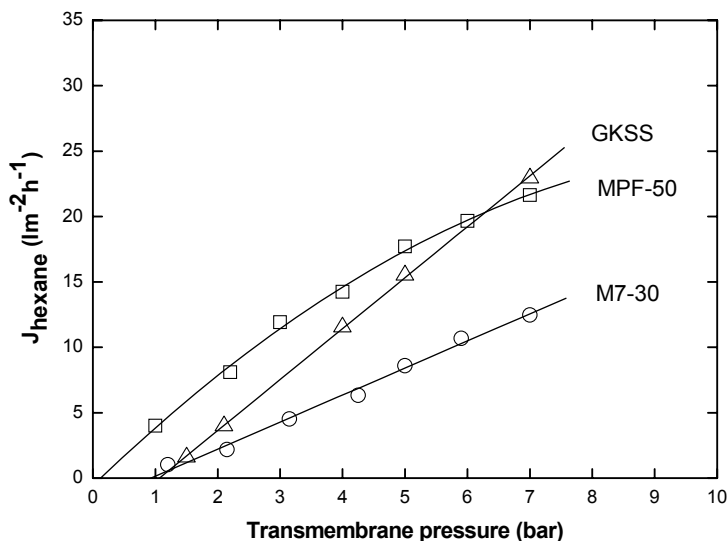


Figure 16: Hexane fluxes as a function of the transmembrane pressure. Experimental conditions: 8 % (w/w) oil/hexane feed solution, at 24 ± 3 °C.

For the GKSS and the M7-30 membranes, the linearity of the hexane flux with applied pressure indicates that no compaction of the membrane occurs over the applied pressure range. However, the MPF 50 membrane shows a non-linear behaviour, suggesting that the membrane is probably compacted during the permeation experiment. Because of the compaction, the membrane resistance towards the flow increases and the permeate flux decreases at applied pressure higher than 4 bar. The compaction behaviour of the MPF-50 is in agreement with the data already reported in literature [2, 24] although these references reported the permeation data at higher pressures compared to the present study.

Table 4 presents the oil retention of the M7-30 PAN/PDMS tailor-made membranes, GKSS and MPF-50 for a 8 % (w/w) oil/hexane feed solution at 7 bar. The presented values are under steady state condition (permeation time up to 120 min).

Table 4: The oil retention for the M7-30, GKSS and MPF-50 membranes. Experimental conditions: feed solution of 8 % (w/w), transmembrane pressure of 7 bar, at 24 ± 3 °C.

Membrane	Oil retention (%)
M7-30	88 ± 3
GKSS	89 ± 3
MPF-50	49 ± 5

For the GKSS and M7-30 membranes, x-intercepts (at $J_{\text{hexane}} = 0$) of around 1 bar are found. For both membranes, this agrees very well with the osmotic pressure difference, $\Delta\pi$, calculated with the van't Hoff equation:

$$\Delta\pi = \frac{R_g T \Delta c}{MW} \quad \text{Equation 11}$$

Δc is the solute concentration difference across the membrane and MW is the solute molecular weight of the solute. In Chapter 3 of this thesis, a systematical investigation of the osmotic phenomena for the PAN/PDMS membrane will be presented.

For the MPF-50 membrane, however, there is a difference between the intercept and the calculated $\Delta\pi$ is found (x-intercept/ $\Delta\pi_{\text{calculate}}$ is 0.2/0.7 bar). This is probably due to the lower membrane retention, around 50 %.

2.5. Conclusions

In this work, tailor-made PAN/PDMS composite membranes are reproducibly prepared and used for the separation of oil/hexane solutions. A composite membrane with good quality of the PDMS top layer was obtained when the 7 % (w/w) PDMS/hexane coating solution was applied. The prepared membranes are stable under the testing conditions and no membrane compaction occurs under the applied pressure range. The results show that the PAN/PDMS composite membrane presents good permeation performance, high hexane permeability (around $3.1 \text{ lm}^2\text{h}^{-1}\text{bar}^{-1}$) and good oil retention (about 90%). The performance of the PAN/PDMS composite is compared with the commercially available silicone type membrane, MPF-50 and the silicone membrane supplied by GKSS, Germany.

2.6. List of symbols

A	Membrane area (m^2)
B	solute permeability coefficient
c_f	Concentration in the feed side (% w/w)
c_p	Concentration in the permeate side (% w/w)
d_{50}	Mean pore size (nm)
$D_{i,k,g}$	Diffusion coefficient
J	Flux through membrane
K	Partition coefficient
l	Membrane thickness (μm)
MW	Molecular weight (g/mol)
$MWCO$	Molecular weight cut off (Da)
n	Number of pores
Δp	Transmembrane pressure (bar)
P	Permeability through the membrane
R	Membrane retention

r_p	Pore radius (m)
R_g	Gas constant ($\text{J mol}^{-1}\text{K}^{-1}$)
t	Time (h)
T	Temperature (K)

Greek symbols

$\alpha_{\text{CO}_2/\text{N}_2}$	Gas selectivity of membrane for CO_2 over N_2
η	Viscosity (cSt)
$\Delta\pi$	Osmotic pressure (bar)
τ	Membrane tortuosity (-)
v	Molar volume (lmol^{-1})

2.7. References

1. K. Ebert, F. P. Cuperus, Solvent resistant nanofiltration membranes in edible oil processing, *Membrane Technology* 107 (1999) p5-8.
2. C.M. Raman LP, N. Rajagopalan, Deacidification of soybean oil by membrane technology, *Journal of American Oil Chemical Society* 73 (1996) p219-224.
3. R. Subramanian, M. Nakajima, T. Kawakatsu, Processing of vegetable oils using polymeric composite membranes, *Journal of Food Engineering* 38 (1998) p41-56.
4. K.K. Reddy, R. Subramanian, T. Kawakatsu, Decolorization of vegetable oils by membrane processing, *European Food Research Technology* 213 (2001) p212-218.
5. D. Bhanushali, S. Kloos, D. Bhattacharyya, Solute transport in solvent-resistant nanofiltration membranes for non-aqueous systems: experimental results and the role of solute-solvent coupling, *Journal of Membrane Science* 208 (2002) p 343-359.
6. N. Scharnagl, H. Buschatz, Polyacrylonitrile (PAN) membranes for ultra- and microfiltration, *Desalination* 139 (2001) p191-198.
7. S.J. Clarson, J.A. Semlyen, *Siloxane Polymers*, PTR Prentice Hall, New Jersey, 1993.
8. J.M. Ziegler, F.W.G. Fearon, *Silicon-based polymer science: a comprehensive resource*, American Chemical Society, Washington DC, 1990.
9. M. Mulder, *Basic principles of membrane technology*, second edition, Kluwer Academic Publishers, Dordrecht, The Netherlands, 1997.
10. J. M. S. Henis, M. K. Tripodi, Composite hollow fiber membranes for gas separation: the resistance model approach, *Journal of Membrane Science* 8 (1981) p233-246.
11. M. Rezac, W. Koros, Preparation of polymer-ceramic composite membranes with thin defect-free separating layers, *Journal of Applied Polymer Science* 46 (1992) p1927-1938.
12. N. Amouroux, L. Léger, Effect of dangling chains on adhesion hysteresis of silicone elastomers, probed by JKR test, *Langmuir* 19 (2003) p1396-1401.

13. T. R. E. Simpson, B. Parbhoo, J. L. Keddie, The dependence of the rate of crosslinking in poly(dimethyl siloxane) on the thickness of coatings, *Polymer* 44 (2003) p4829-4838.
14. L. Germic, K. Ebert, R. Bouma, Z. Borneman, M. Mulder, H. Strathmann, Characterization of polyacrylonitrile ultrafiltration membranes, *Journal of Membrane Science* 132 (1997) p131-145.
15. H. Lonsdale, U. Merten, R. Riley, Transport of cellulose acetate osmotic membranes, *Journal of Applied Polymer Science* 9 (1965) p1341.
16. J.G. Wijmans, and R.W. Baker, The solution-diffusion model: a review, *Journal of Membrane Science* 107 (1995) p1-21.
17. J. Brandrup, E.H. Immergut, *Polymer Handbook*, J. Wiley&Sons, second edition, 1975.
18. D.R. Machado, D. Hasson, R. Semiat, Effect of solvent properties on permeate flow through nanofiltration membranes. Part I: investigation of parameters affecting solvent flux, *Journal of Membrane Science* 163 (1999) p93-102.
19. I.F.J. Vankelecom, K. De Smet, L.E.M. Gevers, A. Livingston, D. Nair, S. Aerts, S. Kuypers, P.A. Jacobs, Physico-chemical interpretation of the SRNF transport mechanism for solvents through dense silicone membranes, *Journal of Membrane Science* 231 (2004) p99-108.
20. M. Schmidt, K.-V. Peinemann, N. Scharnagl, K. Friese, R. Schubert, Patent DE 19507584 C2, 1995.
21. J.P. Robinson, E.S. Tarleton, C.R. Millington, A. Nijmeijer, Solvent flux through dense polymeric nanofiltration membranes, *Journal of Membrane Science* 230 (2004) p29-37.
22. X.J. Yang, A.G. Livingston, L.F.d. Santos, Experimental observations of nanofiltration with organic solvents, *Journal of Membrane Science* 190 (2001) p45-55.
23. D. Bhanushali, S. Kloos, C. Kurth, D. Bhattacharyya, Performance of solvent-resistant membranes for non-aqueous systems: solvent permeation results and modeling, *Journal of Membrane Science* 189 (2001) p1-21.
24. J.A. Whu, B.C. Baltzis, K.K. Sirkar, Nanofiltration studies of larger organic microsolute in methanol solutions, *Journal of Membrane Science* 170 (2000) p159-172.

Appendix I

Effect of stirring rate on the membrane performance

Figure I.1 presents the effect of the stirring rate (range 130-1400 rpm) on the permeate flux and membrane retention, for the M7-30 composite and 8 % (w/w) oil/hexane feed solution.

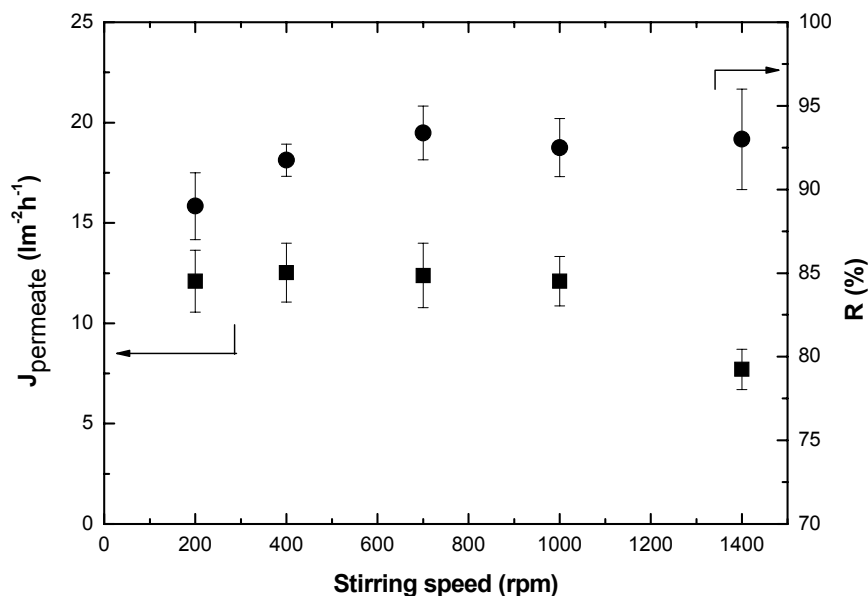


Figure I.1: The permeate flux and membrane retention for the feed solution of 8 % (w/w) oil/hexane. Experimental conditions: 7 bar, 24 ± 3 °C.

The permeate flux is constant for stirring rate up to 700 rpm, however, decreases at higher stirring rates. This phenomenon is reversible and reproducible at various feed concentrations (8 – 30 % (w/w)) and by using different solutes (sunflower oil and polyisobutylene of different MW). Similar behaviour was observed for the commercial MPF-50 membrane using the same feed solutions.

It is well known that the turbulence produced by stirring may have a large effect on the permeate flux through the membrane [I.1]. Agitation and mixing of the solution near the membrane surface could sweep away the accumulated solute, decreasing the thickness of the polarization boundary layer, thus increasing the permeate flow through the membrane. In the present case, however, we observe the opposite: the total transport through the membrane decreases with the increase of the stirring rate.

The triglycerides constitute over 95% of crude vegetables oil; the remaining components include phospholipids, free fatty acids, pigments, sterols, carbohydrates, and proteins. It has been already reported that the phospholipids can form reverse micelles in hexane [I.2]. Therefore, one reason for the decrease of membrane permeability could be the micelle formation induced by the high shear due to vigorous stirring. If that was the case, we would then expect to find an increase in oil retention and changes in the feed concentration due to the deposit of micelles. However, we did not observe any of these phenomena. Most likely, the flux decline at stirring rates higher than 700 rpm is due to the vortex created in the cell, which was visualized in a transparent stirred cell of comparable size and stirrer position with the stainless steel cell – see *Figure I.2*.

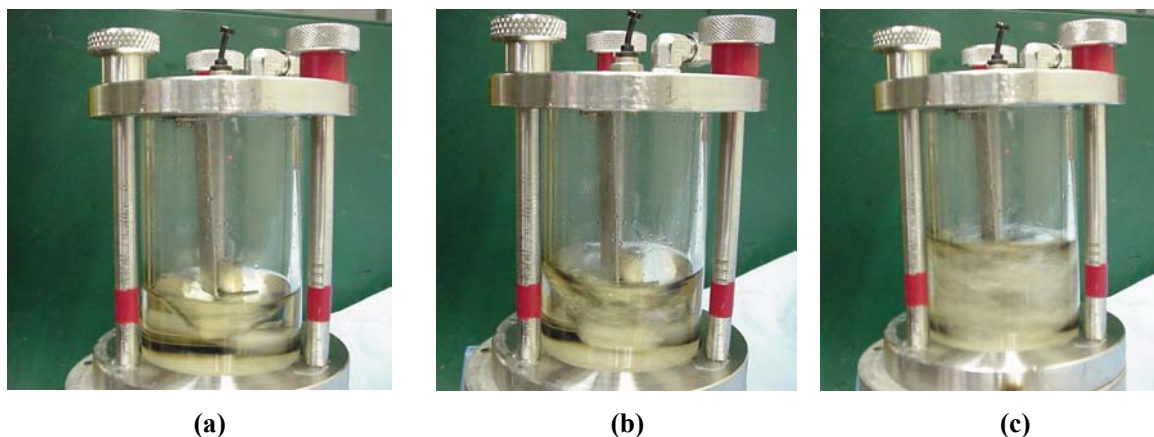


Figure I.2: Visualization of the vortex due to the stirring rate: (a) 300 rpm, (b) 700 rpm (c) 1400 rpm.

At low stirring rates, for the cell with an axial mounted stirrer, the liquid is set in motion, and generates a liquid vortex. At high stirring rates the vortex may reach the stirrer head and gas entrains the liquid [I.3]. The stirrer then partly rotates in gas and therefore the liquid transport is not very effective and the flow through membrane decreases. Based on the above finding, we decided to perform all further permeation experiments at 700 rpm.

References

- I.1.M. H. V. Mulder, Basic Principles of Membrane Technology, second edition, Kluwer Academic Publishers, Dordrecht, 1997
- I.2.L. Lin, K. C. Rhee, S. S. Koseoglu, Bench-scale membrane degumming of crude vegetable oil: process optimisation, Journal of Membrane Science 134 (1997) p101-108.
- I.3. M. Zlokarnik, Stirring-theory and practice, Wiley-VCH Verlag GmbH, 2001

Appendix II

Influence of the PDMS thickness on the membrane performance

In order to check the influence of the PDMS thickness on the membrane performance, we applied more coating steps with a 7% (w/w) pre-cross-linked PDMS/hexane solution onto PAN. In this way, various PDMS thicknesses are obtained by applying a new PDMS layer on the existing one (after each coating step, the thermal treatment in a N₂ oven at 65 °C, 4 h was applied). The prepared PAN/PDMS membranes are defect-free, showing a CO₂/N₂ selectivity of about 10, close to the intrinsic selectivity of PDMS.

Figure II.1 shows typical SEM images of the cross-section of the prepared PAN/PDMS membranes with various PDMS thicknesses.

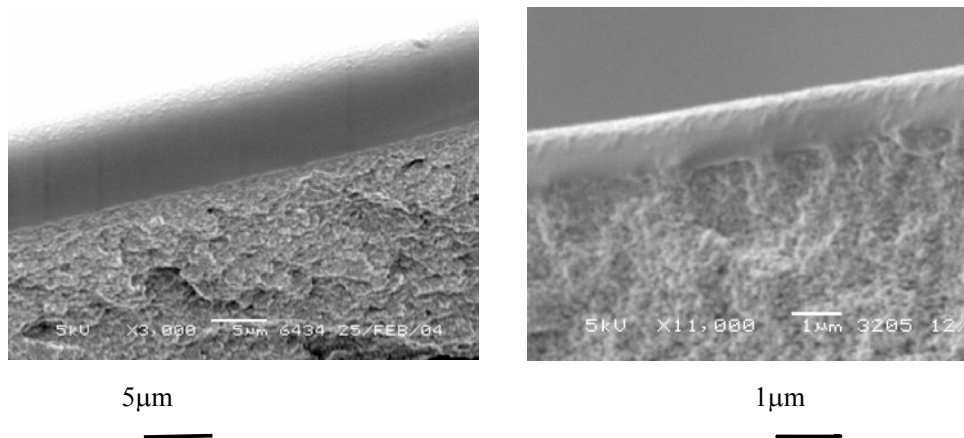


Figure II.1: Typical examples of the SEM images of cross-section of the prepared PAN/PDMS membranes with thicknesses of about: (a) 7 μm and (b) 1 μm.

The PDMS thickness visualized by SEM increases with the number of coating layers, as expected. The PDMS effective thickness was measured from the pure CO₂ permeation experiments, following the procedure described in [II.1]. *Table II.1* summarizes the results for the effective and visualized PDMS thickness.

Table II.1: Effective and visualized PDMS thickness of the PAN/PDMS membranes prepared by various coating steps (coating solution of 7 % w/w PDMS hexane).

Coating steps	$l_{\text{eff}}(\text{CO}_2)$ (μm)	l_{SEM} (μm)
1	2.0 ± 0.2	0.9 ± 0.2
3	3.2 ± 0.3	1.9 ± 0.4
6	8.2 ± 0.4	7.0 ± 1.4

For all the membranes, it seems that the pore intrusion is similar (about $1\mu\text{m}$), as given from the difference between effective and visualized PDMS thickness.

Figure II.2 shows the effect of PDMS thickness on the hexane flux through PAN/PDMS composite membranes, at various transmembrane pressures.

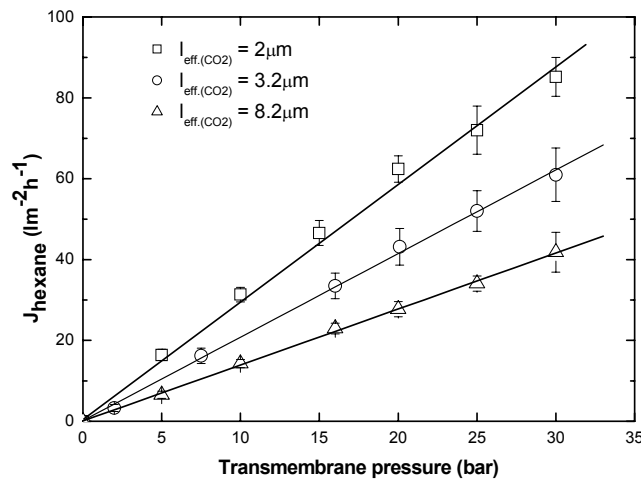


Figure II.2: Hexane flux as a function of transmembrane pressure through PAN/PDMS of various thicknesses, at $24 \pm 3^\circ\text{C}$.

The hexane flux increases linearly with the applied pressure in all cases, indicating that no membrane compaction occurs over the applied pressure range. The hexane flux through PAN/PDMS composite membranes decreases with the increase of the PDMS thickness as expected from the solution-diffusion model discussed in detail earlier (Equation 6 b).

For the PAN/PDMS composite membrane, however, it is difficult to identify the “real” membrane thickness corresponding to l of Equation 6 b. Table II.2 presents an attempt to normalize the hexane permeability (P_{hexane}) through the PAN/PDMS composite membranes with the PDMS thickness.

Table II.2: Normalized hexane permeability for various PDMS thicknesses.

P_{hexane} ($\text{lm}^{-2}\text{h}^{-1}\text{bar}^{-1}$)	$P_{\text{hexane}} \times l_{\text{eff.CO}_2}$ ($\text{lm}^{-2}\text{h}^{-1}\text{bar}^{-1}\mu\text{m}$)	$P_{\text{hexane}} \times l_{\text{SEM}}$ ($\text{lm}^{-2}\text{h}^{-1}\text{bar}^{-1}\mu\text{m}$)
3.0 ± 0.3	6.0 ± 0.5	2.7 ± 0.4
2.0 ± 0.2	6.4 ± 0.6	3.8 ± 0.8
1.4 ± 0.1	11.5 ± 0.8	9.8 ± 1.3

Neither the normalization by the $l_{\text{eff.CO}_2}$ nor by the l_{SEM} gives a constant value for the membranes of various thicknesses. The PDMS swells significantly in hexane, therefore the thickness in the wet state would be different than the PDMS thickness determined in the dry state by gas permeation and SEM. In addition, swelling of the PDMS would be different within the pores (restricted swelling by the pore walls) than when it is on top of the support, exhibiting different mass resistances for the hexane transport. The difference in swelling between the PDMS inside the pores and on the top of the support would probably differ for membranes with thicker top layer.

Figure II.3 shows the effect of the transmembrane pressure on the hexane flux for various PDMS thicknesses, at 8 % w/w oil/hexane solution.

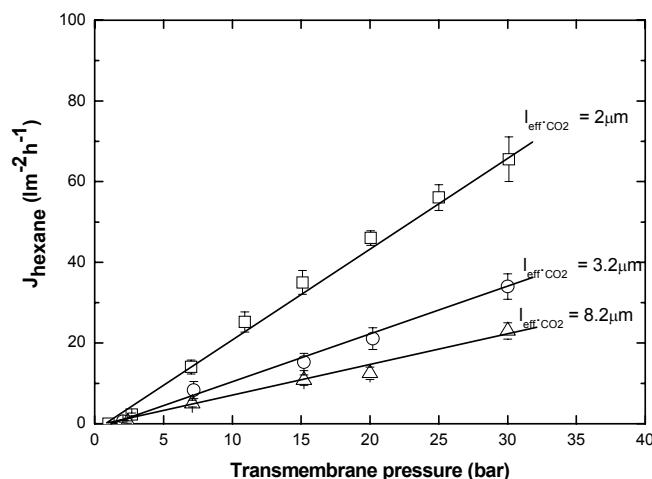


Figure II.3: Hexane flux as a function of transmembrane pressure through PAN/PDMS membranes of various effective thicknesses. Experimental conditions: 8% w/w oil/hexane feed, at 24 ± 3 °C.

The hexane permeability coefficient for each effective thickness (calculated from the slopes of the graphs in *Figure II.3*) decreases with the increase of PDMS thickness. Again the normalized P-values with the $l_{eff.CO_2}$ or the l_{SEM} do not give a constant value for the membranes of various thicknesses (see *Table II.3*).

Table II.3: Normalized hexane permeability through PAN/PDMS membranes of various PDMS thicknesses. Experimental conditions: 8% w/w oil/hexane feed, at 24 ± 3 °C.

P_{hexane} ($l m^{-2} h^{-1} bar^{-1}$)	$P_{hexane} \times l_{eff.CO_2}$ ($l m^{-2} h^{-1} bar^{-1} \mu m$)	$P_{hexane} \times l_{SEM}$ ($l m^{-2} h^{-1} bar^{-1} \mu m$)
2.1 ± 0.2	4.2 ± 0.4	1.9 ± 0.2
1.2 ± 0.2	3.8 ± 0.6	2.3 ± 0.3
0.8 ± 0.1	6.6 ± 0.8	5.6 ± 0.7

Figure II.4 presents the oil retention as a function of the transmembrane pressure for various PDMS effective thicknesses, at 8% w/w oil/hexane solution.

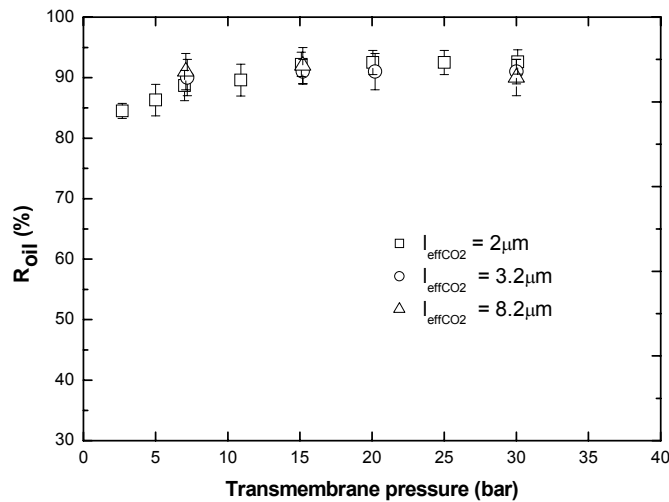


Figure II.4: Oil retention by the PAN/PDMS composite membrane as a function of transmembrane pressure and effective thickness. Experimental conditions: 8 % w/w oil/hexane solution, at 24 ± 3 °C.

In all cases, the oil retention by PAN/PDMS of various PDMS effective thicknesses is similar. Interestingly, it is also similar to the oil retention of GKSS membrane (Chapter 2) even though their hexane permeability is much different. If we consider that the retention of the membrane is given by the ratio of partition coefficients of oil/hexane as well as the ratio of their diffusion coefficients, then it seems that these ratios are constant for the studied systems. This indicates that probably the oil retention is due to its low diffusion coefficient in the highly swollen PDMS network. More about the transport mechanism will be discussed in Chapter 3. Vankelecom et al. [II.3] studied the effect of pore intrusion of PDMS within the polysulfone filled zirconium oxide (Zirfon[®]) support for pervaporation of the water-ethanol mixture. The flux through the PDMS/Zirfon[®] composite membrane was found to be dependent on the pore intrusion extend, while the membrane selectivity was similar.

References

- II.1. L. Germic, K. Ebert, R. Bouma, Z. Borneman, M. Mulder, H. Strathmann, Characterization of polyacrylonitrile ultrafiltration membranes, *Journal of Membrane Science* 132 (1997) p131-145.
- II.2. S. Koike, S. R., N. H., N. M., Separation of oil constituents in organic solvents using polymeric membranes, *Journal of the American Oil Chemists Society* 79 (2002) p937-942.
- II.3. I. F. J. Vankelecom, B. Moermans, G. Verschueren, P. A. Jacobs, Intrusion of PDMS top layers in porous supports, *Journal of Membrane Science* 158 (1999) p289-297.

Insight into the transport of hexane – solute systems through tailor-made composite membranes*

Abstract

This work presents composite membranes comprising poly(acrylonitrile) (PAN) as the support and poly(dimethyl siloxane) (PDMS) as the selective top layer. For sunflower oil/hexane and polyisobutylene (PIB)/hexane, the permeation characteristics of these membranes for various feed concentrations and pressures are studied. For each system, the effect of transmembrane pressure upon the flux and retention of the PAN/PDMS composite membrane is investigated. Osmotic phenomena similar to those of aqueous systems are observed and interpreted using the van't Hoff equation. The hexane flux increases linearly with the applied pressure and the hexane permeability (P_{hexane}) decreases with the increase of the feed concentration. The normalization of P_{hexane} by the apparent viscosity and the membrane swelling indicates that the viscosity may be a measure for the diffusivity of the solvent inside the polymer network and the swelling for the solubility, in the framework of a solution diffusion model. However, the model can not explain the solute-solvent coupling found experimentally. The flux of the solute (oil or PIB) increases linearly with the applied pressure as well, especially at low feed concentrations when the membrane swelling is higher, indicating coupling of solute transport to solvent flux. For the same feed solution concentration, the effect of flux coupling (solvent-induced solute dragging) decreases with the molecular weight of the solute. Ultimately, when the applied pressure increases the increase of hexane flux is much higher than the corresponding solute (oil or PIB) flux resulting to an increase of the membrane retention.

* Parts of this chapter has been published in Journal of Membrane Science 228 (2004), 103-116

3.1. Introduction

Nanofiltration (NF) is the membrane process located between ultrafiltration (UF) and reverse osmosis (RO) with respect to size discrimination. It has the advantage of low operating pressure compared to RO and higher molecule retentions compared to UF. For nanofiltration, research mainly focused on aqueous systems; however, a lot of pharmaceutical and fine chemical conversions as well as extraction applications are carried out in organic, non-aqueous media. Nanofiltration membranes used in organic media are either composite membranes, consisting of an UF support membrane and a thin selective layer of different material [1 - 3], or they are asymmetric membranes prepared from the same material [4].

In the recent years, several papers have been published on the membrane applications in non-aqueous solvent media [5 - 21]. Research focussed on the separation of some particular solvent/solute systems rather than experiments designed to fundamentally understand the influence of individual factors affecting mass transport. In addition, most of the studied membranes were commercial and the exact nature of their selective layer has not been fully revealed. Recently, Bhanushali et al. reviewed the main findings in the field and investigated the permeation of several organic media through various hydrophilic and hydrophobic membranes [5, 6]. They found similarities in the transport mechanisms for the aqueous and non-aqueous systems based on the relative size ratios of solute and solvent; one important conclusion was that coupling of the solute and solvent fluxes could not be neglected. Luthra et al. [10] suggested that the observed flux decline in time for a batch filtration of tetraoctylammonium bromide/toluene systems, through STARMEM 122 membrane could be due to the build up of osmotic pressure, which they estimated to be around 12 bar. Scarpello et al. [11] have reported for the STARMEM™ 122 membranes that the catalyst retention increased with the increase of feed concentration. Zwijnenberg et al. [17], found a constant retention of triglycerides in acetone through the Pebax® composite membrane over the concentration range 0-50 %(w/w) (applied pressure 20 bar). The reason for the constant ratio between acetone and triglyceride remained unexplained. This might be due to the interaction between the hydrophilic membrane in nature and the polar solvent. It is obvious that the parameters affecting the mass transport in organic solvent NF are rather complex. The transport of solvent and solute through the membranes

could be influenced by several factors. To date, the identification and influence of each factor has not been fully sorted out and more thorough and systematic investigations are desired.

In the vegetable oil industry, the oil extraction from different seeds is performed mostly using hexane as the solvent. The hexane recovery by membrane processes is environmentally friendly and safer with respect to health and explosion hazards compared to the evaporation [18]. Up to date, the recovery of solvent and the fractionation of fats and oils by membrane technology have been mainly investigated on the laboratory scale using commercial membrane materials [13, 19 - 21]. However, these materials are relatively expensive and under the experimental conditions have limited stability. In addition, their precise chemical structure and composition is not known and no direct relation between the membrane properties and the transport mechanism can be drawn. In this work, we prepare our own tailor made composite membrane, comprising poly(acrylonitrile) (PAN) as a support and poly(dimethyl siloxane) (PDMS) as the selective top layer. The swelling and the permeation characteristics of these membranes with sunflower oil/hexane and poly(isobutylene) (PIB)/hexane solutions are extensively studied. For both systems, the effect of solute concentration and of the transmembrane pressure upon the flux and retention of the PDMS/PAN composite membrane is investigated. Our work aims to establish a thorough experimental investigation by:

- Preparing reproducible membranes of known composition for the recovery of hexane from oil / hexane and PIB / hexane solutions.
- Identifying and understanding the important parameters, which control the transport mechanism through the composite membrane.

3.2. Theoretical background

According to the solution-diffusion model which was developed by Lonsdale et al [22] and recently revisited by Wijmans and Baker [23], the flux of a species i through the membrane is given by:

$$J_i = \frac{D_i K_i}{\ell} [c_{if} - c_{ip} \exp(\frac{-\nu_i (p_f - p_p)}{R_g T})] \quad \text{Equation 1}$$

where D_i is the diffusion coefficient of i through the membrane, K_i is the partition coefficient, ℓ is the membrane thickness, c_{if} , c_{ip} is the feed and permeate concentrations of species i , respectively, ν_i is the partial molar volume of species i , p_f , p_p is the feed and permeate sides pressures, respectively, R_g is the gas constant and T is the temperature. The primary assumption made in the model is that the flux of the solute and solvent are independent. For the case of the pure solvent and by incorporation of the osmotic pressure, *Equation 1* becomes:

$$J_i = \frac{D_i K_i c_{if}}{\ell} [1 - \exp(\frac{-\nu_i (\Delta p - \Delta \pi)}{R_g T})] \quad \text{Equation 2}$$

where Δp and $\Delta \pi$ is the difference in applied and osmotic pressure across the membrane, respectively. When the exponential term is small (low pressure range and low molar volume) then *Equation 2* can be written to a very good approximation as:

$$J_i = \frac{D_i K_i c_{if} \nu_i}{\ell R_g T} (\Delta p - \Delta \pi) \quad \text{Equation 3a}$$

or

$$J_i = P(\Delta p - \Delta \pi) \quad \text{Equation 3b}$$

where P is a constant equal to the term $\frac{D_i K_i c_{if} \nu_i}{\ell R_g T}$ and is called solvent permeability.

Similarly, the flux of the solute j is:

$$J_j = \frac{D_j K_j}{\ell} [c_{jf} - c_{jp} \exp(\frac{-\nu_j (p_f - p_p)}{R_g T})] \quad \text{Equation 4}$$

If the term $\frac{-v_j(p_f - p_p)}{R_g T}$ is small (low pressure range and low molar volume), the exponential term is close to 1 and *Equation 4* becomes:

$$J_j = \frac{D_j K_j}{\ell} (c_{if} - c_{jp}) \quad \text{Equation 5a}$$

or

$$J_j = B(c_{if} - c_{jp}) \quad \text{Equation 5b}$$

where B is usually constant and is called the solute permeability. *Equation 3b* indicates a linear increase of flux with the transmembrane pressure difference, whereas the solute flux (*Equation 5b*) remains unaffected by the pressure difference.

3.3. Experimental

3.3.1. Materials

The PAN support membranes with MWCO of 30 and 50 kDa were provided by GKSS - Germany. The membranes were delivered in dry state and used without further treatment (their specifications, given by the manufacturer, are presented in Chapter 2). The selective top layer of the composite was PDMS (RTV 615 type, kindly supplied by General Electric, The Netherlands). The silicone kit was a two-component system, consisting of a vinyl-terminated pre-polymer with high molecular weight (RTV A) and a cross-linker containing several hydride groups on shorter polydimethylsiloxane chains (RTV B). The curing of the PDMS-membrane occurs via Pt-catalysed hydrosilylation reaction to form a densely cross-linked polymer network.

The n-hexane (Merck, The Netherlands) and the sunflower oil (Fluka, The Netherlands) were used as supplied, without further purification. The refined sunflower oil (purchased from Fluka – The Netherlands) consisted of a mixture of triglycerides (mostly C₁₈ with traces of C₁₆-C₂₀ fatty acids), of molecular weight of

around 900. Linoleic acid was the major component of unsaturated chains. The polyisobutylenes (PIB), Glissopal® of MW 550, 1000, 1300, and 2300 were kindly provided by BASF - Germany and of MW 350, by Janex S.A. – Switzerland.

3.3.2. Membrane preparation

The PAN/PDMS composite membranes were prepared in a two-step coating procedure:

1. Dip coating of the PAN support membrane in a 1 % (w/w) PDMS/hexane solution and placing in a N₂ oven at 65 °C for 4 h.
2. Dip coating of the membranes with 5 or 7 % (w/w) pre-cross-linked PDMS/hexane solutions (the solutions were pre-cross-linked at 60°C for 3 h, under stirring). The composites were first dried in air at 20 ± 2°C, for about 10 min and then placed in a N₂ oven at 65 °C for 4 h to complete the cross-linking.

The membrane composite is coded Mx-y, where x is the concentration of the second coating solution (5 or 7 %w/w) and y is the MWCO value of the PAN support (30 or 50 kDa). The quality of the coating of the composite membranes was evaluated by performing pure gas permeation measurements with N₂ and CO₂, using the set-up and procedure described in [24]. The gas fluxes through the prepared membrane were measured with a soap-bubble meter (feed pressure in the range of 1 - 2.5 bar and permeate pressure of 1 bar). The selectivity of CO₂/N₂ (α_{CO_2/N_2}) of the composite membranes was calculated by:

$$\alpha_{CO_2/N_2} = \frac{\left(\frac{P_g}{\ell}\right)_{CO_2}}{\left(\frac{P_g}{\ell}\right)_{N_2}} \quad \text{Equation 6}$$

where P_g is the gas permeability. A defect-free composite membrane should have selectivity close to the intrinsic selectivity of the PDMS membrane, $\alpha_{CO_2/N_2} = 11.6$.

The morphology of the composite membranes was visualised by Scanning Electron Microscopy (SEM, Microscope Jeol JSM-5600LV, at 15 kV). The samples were broken in liquid N₂ and sputtered with gold under vacuum for 300 s, at a current of 15 mA.

3.3.3. Permeation set-up and procedure

All the permeation experiments were performed in a dead-end filtration set-up described in Chapter 2, following the protocol described there. The flux through the membrane was calculated by the following equation:

$$J = \frac{V}{A \times t} \quad \text{Equation 7}$$

where J is the permeate flux (in $\text{lm}^{-2}\text{h}^{-1}$), V is the permeate volume (in l), A is the membrane area (in m^2), t is the permeation time (in h). The permeate volume was calculated by dividing the collected weight (determined by an electronic balance, Mettler PM 460 Mettler Toledo, The Netherlands) to the permeate density (measured by a Digital Density Meter, model DMA 50). After each measurement, the system was slowly depressurized, the permeate was collected and analyzed and then returned to the feed reservoir. The sunflower oil or PIB concentration in the feed and the permeate solutions was analyzed by refractive index measurements at 25 °C using a Abbe-3 refractometre, from Carl Zeiss, Germany. The sunflower oil or PIB retention was calculated using the equation:

$$R = \left(1 - \frac{c_{jp}}{c_{jf}} \right) \times 100 \quad \text{Equation 8}$$

For each permeation experiment, new membrane was used and the experiment was performed at least in triplicate. Values and error bars reported in the *Tables* and *Figures* are based on three different membranes.

3.3.4. Swelling experiments

For the swelling experiments, free-standing thick PDMS films were used. They were prepared from 75 %(w/w) PDMS/hexane solution at room temperature by mixing the RTV A and RTV B components in 10:1 ratio. The membranes were cast on a Teflon plate and the cross-linking was completed at 65 °C for 4 h in N₂ atmosphere. The thickness of the dense dry PDMS membranes was 160 ± 30 μm. For the swelling measurements, the pre-weighed dry dense PDMS membranes (M_{dry}) were immersed in pure hexane or sunflower oil/hexane, PIB/hexane solutions. At different time intervals, the swollen samples were removed from the solution, the liquid excess was wiped and they were weighed again (M_{wet}). This process was continued until no further weight increase of the membrane was observed (equilibrium swelling). Each weighing was completed in 30 s to minimize evaporation of hexane from the samples. The swelling degree (SD) of the dense PDMS membrane was calculated by:

$$SD(\%) = \left(\frac{M_{wet} - M_{dry}}{M_{dry}} \right) \times 100 \quad \text{Equation 9}$$

In the end of the swelling experiments, the samples were removed from the liquid solutions and dried. From the difference between the initial and final dry weight, the concentration of the solute (oil or PIB) in the membrane was measured and the solute partition coefficient K_j was calculated by:

$$K_j = \frac{c_{j,membrane}}{c_{j,f}} \quad \text{Equation 10}$$

3.4. Results and discussion

3.4.1. Characterization of the PAN/PDMS composite membranes

For the M5-30 and M5-50 composite membranes, the gas selectivity, α_{CO_2/N_2} , is found to be 8.8 ± 2.5 and 6.5 ± 2.5 , respectively. These values are much lower than the PDMS intrinsic selectivity ($\alpha_{CO_2/N_2} = 11.6$), indicating that probably, due to the low viscosity of the 5%(w/w) PDMS solution, the coating layer has defects (see Chapter 2). This effect seems to be more pronounced for the PAN with the higher MWCO of 50 kDa. However, for the composite membranes prepared with 7%(w/w) PDMS/hexane coating solution, the quality of the top-layer is better. Their gas selectivity, α_{CO_2/N_2} , is found to be 9.5 ± 2.0 and independent of the MWCO of the PAN support. From the gas permeation experiments and following the procedure described in [24], the effective thickness of the selective layer is found to be in the range 1.7 - 2.2 μm . From the SEM pictures, a PDMS dense layer of approximately 1 μm is observed on top of the PAN support (see a typical example for the M7-30 membrane in *Figure 1*).

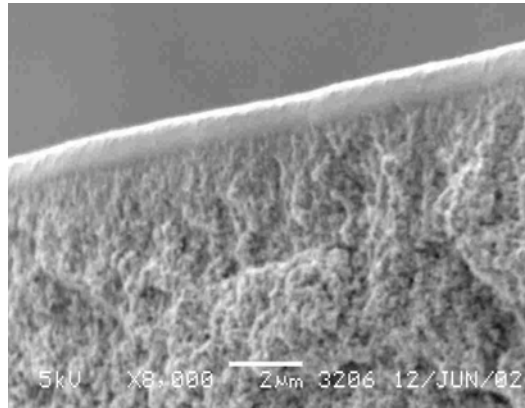


Figure 1: SEM picture of the cross section of the M7-30, PAN/PDMS composite membrane.

In between the support and the dense top layer exists an intermediate layer where the PDMS seems to penetrate into the pores of the support. This pore intrusion might have a positive role. It perhaps provides better anchoring of the selective layer to the

support, preventing delamination even when the PDMS is highly swollen (see later permeation results). Based on the results of the gas permeation experiments, the M7-30 and M7-50 were selected for further permeation measurements.

3.4.2. Swelling measurements

Figure 2 presents typical results of the swelling experiments of dense PDMS membranes in various sunflower oil/hexane and PIB/hexane solutions.

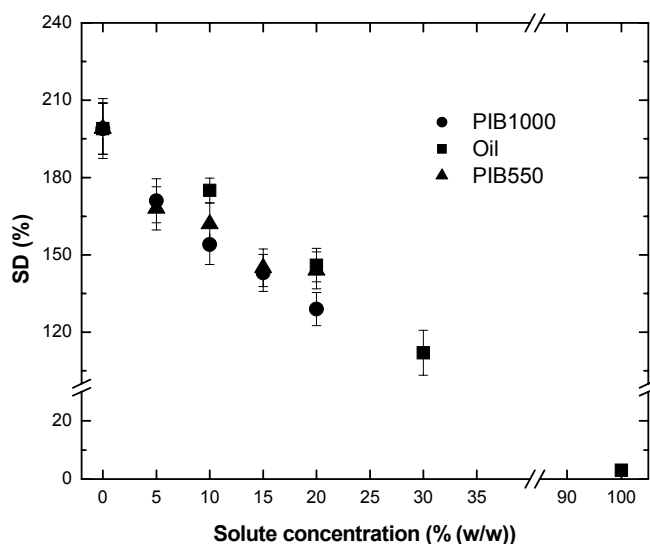


Figure 2: Typical results of the effect of the solution concentration upon the swelling degree of PDMS dense membranes, for various solute/hexane systems.

The swelling of PDMS in pure hexane is high, as should be expected from their comparable solubility parameters (see Table I).

Table 1: Solubility parameters, δ , and molar volumes, ν , of PDMS, hexane, sunflower oil, and PIB.

	PDMS	n-Hexane	Oil	PIB
δ (MPa ^{1/2})	14.9-15.6 ^a	14.9 ^a	16.0 ^b	15.9 - 16.7 ^a
ν (cm ³ /mol)	-	132	980	407-2556 ^c

^a Data from [25]

^b Calculated with group contribution, considering trilinoleate as main component of the oil [26]

^c Molar volume: molecular weight/density; data from Janex S. A. - Switzerland and BASF- Germany.

However, despite the similar solubility parameters of PDMS and sunflower oil (14.9-15.6 MPa^{1/2} and 16 MPa^{1/2}, respectively [25, 26]), the membrane swelling decreases with the increase of oil or PIB concentration and becomes very low (SD = 5%) for 100 (w/w) oil.

According to the Flory - Huggins solution theory, the equilibrium volume fraction of the penetrant, $\phi_{pen.}$, can be related to the activity of the penetrant, $a_{pen.}$, by the following expression [27]:

$$\ln a_{pen.} = \ln \phi_{pen.} + (1 - \phi_{pen.}) \left(1 - \frac{\nu_{pen.}}{\nu_{PDMS}}\right) + \chi (1 - \phi_{pen.})^2 \quad \text{Equation 11}$$

where χ is the PDMS - penetrant interaction parameter. The ratio of penetrant to PDMS molar volumes ($\nu_{pen.} / \nu_{PDMS}$) is assumed negligible. From the results of the swelling experiments for pure hexane and oil ($a_{pen.}=1$) and by using *Equation 11* assuming volume additivity upon mixing, the interaction parameters between PDMS-hexane and PDMS-oil are found to be $\chi_{PDMS-hexane} = 0.58 \pm 0.03$ and $\chi_{PDMS-oil} = 2.11 \pm 0.02$, respectively. The χ value of 2.11 (0.58) for the PDMS-oil (PDMS-hexane) system is high (low) showing small (high) interaction between them. This

indicates that the sorption of hexane in PDMS is thermodynamically more favorable than of oil in PDMS. The interaction parameter is expected to obey the relation [28]:

$$\chi = \chi_S + \chi_H = \chi_S + [\nu_{pen}(\delta_{pen} - \delta_{PDMS})^2/RT] \quad \text{Equation 12}$$

where χ_S, χ_H are the entropic and the enthalpic contributions to χ , respectively and $\delta_{pen}, \delta_{PDMS}$ are the solubility parameters of penetrant and PDMS, respectively. From *Equation 12*, using the results of $\chi_{PDMS\text{-hexane}} = 0.59$ and $\chi_{PDMS\text{-oil}} = 2.11$ in conjunction with the values of $\delta_{PDMS} = 15.2 \text{ MPa}^{1/2}$ [25], $\delta_{\text{hexane}} = 14.9 \text{ MPa}^{1/2}$ [25], $\delta_{\text{oil}} = 16 \text{ MPa}^{1/2}$ [26] and $\nu_{\text{hexane}} = 132 \text{ cm}^3/\text{mol}$, $\nu_{\text{oil}} = 980 \text{ cm}^3/\text{mol}$ (see *Table 2*), the entropic contribution χ_S is derived at 20°C (293°K): $\chi_S(\text{PDMS-hexane}) = 0.55$ and $\chi_S(\text{PDMS-oil}) = 1.85$. The value calculated for the PDMS-hexane is rather close to the value of 0.45 suggested for PDMS [28]. The value for the PDMS-oil however, is high. It is important to note that the χ parameter gives a qualitative estimation of the interactions between the polymer and the penetrant. The *Equations 11, 12* can generally describe quite well the sorption of good solvents (like hexane) in PDMS using χ as adjustable parameter. For poor solvents (like oil or PIB), they lead to large discrepancies suggesting the need for more sophisticated expressions.

In the concentration range 0 – 30 %(w/w), the swelling degree of the dense membrane does not change significantly with molecular weight of the solute (*Figure 2*). In this range, the solute size might not be of importance. Even though the used solutes are relatively large molecules, they might be small in comparison with the mesh size of the silicone network formed by the high swelling in hexane.

Table 2 presents the concentration of oil and PIB in the swollen dense PDMS membranes and the partition coefficients calculated by *Equation 10*.

Table 2: Concentration inside the membrane and solute partition coefficient for the dense PDMS membrane (22 °C).

Solute	Solute MW (gmol ⁻¹)	Feed concentration % (w/w)	c _{membrane} (% (w/w))	K _{solute} (-)
Oil	900	8	4.7 ± 0.3	0.59
		19	8.1 ± 0.6	0.43
		30	12.4 ± 1.3	0.41
PIB	350	8	7.0 ± 0.9	0.88
PIB	550	8	5.6 ± 0.9	0.70
PIB	1000	8	4.4 ± 0.7	0.55
PIB	1300	8	4.2 ± 0.7	0.53
		19	7.7 ± 0.4	0.40
PIB	2300	8	3.9 ± 0.6	0.49
		19	6.4 ± 0.6	0.34

The partition coefficients of the oil and PIB are in the range of 0.34 - 0.88. For the same PIB concentration, the partition of PIB decreases as its MW increases.

In the end of the swelling experiments, when the swollen PDMS samples are rinsed with hexane and dried in the vacuum oven, the weight of the membrane does not differ from its initial dry weight. In addition, for membranes kept for 45 days in pure hexane, the gas selectivity, α_{CO_2/N_2} , is the same as for the freshly prepared membranes (9.5 ± 2.0). Both results prove the stability of the dense PDMS membrane under the studied conditions.

3.4.3. Permeation performance

The filtration performance of the M7-30 and M7-50 composite membranes in oil/hexane and PIB/hexane solutions of concentration between 0 - 30 %(w/w) is

systematically investigated, including the effects of stirring rate, the influence of feed concentration and solute MW, and the effect of the trans-membrane pressure.

Figure 3 shows the effect of the stirring rate on the permeate flux and oil retention, for the 8 %(w/w) oil/hexane solution.

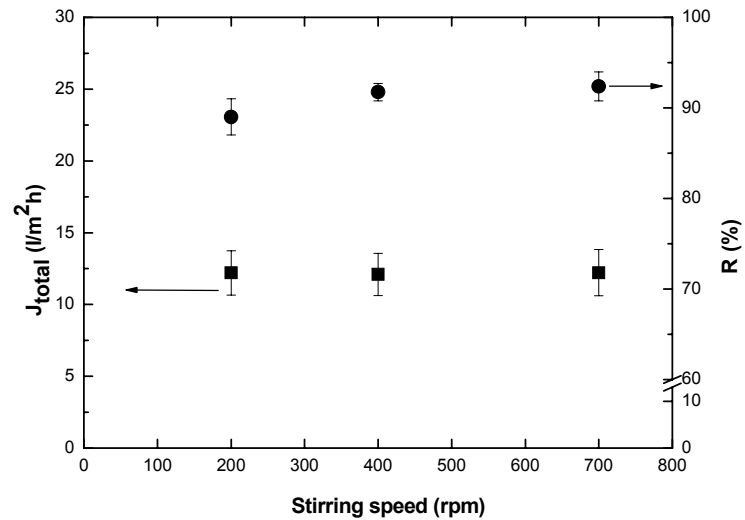


Figure 3: Effect of the stirring speed upon total permeate flux and retention of 8%(w/w) oil/hexane solution, at $\Delta p = 7$ bar and 24 ± 3 °C.

In both cases, no significant changes are observed for stirring rate up to 700 rpm. Similar behavior is found at higher oil/hexane and PIB/hexane concentrations (up to 30 %(w/w)). This might indicate the absence of concentration polarization under the studied conditions or that the mass transfer sub-layer, where the concentration polarization takes place is much smaller than the flow sub-layer so the stirring applied does not influence the concentration polarization. Stirring rates higher than 700 rpm were not applied in order to avoid the vortex described in the Appendix I of Chapter 2. *Figure 4* presents the effect of the operating pressure on the hexane flux for various oil/hexane concentrations.

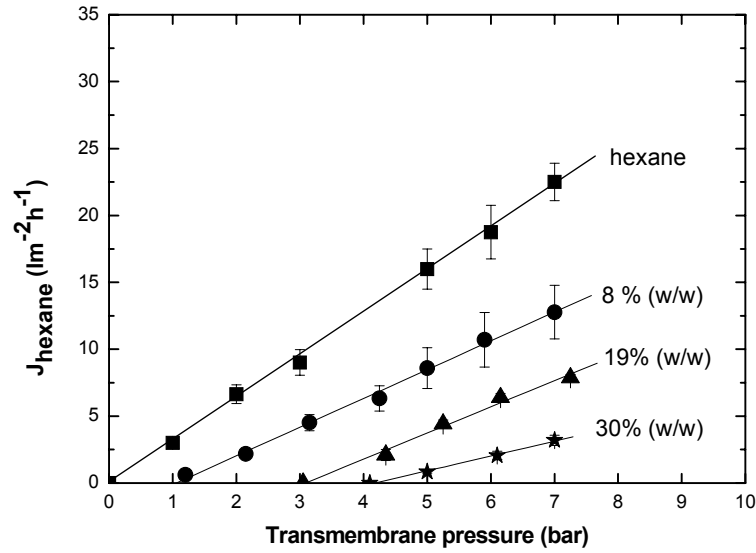


Figure 4: Hexane flux as a function of transmembrane pressure for various oil/hexane feed concentrations.

In all cases, the linearity of flux with the applied pressure indicates that no compaction of the membrane occurs over the applied pressure range. The transport through the membrane can be described by the *Equation 3b*. From the slope of the plot of J_{hexane} versus Δp , the hexane permeability coefficient, P , can be calculated. For the pure hexane, it is found to be $3.1 \pm 0.4 \text{ lm}^{-2}\text{h}^{-1}\text{bar}^{-1}$. For comparison, hexane permeabilities reported by others are: 3 - 4.9 $\text{lm}^{-2}\text{h}^{-1}\text{bar}^{-1}$ for the Pebax[®] composite membranes [3], 1.6 $\text{lm}^{-2}\text{h}^{-1}\text{bar}^{-1}$ for the D membrane from Osmonics [5] and 1.52 $\text{lm}^{-2}\text{h}^{-1}\text{bar}^{-1}$ for the MPF-50 membrane [13]. *Figure 4* allows the quantification of the x -intercepts (at $J_{\text{hexane}} = 0$) for each oil/hexane concentration which can be compared with the osmotic pressures, $\Delta\pi$, calculated using the van't Hoff equation:

$$\Delta\pi = \frac{R_g T \Delta c}{MW}$$

Equation 13

Δc is the solute concentration difference across the membrane (in g/l) and MW is the solute molecular weight. The van't Hoff equation is applicable in our system due to the relative low feed concentrations (0.05-0.21 mol/l). The calculated values of osmotic pressure are in good agreement, within experimental error, with those obtained from x -intercepts (*Table 3*).

Table 3: Comparison between the $\Delta\pi$ calculated by Equation 13 and the x -intercepts of the plots of hexane flux vs Δp for various oil/hexane concentrations (see Figure 6).

Oil conc. (%(w/w))	$\Delta\pi_{\text{calculated}}$ (bar)	x -intercept (bar)
0	0	0
8	1.2 ± 0.1	1
19	2.7 ± 0.2	2.8
30	4.7 ± 0.3	4.3

Similar behaviour is found when using PIB/hexane solutions.

Figure 5 shows the effect of operating pressure on the flux for the 19 %(w/w) PIB/hexane system of various MW, in comparison to the data for oil/hexane mixture.

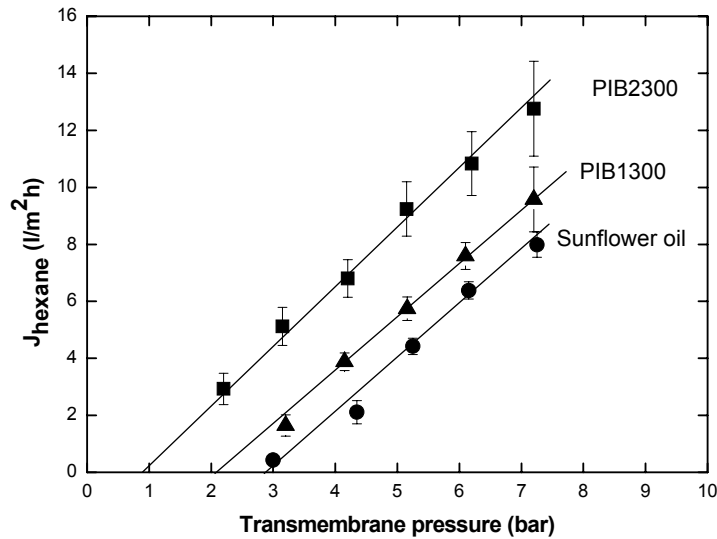


Figure 5: Hexane flux as a function of transmembrane pressure for various solute/hexane systems. Feed concentration: 19 % (w/w).

The x -intercepts are again in very good agreement, within experimental error, with those of $\Delta\pi$ from *Equation 13* (x -intercept/calculated $\Delta\pi$ value: PIB 2300, 0.9 bar/1.2 bar, PIB 1300, 2.1/2.2). In addition, the osmotic pressure difference across the membrane decreases when the MW of the solute increases (see *Figure 5*), as expected from *Equation 13*. The transport characteristics of the investigated systems seem to have great similarities with aqueous systems. Raman et al. [13, 20] have observed osmotic phenomena for oleic acid/methanol using Desal-5 and NTR-759 membranes (concentration range: 0.1 - 0.4 mol/l, Δp up to 25 bar). *Figure 4* and *5* are convincing examples that the organic solvent / solute system, described above behave as ideal systems (comparable to aqueous systems).

The hexane permeability coefficient for each oil/hexane concentration (calculated from the slopes of the graphs in *Figure 4*) decreases with the increase of oil concentration (see *Table 4*).

Table 4: Parameters concerning the transport of oil/hexane solutions through the PAN/PDMS composite membranes.

Oil conc., (%(w/w))	P_{hexane} (l m⁻² h⁻¹ bar⁻¹)	η_{apparent}^a (cSt)	SD/100 (-)	Pη100/SD (l cSt m⁻² h⁻¹ bar⁻¹)
0	3.1 ± 0.4	0.48 ± 0.02	2.0 ± 0.1	0.7 ± 0.1
8	2.4 ± 0.3	0.57 ± 0.01	1.7 ± 0.1	0.8 ± 0.1
19	1.8 ± 0.4	0.63 ± 0.01	1.5 ± 0.1	0.8 ± 0.1
30	1.1 ± 0.3	0.72 ± 0.01	1.2 ± 0.1	0.7 ± 0.1

^a Kinematic viscosity measured at 24 ± 3°C (with Ubbelohde viscometer, from Tamson, The Netherlands).

Similar behavior has also been reported for other systems [17-20]. To identify the parameters affecting the hexane permeability, we normalize it for the viscosity and the swelling degree of the membrane. For the normalization, the value of an apparent viscosity inside the membrane is used. This is estimated from the concentration of solute (oil or PIB) in a hypothetical solvent/solute phase inside the membrane for the dense PDMS membranes (*Table 2*) and the plots of viscosity versus oil/hexane and PIB/hexane concentration at 24 ± 3°C (see *Table 5*).

Table 5: Characteristics of the linear plots of viscosity versus solution concentration [$y = (\text{slope})x + (\text{intercept})$] for various solute/hexane systems.

Solute	Solute MW (gmol^{-1})	Slope (cSt)/% (w/w)	Intercept (cSt)	R ²
Oil	900	0.0178	0.49	0.99
PIB	350	0.0084	0.49	0.98
PIB	550	0.0131	0.49	0.98
PIB	1000	0.0207	0.48	0.98
PIB	1300	0.0275	0.48	0.98
PIB	2300	0.0355	0.47	0.98

For the swelling degree, the results of *Figure 2* concerning the dense PDMS membranes are used. For the various oil/hexane concentrations, the normalized P values do not differ significantly (*Table 4*). It seems that the apparent viscosity inside the membrane and the swelling of the membrane (due to the interaction of PDMS/hexane/solute) are the most critical factors affecting the hexane permeability. A constant value of $P\eta/SD$ (within the experimental error) is also found when comparing the results of PIB / hexane systems using PIB of various MW at various feed concentrations (see *Table 6*).

Table 6: Parameters concerning the transport of PIB / hexane solutions through the PAN/PDMS composite membranes. Experimental conditions: $\Delta p = 7$ bar at 24 ± 3 °C.

Solute	Concentration (% (w/w))	η_{apparent}^a (cSt)	P_{hexane} ($\text{lm}^{-2}\text{h}^{-1}\text{bar}^{-1}$)	SD/100 (-)	$P\eta_{100} / \text{SD}$ ($\text{l cSt m}^{-2}\text{h}^{-1}\text{bar}^{-1}$)
PIB, MW 350	8	0.55 ± 0.06	2.9 ± 0.3	1.8 ± 0.1	0.9 ± 0.2
PIB, MW 550	8	0.56 ± 0.06	2.7 ± 0.3	1.7 ± 0.1	0.9 ± 0.2
PIB, MW 1000	8	0.57 ± 0.06	2.6 ± 0.2	1.6 ± 0.1	0.9 ± 0.2
PIB, MW 1300	8	0.59 ± 0.07	2.7 ± 0.2	1.6 ± 0.1	1.0 ± 0.2
	19	0.69 ± 0.01	1.5 ± 0.3	1.4 ± 0.1	0.7 ± 0.2
PIB, MW 2300	8	0.61 ± 0.08	2.7 ± 0.2	1.7 ± 0.1	1.0 ± 0.2
	19	0.70 ± 0.01	1.6 ± 0.3	1.4 ± 0.1	0.8 ± 0.2

^a Kinematic viscosity measured at 24 ± 3 °C (with Ubbelohde viscometer, from Tamson, The Netherlands).

The effects of viscosity and solute-solvent-membrane interaction have been observed in other systems too [7, 8, 11, 13, 18, 29, 30]. Machado et al. [7], in the study of transport of various solvents through MPF-50 and MPF-60 (silicone type) membranes, found that viscosity and surface tension were major parameters influencing the flux. Scarpello et al. [11] noted that the physico-chemical interactions between solute-solvent and membrane have an important role in the transport of catalysts in tetrahydrofuran/ethyl acetate through STARMEM™ membranes. Raman et al. [13], in the separation of vegetable oils from hexane using various commercial or prototype membranes, reported that due to the high membrane retention, the flux through the membranes decreased due to increase of feed viscosity and the presence of osmotic phenomena. Yang et al. [29] has performed a comprehensive comparison of methanol fluxes through MPF-44, MPF-50 and MPF-60 membranes and concluded that the transport mechanism could not be based solely on viscous flow but also on the interaction between membrane and solvent. Han et al. [30], observed that solute-membrane interaction made a major contribution to the mass transport of hydrophobic compounds, such as toluene through the MPF-50 membrane, suggesting solution

diffusion type mechanism. The effect of swelling on the permeability coefficient is apparent in *Equation 3a*, where the membrane thickness is included. The correction for the “apparent viscosity” is less obvious. In the framework of a solution-diffusion model, we interpret this actually as a measure for the Stokes-Einstein diffusion coefficient.

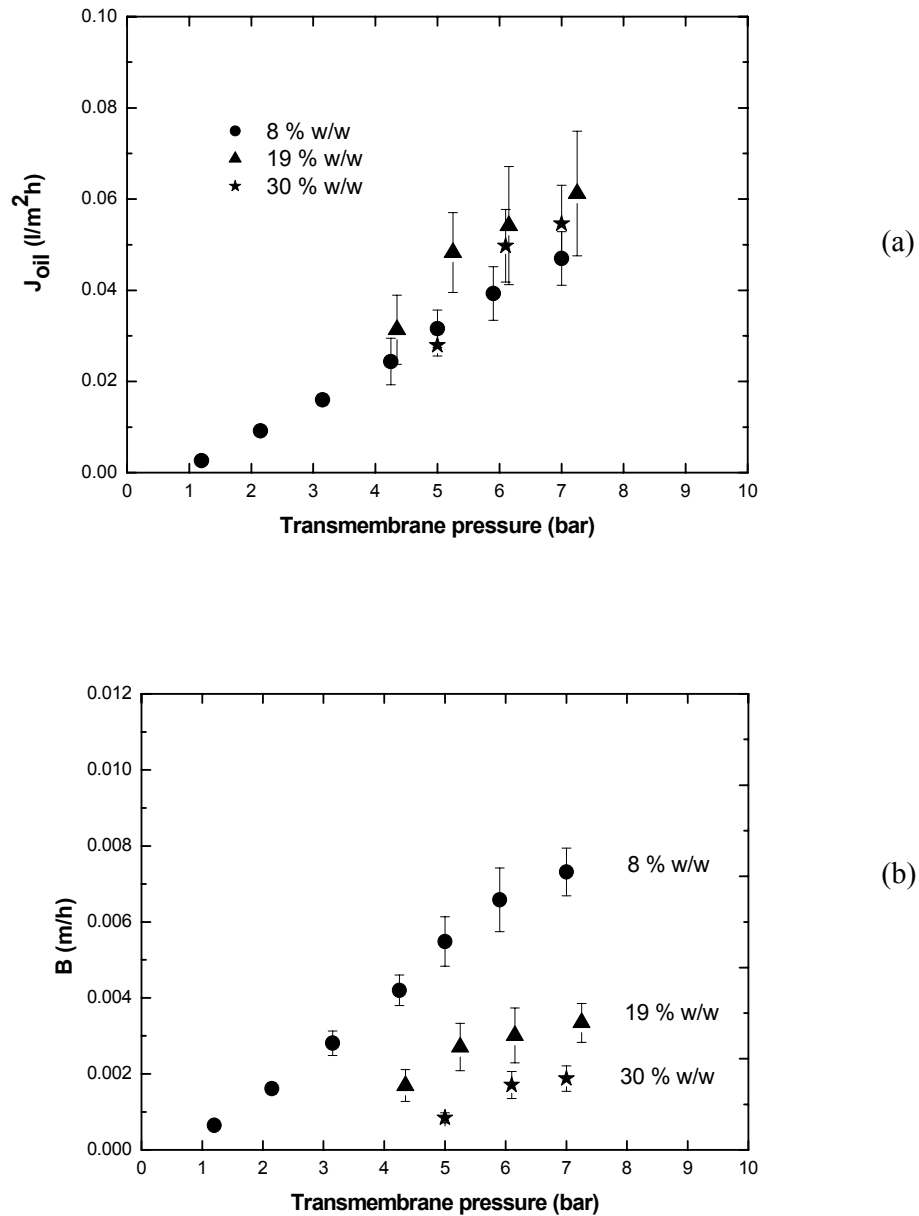


Figure 6: Effect of the transmembrane pressure upon (a) oil flux, J_{oil} and (b) oil permeability coefficient, B , for various oil/hexane concentrations.

Figure 6a depicts the effects of transmembrane pressure on the oil flux at various feed concentrations. Interestingly, the oil flux, J_{oil} , increases with Δp showing that part of the oil transport is related to chemical potential acting on hexane. Apparently, the large hexane flow drags the solute through the swollen network. For 8 % (w/w) oil / hexane solution, the oil permeability, $B = D_{oil}K_{oil} / \ell = J_{oil} / \{[c_{if} - c_{jp} \exp(\frac{-v_j(p_f - p_p)}{R_g T})]\}$, increases significantly with pressure while at higher oil concentrations, the effect is less significant (Figure 6b). Probably, at high oil concentrations where the swelling of the membrane is lower and the “apparent” viscosity inside the membrane is higher (see Table 4), the dragging effect on the oil transport is restricted. Figure 7 shows the effect of the MW of the solute on the solute dragging: for the same solute / hexane solution concentration of 8 %(w/w), the solute flux increases when the MW of the solute decreases.

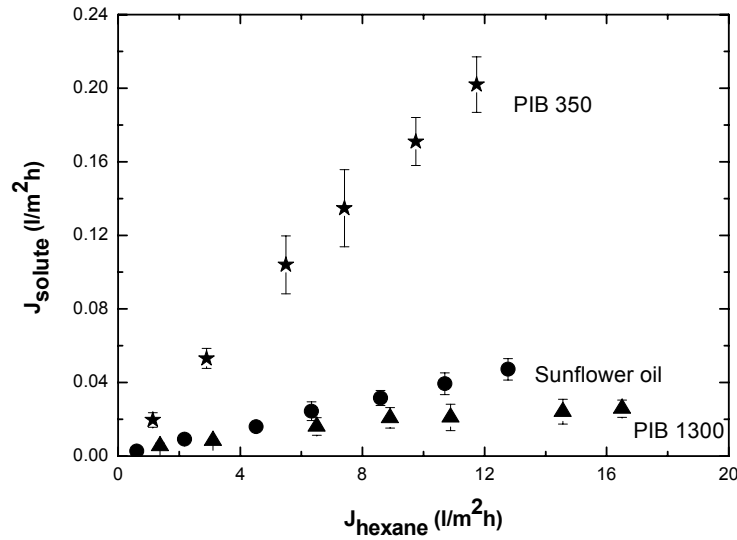


Figure 7: Solute flux as a function of the hexane flux for solutes of various MW. Feed concentration: 8 % (w/w).

Similar behavior is observed at higher solute concentrations, too. In these cases however, the effect of coupling is smaller due to the increase of apparent viscosity and the decrease of the membrane’s swelling (results not shown here). Subramanian et al. [14], studied the transport of oleic acid and triglycerides mixtures through silicone type

composite membranes (NTGS-2200, NittoDenko-Japan). The preferential permeation of oleic acid over triglycerides through the membrane was mainly attributed to the synergistic effect of preferential sorption and concentration dependent solubility as well as diffusivity (according to the solution diffusion model). However, when the operating pressure was increased at constant temperature, the total flux and the relative permeation rates of triglycerides as well as oleic acid increased, showing the significant role of dragging in the transport, in addition to the solution-diffusion.

3.4.4. Retention performance

Figure 8 presents the oil retention as a function of the permeate flux for various sunflower oil / hexane concentrations, in the pressure range of 1 – 7 bar.

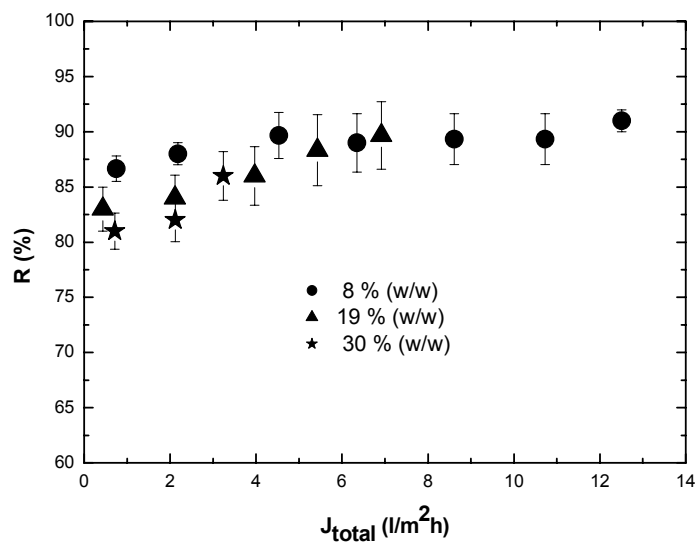


Figure 8: Oil retention by the PAN/PDMS composite membrane as a function of total permeate flux, for various oil/hexane concentrations.

In all cases, the retention increases with permeate flux. As it is shown in *Figures 4* and *6a*, when the pressure increases, the increase of hexane flux is much higher than the relative increase of oil flux leading to increase of retention, at high pressure. At low fluxes, the membrane retention is lower for high oil concentrations probably due to the

decrease of the hexane transport at high oil concentration due to the osmotic phenomena (*Figure 4*). At higher operating pressures, however, when the inherent osmotic pressures are overcome, the hexane flux increases and higher retention is observed.

Figure 9 presents a typical result of the retention of the M7-30 composite membrane for 8 % (w/w) PIB/hexane solutions for transmembrane pressure of 7 bar.

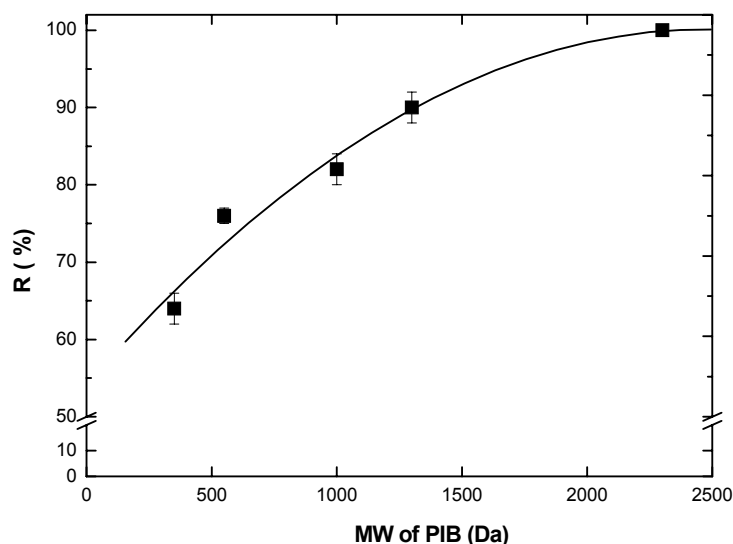


Figure 9: PIB retention by the PAN/PDMS composite membrane as a function of the molecular weight of PIB. Feed concentration: 8 % (w/w), $\Delta p = 7$ bar at 24 ± 3 °C.

The membrane retention increases with the increase of the MW of PIB. We think that the major contribution to retention is due to differences in the diffusion coefficients. The results of *Figure 9* allow us to estimate a MWCO for the M7-30 composite membrane (defined as the MW of the solute that is rejected for 90% by the membrane) of around 1200 - 1250 Da. However, this MWCO is not applicable to all solutions. It is rather a nominal MWCO and will probably change when using other experimental conditions (feed concentration, operating pressure and / or temperature, application of mixtures of PIB) or when moving to other solvents.

Hence, we conclude that the retention of the membranes is given by the ratio of partition coefficients as well as the ratio of diffusion coefficients, the later one being

dominant in the systems studied. Although hexane-induced dragging increases the solute flux, the strong effect of pressure on the chemical potential raises the hexane flux stronger than the dragging raises the solute flux.

3.5. Conclusions

In this work, a tailor-made PAN/PDMS composite membrane is reproducibly prepared and used for the separation of oil/hexane and PIB/hexane solutions. Our main findings are:

- Both the flux and solute (oil or PIB) retention depend on the applied transmembrane pressure and feed concentration. Increased pressure is beneficial in terms of flux and retention. No membrane compaction occurs in pressure range of 1-7 bar.
- Osmotic phenomena similar to those reported in aqueous systems are observed and can be interpreted using the van't Hoff equation.
- The flux of hexane can be normalized by an “apparent viscosity” and the membrane swelling. If we assume the solution-diffusion model to hold for this system, then we can interpret the solvent viscosity as a measure for the diffusion coefficient of the hexane inside the silicone network and the swelling as a measure for the solubility. However, the solution-diffusion model can not explain the solute-solvent coupling that is found experimentally. The flux of the solute (oil or PIB) increases linearly with the applied pressure showing the existence of flux coupling and solvent-induced solute dragging. The phenomenon is more significant at low solute/hexane concentrations (where the membrane swells more) and for solutes of low MW (where the viscosity is lower). However, the increase of hexane flux with the applied pressure is much higher than the respective increase of solute flux causing an increase of the membrane retention at higher pressures.

In Chapter 4 and 7, membranes with selective PDMS top layer of various cross-linking densities and/or more hydrophilic nature will be prepared and investigated. It remains

open whether the osmotic phenomena and the other critical parameters identified in this work (viscosity and membrane swelling) affect the solvent permeability for these systems, too.

3.6. List of symbols

A	Membrane area (m^2)
a_{pen}	Activity of penetrant
B	Solute permeability coefficient (m/h)
$c_{i,j}$	Concentration of species i, j (% w/w)
c_p	Concentration in the permeate side (% w/w)
c_f	Concentration in the feed side (% w/w)
d_{50}	Mean pore size (nm)
$J_{i,j}$	Flux of species i, j through membrane ($\text{lm}^{-2}\text{h}^{-1}$)
ℓ	Membrane thickness (m)
MW	Molecular weight of the solute
p_p	Pressure in the permeate side (bar or MPa)
p_f	Pressure in the feed side (bar or MPa)
P	Solvent permeability through the membrane ($\text{lm}^{-2}\text{h}^{-1}\text{bar}^{-1}$)
P_g	Gas permeability through the membrane ($\text{cm}^3\text{cm}^{-2}\text{s}^{-1}\text{cmHg}^{-1}$)
R	Membrane retention
R_g	Gas constant ($\text{Joule mol}^{-1}\text{K}^{-1}$)
t	Time (h)
T	Temperature (K)
V	Permeate volume (l)
$\alpha_{\text{CO}_2/\text{N}_2}$	Gas selectivity of membrane for CO_2 over N_2

Greek symbols

ϕ_{pen}	Penetrant volume fraction
χ	Interaction parameter
δ	Solubility parameter ($\text{MPa}^{1/2}$)

Δp	Transmembrane pressure equal to $p_f - p_p$ (bar)
$\Delta \pi$	Osmotic pressure difference across the membrane (bar)
η	Viscosity (cSt)
v	Molar volume (cm^3/mol)

3.7. Acknowledgements

- The CW/STW, Shell Global Solution (Amsterdam), Akzo Nobel Chemicals Research (Arnhem), Nederlandse Organisatie voor Toegepast Natuurwetenschappelijk Onderzoek Divisie Materiaaltechnologie (Eindhoven), Solsep B.V. Robust Separation Technologies (Apeldoorn) and DSM-Research CT&A (Geleen) are gratefully acknowledged for the financial support of this work (project number 790.35.249).
- The authors wish to thank: M.A. Hempenius (Materials Science and Technology of Polymers Group, University of Twente, The Netherlands), G-H. Koops and H. Zwijnenberg (European Membrane Membrane Institute – Twente, University of Twente, The Netherlands), A. Nijmeijer (Shell Global Solution), G. Bargeman (Akzo Nobel Chemicals Research), F. P. Cuperus (Solsep B.V. Robust Separation Technologies) and J. Krijgsman (DSM-Research CT&A) for the fruitful discussions.
- GKSS - Germany is gratefully acknowledged for providing the PAN support membranes.

3.8. References

- [1] C. Linder, M. Nemas, M. Perry, R. Katrarro, Silicon-derived solvent stable membranes, US5265734, 1993
- [2] D. M. Koenhen, A. H. A. Tinnemans, A semipermeable composite membrane, a process for the manufacture thereof, as well as application of such membranes for the separation of components in an organic liquid phase or in the vapour phase, US Patent, US5274047, 1992
- [3] K.-V Peinemann, K. Ebert, H.G Hicke, N. Scharnagl, Polymeric composite ultrafiltration membranes for non-aqueous applications, *Environmental Progress* 20(1) (2001) p17-22.
- [4] S. L. White, Transport properties of a polyimide solvent resistant nanofiltration membrane, *Journal of Membrane Science* 205 (2002) p191-202.
- [5] D. Bhanushali, S. Kloos, C. Kurth C, D. Bhattacharyya, Performance of solvent-resistant membranes for non-aqueous systems: solvent permeation results and modelling, *Journal of Membrane Science* 189 (2001) p1-21.
- [6] D. Bhanushali, S. Kloos, D. Bhattacharyya, Solute transport in solvent-resistant nanofiltration membranes for non-aqueous systems: experimental results and the role of solute-solvent coupling, *Journal of Membrane Science* 208 (2002) p 343-359.
- [7] D. R. Machado, D. Hasson, R. Semiat, Effect of solvent properties on permeate flow through nanofiltration membranes. Part I: investigation of parameters affecting solvent flux, *Journal of Membrane Science* 163 (1999) p93-102.
- [8] D. R. Machado, D. Hasson, R. Semiat, Effect of solvent properties on permeate flow through nanofiltration membranes. Part II. Transport model, *Journal of Membrane Science* 166(2000) p63-69.
- [9] G. H. Koops, S. Yamada, S.-I. Nakao, Separation of linear hydrocarbons and carboxylic acids from ethanol and hexane solutions by reverse osmosis, *Journal of Membrane Science* 189 (2001) p241-254.
- [10] S. S. Luthra, X. Yang, L. M. Freitas dos Santos, L. S. White, A. G. Livingston Homogeneous phase transfer catalyst recovery and re-use using solvent resistant membranes, *Journal of Membrane Science* 201 (2002) p65-75.

- [11] J. T. Scarpello, D. Nair, L. M. Freitas dos Santos, L. S. White, A. G. Livingston, The separation of homogeneous organometallic catalysts using solvent resistant nanofiltration, *Journal of Membrane Science* 203 (2002) p71-85.
- [12] J. P. Sheth, Y. Qin, K. K. Sirkar, B. C. Baltazis, Nanofiltration-based diafiltration process for solvent exchange in pharmaceutical manufacturing, *Journal of Membrane Science* 211 (2003) p251-261.
- [13] L.P. Raman, M. Chenyan and N. Rajagopalan, Solvent recovery and partial deacidification of vegetable oils by membrane technology, *Fett / Lipid*, 98 (1996) p10-14.
- [14] R. Subramanian, K.S.M.S. Raghavarao, H. Nabetani, M. Nakajama, T. Kimura and T. Maekawa, Differential permeation of oils constituents in nonporous denser polymeric membranes, *Journal of Membrane Science* 187 (2001) p57-69.
- [15] L. S. White and A. R. Nitsch, Solvent recovery from lube oil filtrates with a polyimide membrane, *Journal of Membrane Science* 179 (2000) p267-274.
- [16] E. Gibbins, M. D'Antonio, D. Nair, L. S. White, L. M. Freitas dos Santos, I. F. J. Vankelecom, A. G. Livingston, Observations on solvent flux and solute rejection across solvent resistant nanofiltration membranes, *Desalination* 147 (2002) p307-313.
- [17] H. J. Zwijnenberg, A. M. Krosse, K. Ebert, K.-V. Peinemann, F. P. Cuperus, Acetone-stable nanofiltration membranes in deacidifying vegetable oil, *Journal of American Oil Chemists Society* 76 (1999) p83-87.
- [18] K. Ebert, F. P. Cuperus, Solvent resistant nanofiltration membranes in edible oil processing, *Membrane Technology* 107 (1999) p5-8.
- [19] L. Lin, K. C. Rhee, S. S. Koseoglu, Bench-scale membrane degumming of crude vegetable oil: process optimisation, *Journal of Membrane Science* 134 (1997) p101-108.
- [20] L. P. Raman, M. Cheryan, N. Rajagopalan, Deacidification of soybean oil by membrane technology, *Journal of American Oil Chemists Society* 73 (1996) p219-224.
- [21] N. S. Krishna Kumar, D. N. Bhowmick, Separation of fatty acids triacylglycerol by membranes, *Journal of American Oil Chemists Society* 73 (1996) p-401.
- [22] H. Lonsdale, U. Merten, and R. Riley, Transport of cellulose acetate osmotic membranes, *Journal of Applied Polymer Science* 9 (1965) p1341.

- [23] J. G. Wijmans, and R. W. Baker, The solution-diffusion model: a review, *Journal of Membrane Science* 107 (1995) p1-21.
- [24] L. Germic, K. Ebert, R. H. B. Bouma, Z. Borneman, M. H. V. Mulder, H. Strathmann, Characterization of polyacrylonitrile ultrafiltration membranes, *Journal of Membrane Science* 132 (1997) p131-145.
- [25] J. E. Mark, *Polymer data handbook*, Oxford University Press, 1999.
- [26] D. W. van Krevelen, P.J. Hoftijzer, *Properties of polymers, their estimation and correlation with chemical structure*, Elsevier, Amsterdam, 1976.
- [27] M. H. V. Mulder, *Basic Principles of Membrane Technology*, Kluwer Academic Publishers, Dordrecht, 1992.
- [28] E. Favre, Q. T. Nguyen, P. Schaetzel, R. Clement and J. Neel, Sorption of organic solvents into dense silicone membranes. Part I. Validity and limitation of Flory Huggins and related theories, *Journal of Chemical Society Faraday Transactions* 89 (1993) p4339-4346.
- [29] X. J. Yang, A. G. Livingston, L. M. Freitas dos Santos, Experimental observations of nanofiltration with organic solvents, *Journal of Membrane Science* 190 (2001) p45-55.
- [30] S. J. Han, S. S. Luthra, L. Peeva, X. J. Yang, A. G. Livingston, Insights into the transport of toluene and phenol through organic solvent nanofiltration membranes, *Separation Science and Technology* 38(9) (2003) p1899-1923.

Effect of cross-linking degree of PDMS on the permeation performance of PAN/PDMS composite membranes

Abstract

This chapter focuses on the effect of poly(dimethyl siloxane) (PDMS) cross-linking degree on the permeation performance of the poly(acrylonitrile) (PAN)/PDMS nanofiltration (NF) composite membrane. PDMS membrane of various cross-linking degrees could be obtained by changing the ratio of a vinyl-terminated pre-polymer over a hydride cross-linker, 10/0.7, 10/1 and 10/2, corresponding to a cross-linker amount of 6.5, 9.1, and 16.7 % w/w, respectively. The swelling of the dense, free-standing PDMS membranes in hexane and polyisobutylene (PIB)/hexane solutions decreases with increasing the amount of cross-linker. The partition coefficient of PIB in the PDMS membrane decreases from 0.95 to 0.39, depending on the cross-linker content of silicone network and on the molecular weight of PIB.

The hexane permeability (P_{hexane}) through the PAN/PDMS prepared at pre-polymer/cross-linker ratio of 10/0.7 is higher than at pre-polymer/cross-linking ratio of 10/1 (4.5 and 3.1 $\text{lm}^{-2}\text{h}^{-1}\text{bar}$, respectively), due to the higher membrane swelling. The P_{hexane} through the PAN/PDMS prepared at pre-polymer/cross-linker ratio of 10/2 is higher than through the composite membrane prepared at 10/1 pre-polymer/cross-linking ratio (4.1 and 3.1 $\text{lm}^{-2}\text{h}^{-1}\text{bar}$). This result is not consistent with the swelling findings of the dense, freestanding PDMS membranes. This might be due to less pore intrusion of PDMS for the composite membrane prepared at pre-polymer/cross-linker ratios of 10/2 compared to 10/1 and/or due to the heterogeneous quality of the silicone network. However, the composite membranes prepared at various pre-polymer/cross-linker ratios have similar oil and/or PIB retention, indicating that PAN/PDMS prepared at pre-polymer/cross-linker ratios of

10/0.7 and 10/2 might be attractive for a practical application due to the higher hexane flux.

The “apparent” viscosity inside the membrane and the membrane swelling are the most critical factors affecting the hexane permeability through the PAN/PDMS of various cross-linking degrees. The cross-linking degree of PDMS has, however, no effect on the MWCO of the membrane probably due to the high swelling of the silicone network.

4.1. Introduction

In Chapter 2 and 3, we have described the preparation and characterization of the PAN/PDMS composite membranes that exhibit nanofiltration separation characteristics for oil and polyisobutylene (PIB)/hexane solutions. The mass transport of organic molecules through the dense NF membranes is based on the solubility and diffusivity of the penetrants into the PDMS network [1-4]. The solubility and diffusivity of the organic penetrants may be influenced by the structure of the PDMS network. By introducing extra cross-links in the PDMS network, the membrane swelling may be restricted and the diffusivity of the penetrant through the PDMS would decrease. Several studies [1, 2, 5-8] used the PDMS-based NF membranes in various non-aqueous media due to the high affinity of PDMS for non-polar organic solvents. However, no information about the cross-linking density of PDMS in these membranes was given. Bhanushali et al. [5] indicated already that cross-linking degree of the silicone network may be a very important parameter determining the permeation characteristics of the NF membranes. However, no systematical study has been undertaken concerning the influence of the PDMS cross-linking degree on the transport properties of silicone-based NF membrane, mainly because the studied membranes are commercial and the exact nature of their selective layer has not been fully revealed. In Chapter 2, we compared the hexane permeability through two dense, gas selective PDMS-based composite membranes (GKSS membranes and our PAN/PDMS tailor-made composites). The results indicate that the cross-linking of the silicone network might be different for these membranes. Concerning gas and vapor transport through dense silicone membranes, Hagg et al. [9] reported a significant effect of the PDMS cross-linking degree on the permeability of Cl_2 , O_2 , and N_2 while Nguyen et al. [10] studied the significance of the cross-linking degree on the pervaporation of water-ethyl acetate mixtures through the dense PDMS membranes.

In Chapter 2 and 3 we used PAN/PDMS membranes prepared at prepolymer/cross-linker ratio of 10/1 w/w, which is the recommended ratio by the

supplier (General Electric, The Netherlands). It may correspond to the stoichiometry of the reaction between the pre-polymer of vinyl-type and the cross-linker of hydrosilane-type (information give by the supplier). However, when the pre-polymer/cross-linker ratio varies, the PDMS swelling is expected to change considerably [11-13]. This may improve the performance of the PAN/PDMS composite membranes, in particular their flux. Therefore, we systematically study the influence of cross-linker amount (6.5, 9.1, and 16.7 % w/w, corresponding to the pre-polymer/cross-linker ratios of 10/0.7, 10/1, and 10/2, respectively) on the membrane swelling and PIB/hexane solution permeation through PAN/PDMS composite membranes. For the PAN/PDMS prepared at pre-polymer/cross-linker ratio of 10/1, we reported in Chapter 3 that the “apparent viscosity” inside the membrane and the swelling of the membrane (due to the interaction of PDMS/hexane/solute) are the most critical factors affecting the hexane permeability. It would be interesting to see if similar conclusion can be drawn for the hexane transport through the PDMS membranes prepared at pre-polymer/cross-linker ratios of 10/0.7 and 10/2.

4.2. Theoretical background

The hydrosilylation (addition) reaction relies on the ability of the hydrosilane bond of the cross-linker (SiH) to add across a carbon-carbon double bond that belongs to the pre-polymer in the presence of Pt catalyst – see *Figure 1* [14, 15].

In the ideal case, the SiH may react only with the $-\text{CH}=\text{CH}_2$ groups along the pre-polymer chains, allowing a good control over the cross-links distribution. The stoichiometric ratio of the PDMS system is defined as the ratio of hydrosilane to vinyl groups, being 1/1. For the ideal case, the molecular weight and molecular weight distribution of chains in the network are those of the pre-polymer chains prior to their end linking into the network structure [14, 15]. In practice, the

formed network may deviate from the ideality due to the steric hindrance or the un-balanced stoichiometry of the curing reaction.

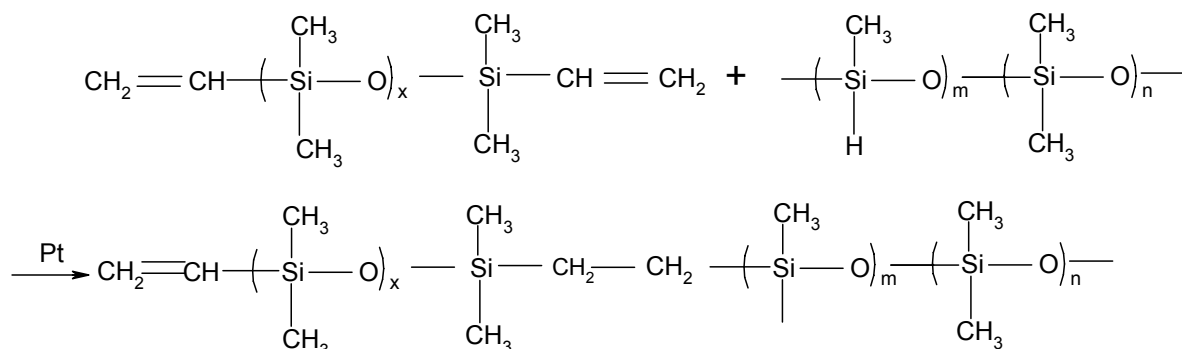


Figure 1: Scheme of the cross-linking reaction for the silicone network formation.

Few experimental studies on the effect of the pre-polymer/cross-linker ratio upon some physical properties of the PDMS as well as the gas/vapour transport are available in literature [9, 10, 16-19]. Simpson et al. [16] reported that an excess of the cross-linker (from the stoichiometric amount) slowed down the curing rate for the PDMS films of various thicknesses. The excess of tetrafunctional cross-linker (tetrakis(dimethylsiloxy) silane) was reported to improve the adhesion of the silicone to the fluorinated glass substrate [17]. Venkataraman et al. [18] studied the dynamic storage modulus as a function of the pre-polymer/cross-linker ratio. In the absence of any side reaction, balanced stoichiometry led to the PDMS network with a high elasticity. Shefer et al. [19] studied the changes in the glass transition temperature (T_g) of PDMS as a result of various cross-linking degree, indicating that the highest T_g is at the stoichiometrical ratio of the silicone network. Hagg et al. [9] measured the permeability of Cl_2 , O_2 , and N_2 through the “standard”, stoichiometrically cross-linked PDMS and the γ -radiated PDMS composite membranes (with a higher degree of cross-linking than the “standard” PDMS), at pressure range of 1-3 bar. The membranes showed a decrease in gas permeability and a slight increase in gas selectivity with the increase of PDMS cross-linking degree. For example, at 25 °C, the N_2 permeability for “standard”

PDMS samples was reported to be 0.8×10^{-6} (m³(STP)m)/(m²hbar), while for γ -radiated samples 0.2×10^{-6} (m³(STP)m)/(m²hbar) was found. Nguyen et al. [10] performed pervaporation of water-ethyl acetate mixtures through PDMS cross-linked membranes in different conditions (pre-polymer/cross-linker ratios and temperatures). They observed a decrease of both water and ester permeation fluxes, attributed to the decrease in the sorption of the components in the PDMS membrane.

Non-porous, gel membranes are swollen polymeric networks with “pores” of molecular size, usually between 20 and 100 Å [20, 21]. In fact, the term “pore” might be misleading, and, as de Gennes pointed out [22], a more appropriate term would be “macromolecular mesh”. Non-porous, gel membranes include most types of hydrogels such as water-swollen networks of poly(vinylalcohol) and related polymers, as well as other hydrophobic polymers swollen in the appropriate organic solvents (as PDMS in hexane).

The investigation of swelling equilibrium can help to elucidate the structure of the PDMS network. According to the Flory-Huggins solution theory (applicable for the good solvents in PDMS [9, 23]), the equilibrium volume fraction of the penetrant, $\phi_{pen.}$, can be related to the activity of the penetrant, $a_{pen.}$, by the following expression:

$$\ln a_{pen.} = \ln \phi_{pen.} + (1 - \phi_{pen.}) \left(1 - \frac{v_{pen.}}{v_{PDMS}}\right) + \chi (1 - \phi_{pen.})^2 \quad \text{Equation 1}$$

where χ is the PDMS - penetrant interaction parameter. The ratio of penetrant to PDMS molar volumes ($v_{pen.}/v_{PDMS}$) is assumed negligible. For the pure liquid, the χ parameter of PDMS prepared at each pre-polymer/cross-linker ratio is calculated by setting $\ln a_{pen.} = 0$. In order to gain further insight into the swelling process in relation to the morphological characteristics of the network, the PDMS volume fraction in the swollen state, ϕ_{PDMS} , is estimated by using the equation [12]:

$$\phi_{PDMS} = \frac{w_{PDMS} / \rho_{PDMS}}{(1 - w_{PDMS}) / \rho_{hexane} + w_{PDMS} / \rho_{PDMS}} \quad \text{Equation 2}$$

where w_{PDMS} is the weight fraction of the polymer at the swelling equilibrium and ρ_{PDMS} and ρ_{hexane} is the density of the PDMS and hexane, respectively. The polymer volume fraction is calculated assuming the polymer-solvent volume additivity.

The Flory-Rehner equation [23] however takes into account the effect of cross-linking degree on the elastic forces contribution and may be used for the systems involving the same polymer at various cross-linking degree [12]:

$$\ln a_{pen.} = \ln(1 - \phi_{PDMS}) + \phi_{PDMS} \left(1 - \frac{v_{pen.}}{v_{PDMS}} \right) + \chi \phi_{PDMS}^2 + \frac{v_{pen.} \rho_{PDMS}}{M_c} \left(1 - 2 \frac{M_c}{M^*} \right) \left(\phi_{PDMS}^{1/2} - \frac{1}{2} \phi_{PDMS} \right) \quad \text{Equation 3}$$

where M_c is the molecular weight between cross-links and M^* is the average molecular weight of the initial pre-polymer, before cross-linking.

The solution-diffusion model [24, 25] has already been used to describe the mass transport through the swollen PDMS membrane in Chapters 2 and 3. We will briefly remind the main equations. The flux of the pure solvent i can be calculated by:

$$J_i = P_i(\Delta p - \Delta \pi) \quad \text{Equation 4}$$

where P is a constant equal to the term $\frac{D_i K_i c_{if} v_i}{l R_g T}$ and is called the solvent permeability, where D_i is the diffusion coefficient of i through the membrane, K_i is the sorption coefficient, l is the membrane thickness, c_{if} , c_{ip} is the feed and permeate concentrations of species i , respectively, v_i is the partial molar volume of

species i , Δp and $\Delta\pi$ is the difference in applied and osmotic pressure across the membrane, respectively, R_g is the gas constant and T is the temperature, respectively. Similarly, the flux of the solute j is:

$$J_j = \frac{D_j K_j}{l} \left[c_{jf} - c_{jp} \exp\left(\frac{-v_j(p_f - p_p)}{R_g T}\right) \right] \quad \text{Equation 5}$$

Equation 4 indicates a linear increase in solvent flux with increasing transmembrane pressure difference, whereas *Equation 5* indicates that the solute flux is less affected by the pressure difference. This leads in general to an increasing solute retention with increasing solvent flux. The primary assumption made in the model is that the flux of the solute and solvent are independent.

4.3. Experimental

4.3.1. Materials

The PAN support membranes with molecular weight cut-off (MWCO) of 30 kDa were provided by GKSS - Germany. The selective top layer of the composite was PDMS (RTV 615 type, kindly supplied by General Electric, The Netherlands). The silicone kit was a two-component system, consisting of a vinyl-terminated pre-polymer (RTV A) and a cross-linker containing several hydrosilane groups (RTV B). The curing of the PDMS-membrane occurs via Pt-catalysed hydrosilylation reaction to form a densely cross-linked polymer network.

The polyisobutylenes (PIB), Glissopal[®] of MW 550, 1000, 1300, and 2300 were kindly provided by BASF - Germany and of MW 350, by Janex S.A.–Switzerland (see *Table 1*).

Table 1: Specifications of the PIB used in this work.

MW_{PIB}^a (g mol⁻¹)	Producer	Polydispersity^b (-)
350	Janex	1.8
550	BASF	2.1
1000	BASF	2.9
1300	BASF	3.6
2300	BASF	1.8

^a Given by the producer

^b Defined as the ratio of M_w to M_n , determined by GPC.

The n-hexane (Merck, The Netherlands) and the PIB were used as supplied, without further purification.

4.3.2. Membrane preparation and characterization

The free-standing, thick PDMS films were prepared from 75 %(w/w) PDMS/hexane solution at room temperature by mixing the pre-polymer and cross-linker at 10/0.7, 10/1, 10/2 w/w ratios.

The PAN/PDMS tailor-made composite membranes were prepared in a two-step coating procedure, as described in Chapter 2.

The density of the dense PDMS films was measured with a pycnometer (Micrometrics Accupyc 1330). The elastic modulus of the dense PDMS films was determined by performing tensile testing on a Zwick Z020 (Germany) machine. In order to obtain the stress-strain diagrams, the uniaxial deformation of the sample (dumb-bell test piece, according to ISO37, type 2) was measured under 10 N loading. The molecular weight between cross-links (M_c) was calculated [26, 27] by:

$$M_c = \frac{3\rho_{PDMS} R_g T}{E_m} \quad \text{Equation 6}$$

where E_m is the elastic modulus.

Pure gas permeation measurements with N_2 and CO_2 were performed, using the set-up and procedure described in Chapter 2. No significant differences in gas permeability through the composites as a function of cross-linking degree were found. For the PAN/PDMS composite membranes, the gas selectivity, α_{CO_2/N_2} was found to be 9.8 ± 1.4 , independent on the cross-linking degree. These values are close to the PDMS intrinsic selectivity, indicating the good quality of the PDMS top-layer.

For the swelling measurements, the pre-weighed dry dense PDMS membranes (M_{dry}) were immersed in pure hexane or PIB/hexane solutions until the equilibrium swelling was reached, M_{wet} . Swelling degree (SD) of the dense PDMS membrane was calculated by:

$$SD(\%) = \left(\frac{M_{wet} - M_{dry}}{M_{dry}} \right) \times 100 \quad \text{Equation 7}$$

For PIB/hexane solutions, at the end of the swelling experiments, the samples were removed from the liquid solutions and dried. From the difference between the initial and final dry weight, the concentration of the PIB in the membrane ($c_{PIB,membrane}$, % w/w) was measured and the PIB partition coefficient K_{PIB} was calculated by:

$$K_{PIB} = \frac{c_{PIB,membrane}}{c_{PIB,f}} \quad \text{Equation 8}$$

where $c_{PIB,f}$ is the PIB concentration in the immersed solution, % w/w.

Attenuated total reflectance Fourier transform infrared spectroscopy (ATR-FTIR) was used for the characterization of PDMS at various cross-linking degrees. The penetration depth of the infrared beam ranged from 0.5 μm at 3000 cm^{-1} to 2 μm at 700 cm^{-1} for the ZnSe crystal with a 90° angle of incidence for PDMS network analysis. Gel permeation chromatography (GPC) was used to determine the molecular weight of the pre-polymer and cross-linker. The GPC analysis for the PDMS components (pre-polymer and cross-linker) as supplied by General Electric was performed by Waters 515 GPC instrument, using tetrahydrofuran as solvent. ^1H NMR spectroscopy was used to determine the structure of the pre-polymer and cross-linker (Bruker AC 250 spectrometer, 400 MHz, using deuterated chloroform). The morphology of the composite membranes was visualized by Scanning Electron Microscopy (SEM, Microscope Jeol JSM-5600LV, at 15 kV). All the liquid permeation experiments through the composite membranes were performed at room temperature (24 ± 3 °C), with the set-up and the experimental protocol described in Chapter 2. Helium gas was used to apply pressures in the range of 1-7 bar. The flux through the membrane was calculated by dividing the amount of the collected permeate over the membrane area and permeation time. The permeate volume was calculated by dividing the collected weight to the permeate density (measured by a Digital Density Meter, model DMA 50). The PIB concentration in the feed ($c_{PIB,f}$, % w/w) and the permeate ($c_{PIB,p}$, % w/w) solutions was analyzed by refractive index measurements at 25 °C using a Abbe-3 refractometer, from Carl Zeiss, Germany. The PIB retention was calculated using the equation:

$$R = \left(1 - \frac{c_{PIB,p}}{c_{PIB,f}} \right) \times 100 \quad \text{Equation 9}$$

Values and error bars reported in the tables and figures are based on three different membranes samples.

4.4. Results and discussion

4.4.1. Pre-polymer and cross-linker characterization

Figure 2 presents a typical result of the GPC analysis for the pre-polymer and cross-linker, as received from the supplier.

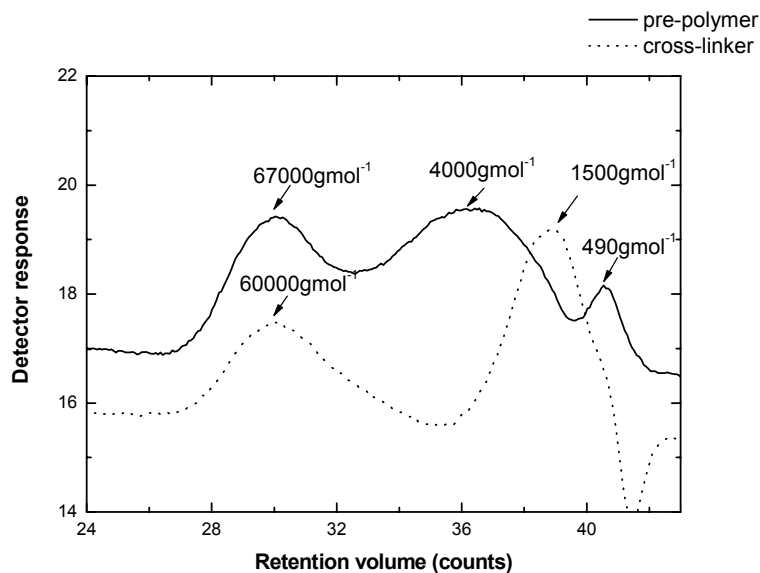


Figure 2: The molecular weight of the PDMS pre-polymer and cross-linker determined by GPC.

The data indicate that the pre-polymer and cross-linker have mainly a bimodal character of widely differing molecular weight (for pre-polymer: 4000 and 67000 gmol⁻¹ and for cross-linker: 1500 and 60000 gmol⁻¹). The molar masses of the pre-polymer and cross-linker obtained by ¹H-NMR analysis (data not shown here) are in good agreement with the GPC results.

Theoretically, the hydrosilylation reaction is very specific since the hydrosilane groups should react only with the vinyl groups at the end of the chains, the stoichiometric ratio being 1/1. Generally, an excess of the hydrosilane part is used in order to compensate for the steric hindrance: the reaction between vinyl and hydrosilane groups becomes more and more difficult since reactive species

become scarcer, and the network becomes tighter as the reaction progresses [14]. In the absence of any significant side-reaction, balanced stoichiometry should lead to a network with average molecular weight between cross-links, M_c , that equals the molecular weight of the pre-polymer chains prior to their end linking and few, if any, dangling-chains (those chains attached to the network at one end only) [14, 15].

4.4.2. ATR-FTIR and mechanical analysis of the dense PDMS membrane

ATR-FTIR was used for the spectroscopic characterization of the dense, freestanding PDMS membranes prepared at various pre-polymer/cross-linker ratios. *Figure 3* presents a typical result for the membrane prepared at the “reference” ratio, 10/1.

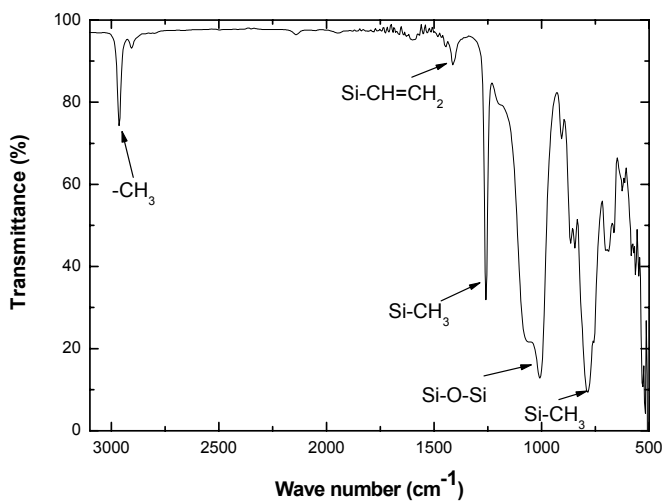


Figure 3: ATR-FTIR spectra of the PDMS membrane prepared at ratio of 10/1.

The typical peaks of the C-H methyl stretch at 2965 cm^{-1} , the silicon-methyl bond at 1260 cm^{-1} , and the broad polymer backbone absorption band between $1130 - 1000\text{ cm}^{-1}$ are found [28].

The amount of the unreacted vinyl and hydrosilane (SiH) groups (after cross-linking at 65°C for 4 h in N₂ oven) can be determined by following the change in intensity of the absorption band at 1410 cm⁻¹ (for vinyl) and 2140 cm⁻¹ (for SiH). If no side reaction occurs, the changes in the intensity of these bands should be attributed to the consumption of these groups upon cross-linking reaction. *Figure 4* presents typical ATR-FTIR spectra of the dense PDMS films of various pre-polymer/cross-linker ratios at these specific wavelengths.

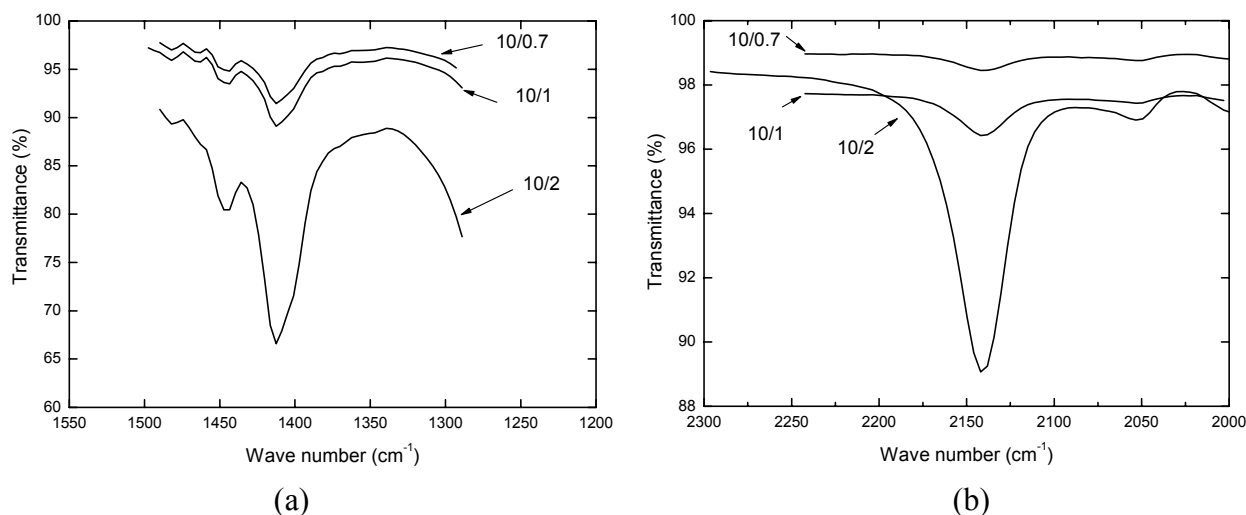


Figure 4: ATR-FTIR spectra of the dense PDMS membrane prepared at pre-polymer/cross-linker of various ratios for (a) vinyl group (b) SiH group, respectively.

For the PDMS prepared at pre-polymer/cross-linker ratio of 10/2, the intensity of the absorption band at 1410 cm⁻¹ is high, indicating an excess of the vinyl groups. In *Figure 4* (b), the SiH absorption band can not be clearly detected for the PDMS membranes prepared at pre-polymer/cross-linker ratios of 10/0.7 and 10/1, indicating the total SiH consumption upon the cross-linking reaction. In contrary, for PDMS of 10/2 ratio, the SiH peak is high, suggesting that not all the hydrosilane groups reacted. Nguyen et al. [10] reported similar results for an excess of cross-linker amount in the pre-polymer/cross-linker mixture. They suggested that the silicone network might be considered to be a blend of unreacted

silicone (still containing vinyl and SiH groups) and fully-cured silicone (without unreacted groups) [10]. The experimental findings may support the hypothesis of heterogeneous cross-linker “agglomeration” or “branching” [29] that decreases the extend of cross-linking reaction due to the steric hindrance. This leads to the formation of an “imperfect” PDMS network at pre-polymer/cross-linker ratio of 10/2, which is spatially as well as compositionally heterogeneous. Such network is expected to have a lower swelling degree compared to the homogeneous network. *Table 2* presents the density (ρ), the Young’s modulus (E_m), and the calculated average molecular weight of chain between the cross-links (M_c – see *Equation 6*) of the PDMS prepared at various pre-polymer/ cross-linker ratios.

Table 2: Density, Young’s modulus and average molecular weight of chains between cross-links for PDMS prepared at pre-polymer/cross-linker of various ratios.

Pre-polymer/cross-linker ratio	ρ (gcm^{-3})	E_m (MPa)	M_c (10^3gmol^{-1})
10/0.7	1.052 ± 0.009	0.35 ± 0.08	22.3 ± 4.5
10/1	1.055 ± 0.006	0.50 ± 0.02	15.6 ± 0.8
10/2	1.064 ± 0.007	0.77 ± 0.06	10.3 ± 0.7

The elastic modulus of the dense, freestanding PDMS membrane increases with the amount of cross-linker, as expected, since an increase in cross-linker content forms a tighter network. Similar trend was reported by Nguyen et al. [10]. Thus, the average molecular weight between cross-links decreases from 22300 to 10300 gmol^{-1} .

4.4.3. Swelling experiments of dense PDMS membrane in hexane

Figure 5 presents the effect of the cross-linker content upon the swelling of freestanding, dense PDMS membranes prepared at pre-polymer/cross-linker ratios of 10/0.7, 10/1, and 10/2, corresponding to 6.5, 9.1, and 16.7 %w/w cross-linker content, respectively.

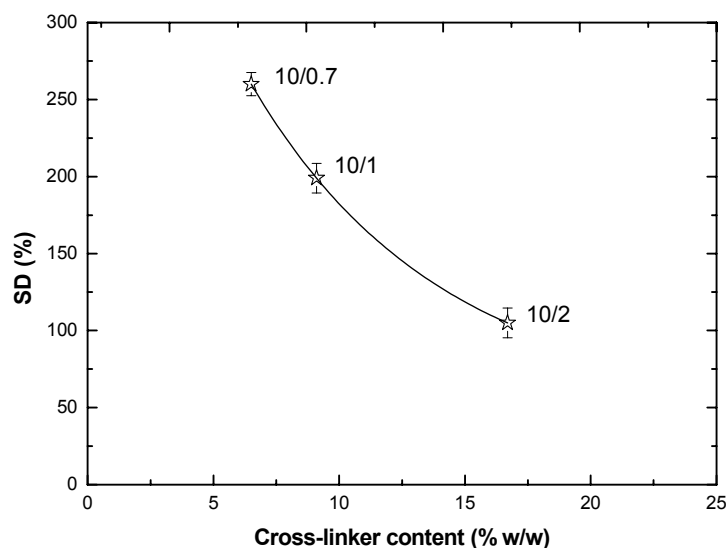


Figure 5: The effect of the cross-linker content upon the swelling degree (SD) of PDMS dense membranes in hexane.

The lower the amount of cross-linker in the pre-polymer-cross-linker mixture, the higher the swelling degree of the membrane. Such behavior can be explained by the decrease in the chain length between cross-links with the increase of the cross-linker amount (see *Table 2*): the shorter the chains between cross-links, the stronger the elastic resistance to the swelling stress (higher elastic modulus), and the lower the swelling degree of the membrane [14].

Table 3 summarizes the results of swelling experiments of the dense PDMS membranes in hexane: the weight fraction of PDMS (w_{PDMS}), the volume fraction of PDMS (ϕ_{PDMS}), and the interaction parameter (χ) calculated by using the Flory-

Huggins and the Flory-Rehner equations. For the Flory-Rehner equation (Equation 3), the M_c obtained from the mechanical analysis (Table 2) and the M^* of 35000 g mol^{-1} taken from the GPC analysis, Figure 2) are used.

Table 3: Equilibrium data from the swelling experiments.

Pre-polymer/cross-linker ratio	w_{PDMS} (-)	ϕ_{PDMS} (-)	$\chi_{\text{Flory-Huggins}}$ (-)	$\chi_{\text{Flory-Rehner}}$ (-)
10/0.7	0.28 ± 0.02	0.19 ± 0.02	0.57 ± 0.02	0.58 ± 0.02
10/1	0.33 ± 0.03	0.24 ± 0.02	0.59 ± 0.02	0.59 ± 0.02
10/2	0.50 ± 0.03	0.38 ± 0.03	0.68 ± 0.02	0.66 ± 0.02

The data show that the volume fraction of PDMS in the swollen network increases with the amount of cross-linker. This increase does not affect much the interaction parameters of the hexane-PDMS membranes prepared at pre-polymer/cross-linker ratios of 10/0.7 and 10/1. However, for PDMS prepared at pre-polymer/cross-linker ratio of 10/2, the χ parameter is higher, suggesting that the χ parameter depends upon the cross-linking degree of the PDMS for the studied system. Such finding has been already reported in literature [10, 30-32], the origin of this behavior being attributed to the fact that the mixing and the elastic free energies are not strictly separable in the description of swelling equilibrium [10, 32]. Therefore, the increase in cross-linking degree determines an increase in the elastic energy for polymer network deformation, which reduces the free energy of mixing [10]. Another potential cause of this behavior may be the difference in the quality of the PDMS network prepared at pre-polymer/cross-linker of various ratios. The ATR-FTIR spectra of PDMS prepared at pre-polymer/cross-linker ratio of 10/2 indicate that the silicone network contains unreacted hydrosilane and vinyl groups. The response of such “imperfect” network to the swelling stress would not be as ideal as supposed in the Flory-Huggins and Flory-Rehner models. Two main simplifications employed, namely the Gaussian distribution of the polymer chains (which was found to not be always valid for the bimodal PDMS elastomers [33])

and the phantom network (which ignores the intermolecular effects, therefore the topological constraints), may not be valid for the prepared silicone network [34]. More sophisticated theories are available (e.g. using self-avoiding walk statistics for the polymer chain distribution) but they are more difficult to apply because they contain parameters that are not always available in the literature [34].

Interestingly, the values of χ parameter calculated using Flory-Huggins and Flory-Rehner equations are similar, indicating that the elastic contribution of the PDMS network towards the swelling in hexane is negligible. We attribute this to the high M_c (10300 and 22300 g mol^{-1}). Actually, the elastic part of the Flory-Rehner equation induces very little modification to the Flory-Huggins equation, unless the PDMS network has a very small M_c [9]. Similar findings were reported [9, 10] for the PDMS network with the M_c in the range of 640-12700 g mol^{-1} .

4.4.4. Swelling of dense PDMS membranes in PIB 550 /hexane solutions

The equilibrium swelling degree of the dense, freestanding PDMS membrane in PIB/hexane solutions was investigated as well. For this study, PIB of various MW have been used. *Figure 6* presents a typical result concerning the PIB of MW 550 g mol^{-1} . Similar results were obtained for PIB of other MW, too. In the concentration range of 0-30% (w/w), the swelling degree of the PDMS prepared at pre-polymer/cross-linker of various ratios does not change significantly with molecular weight of the solute (see *Figure 2* in Chapter 3). In this range, the solute size might be smaller than the mesh size of the silicone gel formed by the highly swollen network in hexane.

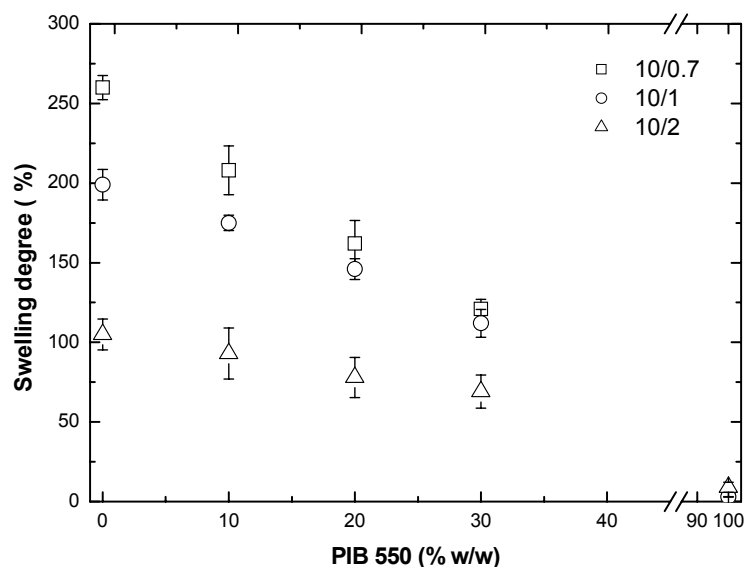


Figure 6: The effect of the solution concentration upon swelling degree of the PDMS dense membranes prepared at pre-polymer/cross-linker of various ratios.

The effect of pre-polymer/cross-linker ratio on the swelling degree of the PDMS membrane in PIB/hexane solutions is similar to the pure hexane, i.e. the lower the amount of cross-linker, the higher the membrane swelling. In addition, the PDMS swelling degree decreases when the concentration of the PIB/hexane solution increases, for all the cross-linking degrees. From the results of the swelling experiments for pure PIB ($a_{pen.}=1$) and by using *Equation 1*, the interaction parameter between PDMS/PIB is found to be 2.11 ± 0.02 [1]. This value is higher than the χ value of 0.58 corresponding to PDMS/hexane system. This indicates that the sorption of hexane in PDMS is thermodynamically much more favorable compared to sorption of PIB.

Swelling experiments of PDMS membranes prepared at pre-polymer/cross-linker of various ratios in the PIB of various MW/hexane solutions of 8 % w/w (at $22 \pm 1^\circ\text{C}$) were performed. From the difference between the initial and final dry weight, the concentration of the PIB (c_{PIB} , % w/w) within the membrane is determined (see *Figure 7*).

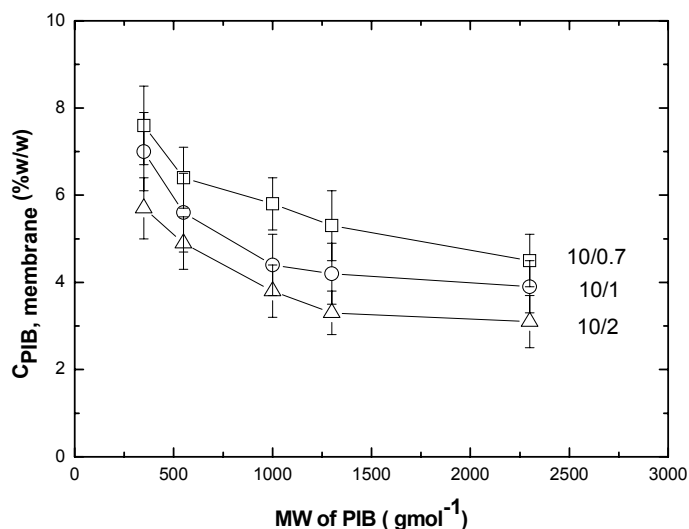


Figure 7: The effect of MW of PIB on the concentration of PIB/hexane solution inside the PDMS dense membrane prepared at pre-polymer/cross-linker of various ratios.

The concentration of PIB inside the PDMS network decreases when the MW of PIB increases, indicating a decrease in PDMS-PIB/hexane solution interaction with increasing PIB MW. The experimental finding is consistent with the dependence of the interaction parameter on the molar volume of the penetrant [1, 35]. In addition, the concentration of PIB inside the PDMS network decreases slightly with increasing the amount of the cross-linker. Such behavior can be explained by the decrease of the chain length between cross-links with the increase of the cross-linker amount: the shorter the chains between cross-links, the stronger the elastic resistance to the swelling stress, thus the lower the swelling of the membrane, and therefore, the lower the PIB amount inside the PDMS network. The PIB partition coefficient, $K_{PIB,membrane}$ is calculated from the results of *Figure 7* over the concentration of the immersing PIB/hexane solution (8 % w/w), using *Equation 8*. The $K_{PIB,membrane}$ in highly swollen, freestanding silicone membranes (PDMS gel) is affected by the cross-linked density, as well as by the penetrant

size. It decreases slightly with increasing pre-polymer/cross-linker ratio of the PDMS-gel membranes.

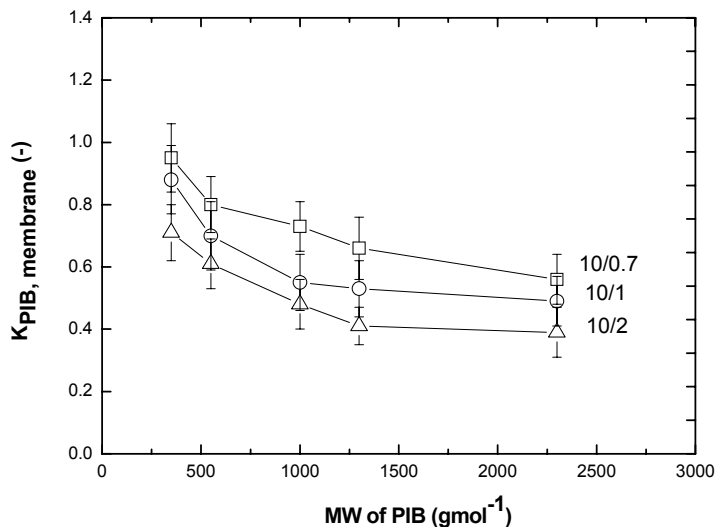


Figure 8: The PIB partition coefficient for the PDMS dense membranes prepared at pre-polymer/cross-linker of various ratios.

When the molecular weight of the PIB increases, the PIB partition coefficient into the PDMS decreases. Similar effect of the cross-linking degree on the partition coefficient of myoglobin in block copolymer membrane of PEO-PDMS membrane was reported by Harland et al. [36].

4.4.5. Permeation experiments

Figure 9 presents the hexane flux through the PAN/PDMS composites of various cross-linking degrees as a function of transmembrane pressure. The hexane flux increases linearly with the applied pressure in all cases, indicating that no compaction of the membrane occurs over the applied pressure range. From the slopes of the plots of Figure 9, the hexane permeability coefficient, P_{hexane} , can be calculated. Hexane permeability through the PAN/PDMS composites prepared at

pre-polymer/cross-linker ratio of 10/0.7 is found to be $4.5 \text{ lm}^{-2}\text{h}^{-1}\text{bar}^{-1}$, of 10/1 is $3.1 \text{ lm}^{-2}\text{h}^{-1}\text{bar}^{-1}$, and of 10/2 is $4.1 \text{ lm}^{-2}\text{h}^{-1}\text{bar}^{-1}$, respectively.

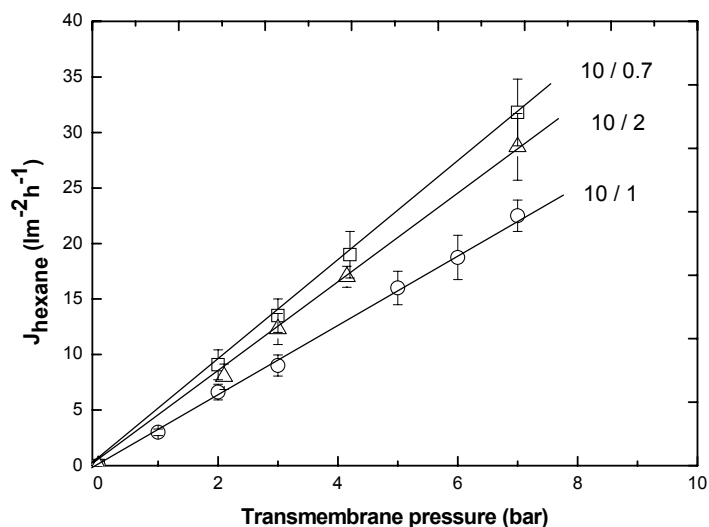


Figure 9: Hexane flux as a function of the transmembrane pressure for the PAN/PDMS membranes prepared at various pre-polymer/cross-linker ratios.

For the PAN/PDMS composites prepared at pre-polymer/cross-linker ratio of 10/0.7, the hexane permeability is higher in comparison to that through the membrane composite prepared at 10/1 pre-polymer/cross-linker ratio. This finding is consistent with the swelling results of the corresponding dense, free-standing PDMS membranes: PDMS network prepared at pre-polymer/cross-linker ratio of 10/0.7 swells much more (260 % (w/w)) than that at 10/1 (200 % (w/w)). The hexane permeability through the PAN/PDMS membrane prepared at pre-polymer/cross-linker ratio of 10/2 ratio is not consistent with the swelling results of the corresponding dense membranes: the P_{hexane} through the PAN/PDMS prepared at ratio of 10/2 is higher ($4.1 \text{ lm}^{-2}\text{h}^{-1}\text{bar}^{-1}$) than of 10/1 ($3.1 \text{ lm}^{-2}\text{h}^{-1}\text{bar}^{-1}$) although the swelling degree of the corresponding dense PDMS membrane is lower. This indicates that another parameter, besides swelling of the cross-linked network, might be important in this case. Probably the pore intrusion is different for the PAN/PDMS prepared at pre-polymer/cross-linker ratios of 10/1 and 10/2.

To study this hypothesis, we compare the effective thickness of the PDMS coating layer determined by CO₂ permeation experiments with the thickness visualized by SEM. Typical SEM pictures of the cross-section of the PAN/PDMS prepared at pre-polymer/cross-linker of various ratios are shown in *Figure 10*.

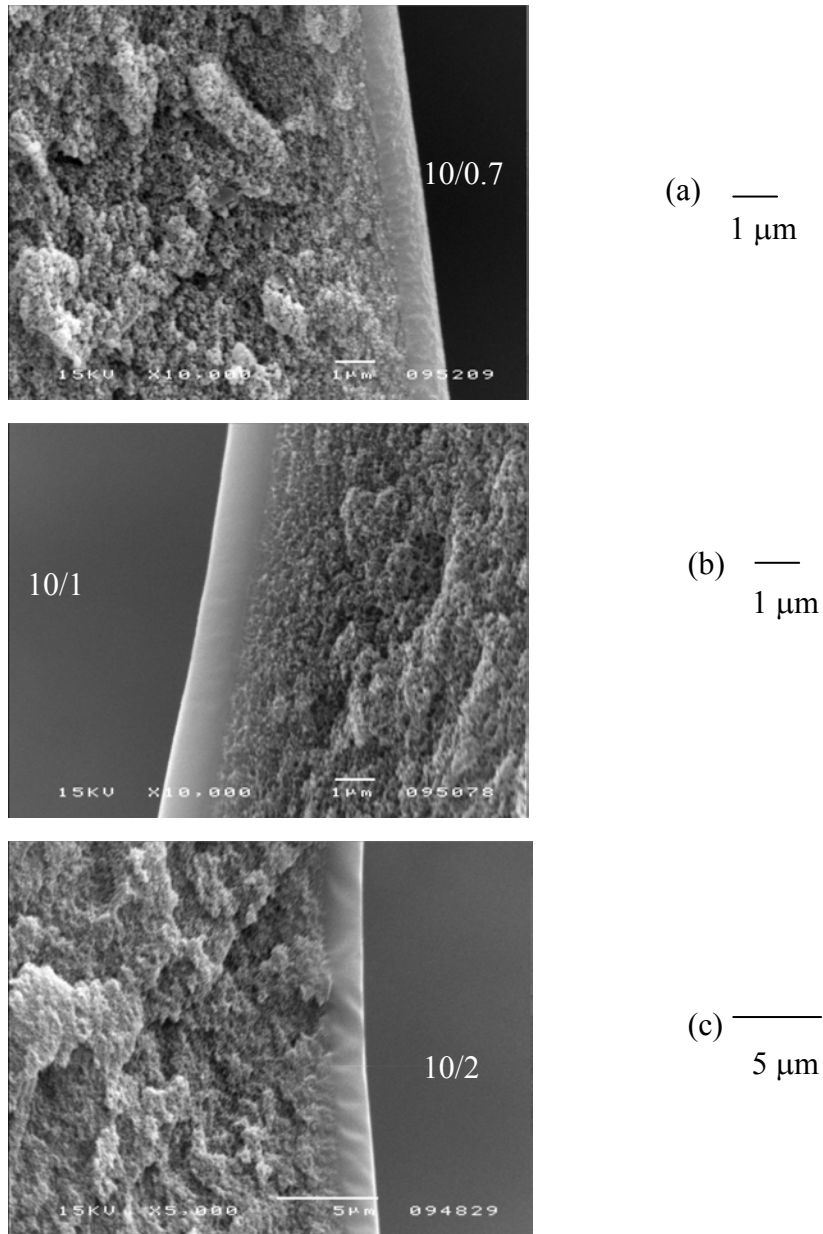


Figure 10: SEM pictures of the cross-section of PAN/PDMS composite membranes prepared at pre-polymer/cross-linker ratio of (a) 10/0.7 (magnification 10000x), (b) 10/1 (magnification 10000x) and (c) 10/2 (magnification 5000x).

Table 4 compares the PDMS thickness visualized by SEM and the effective thickness of the PDMS calculated from CO₂ permeability measurements, assuming that the gas transport is completely determined by the PDMS.

Table 4: Effective and visualized PDMS thickness, and hexane permeability of the PAN/PDMS membranes prepared at pre-polymer/cross-linker of various ratios.

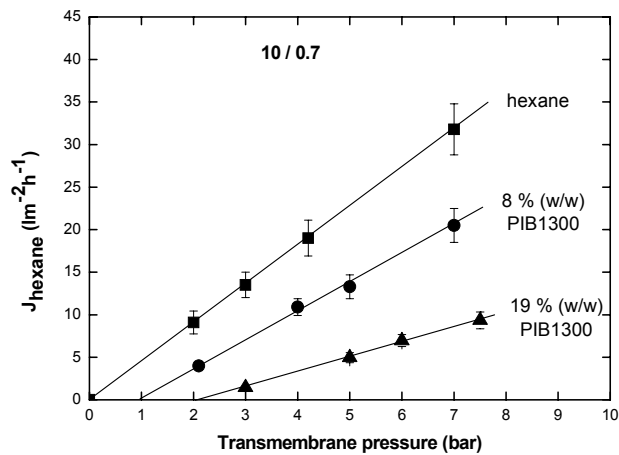
Pre-polymer/cross-linker ratio	$l_{\text{eff(CO}_2\text{)}}$ (μm)	l_{SEM} (μm)	P_{hexane} ($\text{lm}^{-2}\text{h}^{-1}\text{bar}^{-1}$) ¹
10/0.7	1.9 ± 0.2	0.9 ± 0.2	4.5 ± 0.5
10/1	2.0 ± 0.2	1.0 ± 0.2	3.1 ± 0.4
10/2	2.2 ± 0.3	1.8 ± 0.3	4.1 ± 0.5

For the PAN/PDMS composite membranes prepared at pre-polymer/cross-linker ratios of 10/0.7 and 10/1, the difference between the effective and visualized thickness is of about 1 μm . At the top of PAN support an intermediate layer probably exists where the PDMS penetrates into the pores of the support. For the composite membrane prepared at pre-polymer/cross-linker ratio of 10/2, however, the difference between the effective and visualized thickness is not as much, indicating that the pore intrusion in this membrane is less than for the other two composites. This might be the reason for the relatively high hexane permeability observed for this membrane, even though the membrane swelling is less than for the other two membranes. A pore confinement restricts the swelling of the PDMS network immobilized inside the pores due to the rigidity of the support matrix. Similar results are reported by Vankelecom et al. [37] for the pervaporation of water/ethanol with a PDMS/Zirfon composite membrane that had various degrees of pore intrusion.

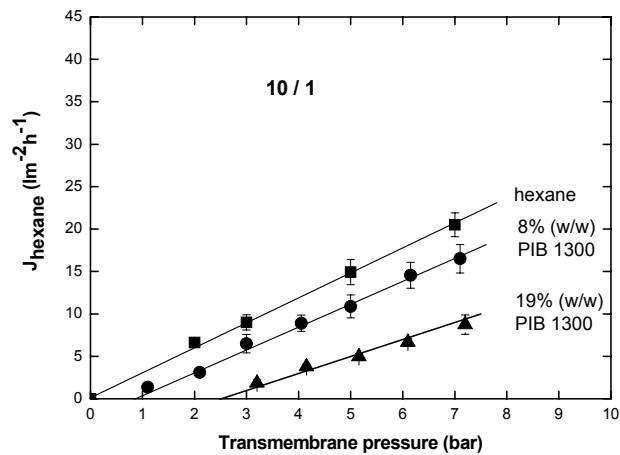
Apparently, the cross-linking degree and the pore intrusion of the silicone network influence the hexane flux through the dense PDMS-based NF composite

membranes. In Chapter 2 we reported a hexane permeability of $5.9 \text{ lm}^{-2}\text{h}^{-1}\text{bar}$ for the gas-selective GKSS membrane with an effective thickness of $2\mu\text{m}$ and without pore intrusion. Our PAN/PDMS composite membrane prepared at 10/2 pre-polymer/cross-linker ratio presents similar features concerning pore intrusion and effective thickness. However, its hexane permeability is found to be $4.1 \text{ lm}^{-2}\text{h}^{-1}\text{bar}$, indicating that the different cross-linking degree of the network may cause the difference in hexane permeability. Koike et al. [38] and Robinson et al. [7] reported also various hexane permeabilities ($4.7 \text{ lm}^{-2}\text{h}^{-1}\text{bar}$, effective thickness not revealed and $10 \text{ lm}^{-2}\text{h}^{-1}\text{bar}$, for $2\mu\text{m}$) through dense, gas selective, PDMS-based NF composite membranes. The gas selectivity of all those membranes was the intrinsic PDMS gas selectivity, suggesting that the differences in hexane permeability might be given by the various cross-linking degree of the silicone network.

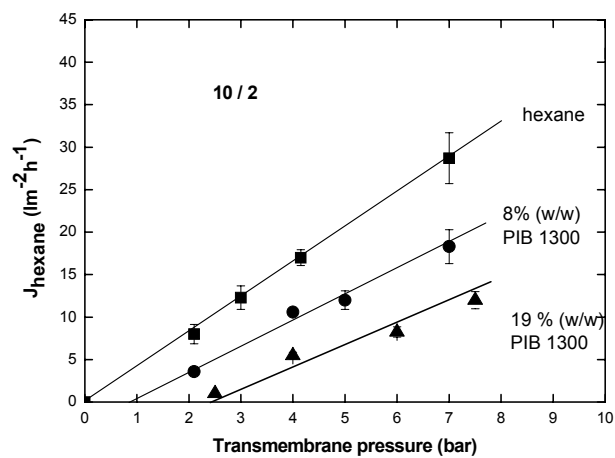
Figure 11 presents the effect of the feed pressure on the hexane flux for various PIB1300/hexane concentrations, for the PAN/PDMS prepared at pre-polymer/cross-linker of various ratios. The hexane permeability coefficient (calculated from the slopes of the graphs in *Figure 11*) through the PAN/PDMS composite prepared at pre-polymer cross-linker of various ratios decreases with the increase of PIB1300 concentration. Similar trend has also been reported in literature [1, 39-42] for various organic systems. The decrease of solvent permeability with increase of solute concentration is due to the increase in feed viscosity.



(a)



(b)



(c)

Figure 11: Hexane flux through PAN/PDMS membrane prepared at pre-polymer/cross-linker ratios of (a) 10/0.7, (b) 10/1 and (c) 10/2 as a function of transmembrane pressure for various PIB 1300/hexane feed concentrations.

In all cases, the linearity of the J_{hexane} with the applied pressure indicates that no compaction of the membrane occurs over the applied pressure range. Hence the hexane transport through the membrane can be described by the *Equation 4*. For the PAN/PDMS composite membranes prepared at pre-polymer/cross-linker ratios of 10/0.7 and 10/2, osmotic phenomena similar to those already reported at pre-polymer/cross-linker ratios of 10/1 [1] are observed and can be interpreted using the van't Hoff equation:

$$\Delta\pi = \frac{R_g T \Delta c}{MW} \quad \text{Equation 11}$$

$\Delta\pi$ is the osmotic pressure (in bar), Δc is the solute concentration difference across the membrane (in g/l) and MW is the solute molecular weight (in gmol^{-1}). The x -intercepts (at $J_{\text{hexane}} = 0$) for each PIB1300/hexane concentration are again in very good agreement, within experimental error, with those of $\Delta\pi$ calculated by using *Equation 11*. For example, for PAN/PDMS composite prepared at pre-polymer/cross-linker ratio of 10/0.7, x -intercept/calculated $\Delta\pi$ value is 1.0 bar/0.8 bar for 8 % (w/w) feed and 2.3 bar/2.1 bar for 19 % (w/w) feed.

For the PAN/PDMS prepared at pre-polymer/cross-linker ratio of 10/1, we reported in Chapter 3 that the “apparent viscosity” inside the membrane and the swelling of the membrane (due to the interaction of PDMS/hexane/solute) are the most critical factors affecting the hexane permeability. It is interesting to see if similar conclusion can be drawn for the hexane transport through the PDMS membranes prepared at pre-polymer/cross-linker ratios of 10/0.7 and 10/2. *Table 5* presents this normalization for the PAN/PDMS membranes prepared at pre-polymer/cross-linker of various ratios, at the same experimental conditions: feed of 8 % (w/w) PIB/hexane, at 24 ± 3 °C. For the normalization, the value of an “apparent viscosity” of the solution inside the membrane is used. This is estimated from the concentration of PIB in a hypothetical hexane/PIB phase inside the dense PDMS membranes (*Figure 7*) and the plots of viscosity versus PIB/hexane

concentration already presented elsewhere [1]. For the swelling degree, the results of the dense PDMS membranes are used.

For all membranes, a constant normalized value is found for each pre-polymer/cross-linker ratio, the magnitude of which depends on the cross-linking degree of the PDMS. For the PAN/PDMS membranes prepared at pre-polymer/cross-linker ratios of 10/0.7 and 10/1, the normalized hexane permeability, $P\eta/SD$, is similar (about 1). However, for the composites prepared at pre-polymer/cross-linker ratio of 10/2, the normalized value is higher (range of 2.1-2.4) due to the lower SD of the dense PDMS membrane of 10/2 ratio compared to 10/0.7 and 10/1. If we assume the solution-diffusion model to hold for this system, then we can interpret the solvent viscosity as a measure for the diffusion coefficient of hexane inside the silicone network and the swelling as a measure for the solubility. However, the solution-diffusion does not consider the solute-solvent coupling (solvent-induced solute dragging) that is found experimentally, as we will discuss below.

For the PAN/PDMS composite membrane prepared at pre/polymer/cross-linker ratio of 10/1, we have already found [1] that the flux of the solute increases linearly with the applied pressure, showing the existence of flux coupling or solvent-induced solute dragging.

Figure 12 shows that the dragging effect of the hexane flux on the solute occurs for the PAN/PDMS composites at various cross-linking degrees. At the same PIB1300/hexane feed concentration, the PIB flux increases linearly with the hexane flux. The flux of PIB 1300 through the PAN/PDMS composite prepared at pre-polymer/cross-linker ratio of 10/0.7 is higher than that through the composite of 10/1 (similar pore intrusion), indicating its correlation with cross-linking degree of the silicone network (result consistent with the partition experiments of *Figure 8*).

Table 5: Parameters concerning the transport of PIB/hexane solutions through the PAN/PDMS membranes prepared at pre-polymer/cross-linker ratio of (a) 10/0.7 , (b) 10/1, (c) 10/2. Experimental conditions: feed of 8 % (w/w), at 24 ± 3 °C.

(a)

MW of PIB, (gmol^{-1})	η_{apparent} (cSt)	P_{hexane} ($\text{lm}^{-2}\text{h}^{-1}\text{bar}^{-1}$)	SD/100 (-)	$P\eta_{100}/\text{SD}$ ($\text{l cSt m}^{-2}\text{h}^{-1}\text{bar}^{-1}$)
350	0.56 ± 0.06	4.1 ± 0.5	2.1 ± 0.1	1.0 ± 0.2
550	0.57 ± 0.06	3.7 ± 0.6	2.1 ± 0.1	1.0 ± 0.2
1000	0.60 ± 0.06	3.3 ± 0.6	2.1 ± 0.1	0.9 ± 0.2
1300	0.62 ± 0.07	3.2 ± 0.5	2.1 ± 0.1	0.9 ± 0.2
2300	0.63 ± 0.08	3.0 ± 0.4	2.1 ± 0.1	0.9 ± 0.2

(b)

MW of PIB, (gmol^{-1})	η_{apparent} (cSt)	P_{hexane} ($\text{lm}^{-2}\text{h}^{-1}\text{bar}^{-1}$)	SD/100 (-)	$P\eta_{100}/\text{SD}$ ($\text{l cSt m}^{-2}\text{h}^{-1}\text{bar}^{-1}$)
350	0.55 ± 0.06	2.8 ± 0.3	1.8 ± 0.1	0.9 ± 0.2
550	0.56 ± 0.06	2.7 ± 0.3	1.7 ± 0.1	0.9 ± 0.2
1000	0.57 ± 0.06	2.6 ± 0.2	1.6 ± 0.1	0.9 ± 0.2
1300	0.59 ± 0.07	2.7 ± 0.2	1.6 ± 0.1	1.0 ± 0.2
2300	0.61 ± 0.08	2.7 ± 0.2	1.7 ± 0.1	1.0 ± 0.2

(c)

MW of PIB, (gmol^{-1})	η_{apparent} (cSt)	P_{hexane} ($\text{lm}^{-2}\text{h}^{-1}\text{bar}^{-1}$)	SD/100 (-)	$P\eta_{100}/\text{SD}$ ($\text{l cSt m}^{-2}\text{h}^{-1}\text{bar}^{-1}$)
350	0.54 ± 0.07	3.9 ± 0.6	0.9 ± 0.1	2.4 ± 0.4
550	0.55 ± 0.06	3.5 ± 0.5	0.8 ± 0.1	2.4 ± 0.4
1000	0.56 ± 0.07	3.1 ± 0.6	0.8 ± 0.1	2.2 ± 0.4
1300	0.57 ± 0.08	2.9 ± 0.4	0.8 ± 0.1	2.1 ± 0.3
2300	0.58 ± 0.08	2.8 ± 0.4	0.8 ± 0.1	2.1 ± 0.3

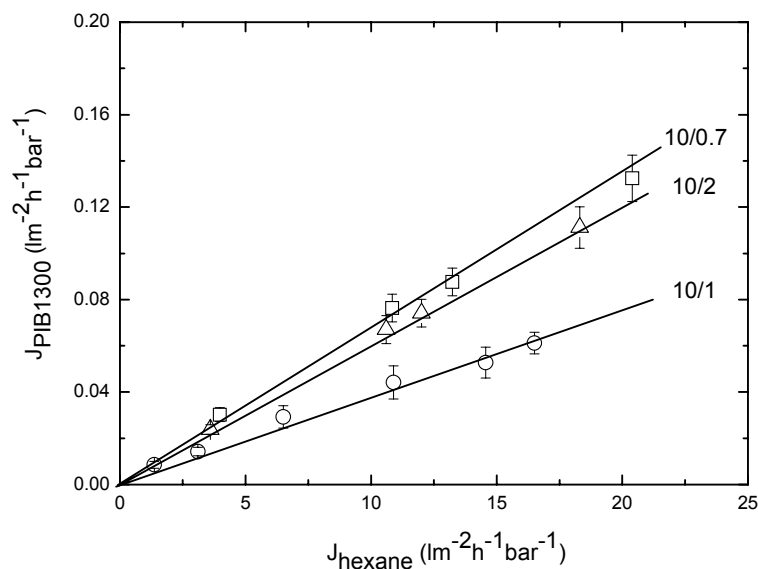


Figure 12: The flux of PIB 1300 as a function of the hexane flux for various cross-linking degrees of PDMS. Feed concentration: 8 % (w/w).

4.4.6. Retention performance

The effect of the PDMS cross-linking degree on the membrane retention for the tailor-made PAN/ PDMS membrane was investigated by determining the MWCO (defined as the MW of the solute that is rejected for 90 % by the membrane). *Figure 13* presents the results of the membrane retention for 8 % (w/w) PIB/hexane solutions at transmembrane pressure of 7 bar, for the PAN/PDMS composites prepared at pre-polymer/cross-linker of various ratios. The indicated MW of PIB is provided by the manufacturers (the polydispersity of PIB of various MW is presented in *Table 1*).

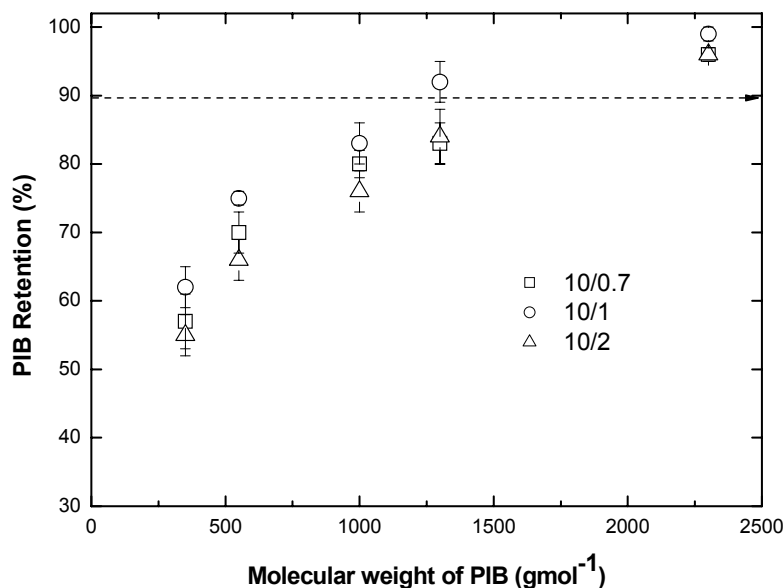


Figure 13: PIB retention by the PAN/ PDMS composite membranes prepared at pre-polymer/cross-linker of various ratios as a function of the molecular weight of PIB. Experimental conditions: feed concentration of 8 %(w/w), $\Delta p=7$ bar, at 24 ± 3 °C.

The relatively high membrane retention is probably based on the difference in solubility/diffusivity of hexane compared to PIB as discussed in Chapter 3. The membrane retention increases with the increase of the molecular weight of PIB. Although hexane-induced dragging increases the PIB flux, the strong effect of pressure on the chemical potential raises the hexane flux stronger than the dragging raises the PIB flux. Paul [43] stated recently that the consequence of the coupling effects in reverse osmosis might exist but they are too small to be noticeable.

Having in mind the polydispersity of the PIB, we can conclude that the retention performance is the same for all the PAN/PDMS composite membranes. The results of *Figure 9* allow us to estimate a MWCO of around 1200 - 1250 Da. The fact that the cross-linking degree of PDMS has no effect on the MWCO of the membrane might be attributed to the highly swollen state of the silicone network.

This hypothesis may be confirmed by the similar rejection performances of various dense, gas selective PDMS-based NF composite membranes were reported [38 and Chapter 2] although their PDMS layer had different cross-linking or thickness, resulting to differences in hexane permeability (4.4.5.).

In conclusion, for the PAN/PDMS composite membranes prepared at ratios of 10/0.7 and 10/2, the hexane permeability is higher than for the composite at 10/1, their retention, however, is similar. Therefore, the composite membranes with 10/0.7 or 10/2 might be more attractive for a practical (industrial) application due to their higher hexane flux without any compromise for the membrane retention.

4.5. Conclusions

In this chapter, PAN/PDMS composite membranes of various cross-linking degrees were prepared. Their transport properties for pure hexane and PIB/hexane solutions were systematically investigated.

The swelling of the dense, free-standing PDMS membrane of various cross-linking degrees in hexane and PIB/hexane solutions slightly decreases when the pre-polymer/cross-linker ratio increases. The partition coefficient of PIB decreases with the increase of cross-linker content and with the increase in PIB molecular weight.

For the PAN/PDMS composite membranes the main findings are:

- The hexane permeability (P_{hexane}) through the PAN/PDMS prepared at pre-polymer/cross-linker ratio of 10/0.7 is higher than at pre-polymer/cross-linking ratio of 10/1 (4.5 and 3.1 $\text{lm}^{-2}\text{h}^{-1}\text{bar}$, respectively) due to the higher membrane swelling. The P_{hexane} through the PAN/PDMS prepared at pre-polymer/cross-linker ratio of 10/2 is higher than that through the composite prepared at ratio of 10/1 (4.1 and 3.1 $\text{lm}^{-2}\text{h}^{-1}\text{bar}$). This is not consistent with the swelling findings of the corresponding free-standing PDMS membranes. The higher P_{hexane} for the composite at ratio 10/2 might be due to less pore

intrusion of PDMS compared to 10/1 and/or due to the heterogeneity of the silicone network.

- Osmotic phenomena are observed for the PAN/PDMS prepared at pre-polymer/cross-linker of various ratios and can be interpreted using the van't Hoff equation.
- The cross-linking degree of PDMS has, however, no effect on the membrane retention probably due to the highly swollen state of the silicone network. Therefore, the PAN/PDMS membrane prepared at pre-polymer/cross-linker ratios of 10/0.7 and 10/2 might be attractive for a practical application due to their higher hexane permeability.

4.6. List of symbols

a_{pen}	Penetrant activity
B	Solute permeability coefficient
$c_{PIB,f}$	Concentration in the feed side (% w/w)
$c_{PIB,p}$	Concentration in the permeate side (% w/w)
$D_{i,j}$	Diffusion coefficient
E_m	Elastic modulus (MPa)
J	Flux through membrane
K	Partition coefficient
l	Membrane thickness (μm)
M_c	Average molecular weight between cross-links (gmol^{-1})
MW	Molecular weight (gmol^{-1})

$MWCO$	Molecular weight cut off (Da)
Δp	Transmembrane pressure (bar)
P	Permeability of hexane through the membrane
R	Membrane retention
SD	Swelling degree (%)
t	Time (h)
T	Temperature (K)
w_{PDMS}	Weight fraction of PDMS at swelling equilibrium

Greek symbols

α_{CO_2/N_2}	Gas selectivity of membrane for CO ₂ over N ₂
η	Viscosity (cSt)
ρ	Density (gcm ⁻³)
$\Delta\pi$	Osmotic pressure (bar)
ϕ_{pen}	Penetrant volume fraction
χ	Interaction parameter
v	Molar volume (cm ³ mol ⁻¹)

4.7. Acknowledgements

M.A. Hempenius (Materials Science and Technology of Polymers Group, University of Twente, The Netherlands) is acknowledged for his assistance in performing GPC and ¹H NMR experiments, as well as for the fruitful discussions.

4.8. References

1. N. Stafie, D. F. Stamatialis, M. Wessling, Insight into the transport of hexane-solute systems through tailor-made composite membranes, *Journal of Membrane Science* 228 (2004) p103-116.
2. I. F. J. Vankelecom, K. De Smet, L. E. M. Gevers, A. Livingston, D. Nair, S. Aerts, S. Kuypers, P. A. Jacobs, Physico-chemical interpretation of the SRNF transport mechanism for solvents through dense silicone membranes, *Journal of Membrane Science* 231 (2004) p99-108.
3. L. White, Transport properties of a polyimide solvent resistant nanofiltration membrane, *Journal of Membrane Science* 205 (2002) p191-202.
4. L. G. Peeva, E. Gibbins, S. S. Luthra, L. S. White, R. P. Stateva, A. G. Livingston, Effect of concentration polarisation and osmotic pressure on flux in organic solvent nanofiltration, *Journal of Membrane Science* 236 (2004) p121-136.
5. K. S. Bhanushali D, Kurth C, Bhattacharyya D, Performance of solvent-resistant membranes for non-aqueous systems: solvent permeation results and modeling, *Journal of Membrane Science* 189 (2001) p1-21.
6. D.R. Machado, D. Hasson, R. Semiat, Effect of solvent properties on permeate flow through nanofiltration membranes. Part I: investigation of parameters affecting solvent flux, *Journal of Membrane Science* 163 (1999) p93-102.
7. J. P. Robinson, E. S. Tarleton, C. R. Millington, A. Nijmeijer, Solvent flux through dense polymeric nanofiltration membranes, *Journal of Membrane Science* 230 (2004) p29-37.
8. R. Subramanian, M. Nakajima, K. S. M. S. Raghavarao, T. Kimura, Processing vegetable oils using nonporous denser polymeric composite membranes, *Journal of American Oil Chemists Society* 81 (2004) p313-322.

9. M.-B. Hagg, Membrane purification of Cl₂ gas: I. Permeabilities as a function of temperature for Cl₂, O₂, N₂, H₂ in two types of PDMS membranes, *Journal of Membrane Science* 170 (2000) p173-190.
10. Q. T. Nguyen , Z. Bendjama, R. Clément, Z. Ping, Poly(dimethylsiloxane) crosslinked in different conditions. Part II. Pervaporation of water-ethyl acetate mixtures, *Physical Chemistry Chemical Physics* 2 (2000) p395-400.
11. E. Favre, Q.T. Nguyen, P. Schaetzel, R. Clement, J. Neel, Sorption of organic solvents into dense silicone membranes. Part 1-Validity and limitations of Flory-Huggins and related theories, *Journal of Chemical Society Faraday Transaction* 89 (1993) p4339-4346.
12. Z. J. Tan, R. Jaeger, G. J. Vancso, Crosslinking studies of poly(dimethylsiloxane) networks: a comparison of inverse gas chromatography, swelling experiments and mechanical analysis, *Polymer* 35 (1994) p3230-3236.
13. J.S. Yoo, S. J. Kim, J. S. Choi, Swelling Equilibria of Mixed Solvent-Poly(dimethylsiloxane) Systems, *Journal of Chemical and Engineering Data* vol. 44 (1999) p16-22.
14. S.J. Clarson, J.A. Semlyen, *Siloxane Polymers*, PTR Prentice Hall, New Jersey, 1993.
15. J. M. Ziegler, F. W. G. Fearon, *Silicon-based polymer science: a comprehensive resource*, American Chemical Society, Washington DC, 1990
16. T. R. E. Simpson, B. Parbhoo, J. L. Keddie, The dependence of the rate of crosslinking in poly(dimethyl siloxane) on the thickness of coatings, *Polymer* 44 (2003) p4829-4838.
17. K. E. Perutz S., Baney J, Hui CY, Cohen C, Investigation of adhesion hysteresis in poly(dimethylsiloxane) networks using the JKR technique, *Journal of Polymer Science- Polymer Physics* 36 (1998) p2129-213936
18. S. K. Venkataraman, L. Coyne, F. Chambon, M. Gottlieb, H. H. Winter, Critical extent of reaction of a polydimethylsiloxane polymer network, *Polymer* 30 (1989) p2222-2226.

19. M. G. A. Shefer, Effect of crosslinks on the glass transition temperature of end-linked elastomers, *Macromolecules* 25 (1992) p4036-4042.
20. N. A. Peppas, C. T. Reinhart, Solute diffusion in swollen membranes. Part I. A new theory, *Journal of Membrane Science* 15 (1983) p275-287.
21. N. A. Peppas, *Hydrogels in medicine and pharmacy*, CRC Press, Boca Raton, 1986
22. P. G. de Gennes, *Scaling concepts in polymer physics*, Cornell University Press, 1979
23. P. J. Flory, *Principles of polymer chemistry*, Cornell University Press, Ithaca, NY, 1964
24. H. Lonsdale, U. Merten, and R. Riley, Transport of cellulose acetate osmotic membranes, *Journal of Applied Polymer Science*, 9 (1965) 1341.
25. J.G. Wijmans, and R.W. Baker, The solution-diffusion model: a review, *Journal of Membrane Science*, 107 (1995) p 1-21.
26. Q. T. Nguyen, Z. Bendjama, R. Clement, Z. H. Ping, Poly(dimethylsiloxane) crosslinked in different conditions Part I. Sorption properties in water-ethyl acetate mixtures, *Physical Chemistry Chemical Physics* 1 (1999) p2761-2766.
27. E. M. Barrall II, M. A. Flandera, J. A. Logan, A thermodynamic study of the crosslinking of methyl silicone rubber, *Thermochimica Acta* 5 (1973) p415-432.
28. J. Pickering, D. van der Meer, G. Vancso, Effects of contact time, humidity, and surface roughness on the adhesion hysteresis of polydimethylsiloxane, *Journal of Adhesion Science and Technology* 15 (2001) p1429-1441.
29. J. E. Mark, Recent studies of rubber elasticity, *Macromolecules Chem. Suppl.* 2 (1979) p87-97.
30. G. B. McKenna, K. M. Flynn, Mechanical and swelling behaviour of crosslinked natural rubber: consequences of the Flory-Rehner hypothesis, *Polymer Communications* 29 (1988) pp272-275.

31. L. Y. Yen, B. E. Eichinger, Vapor sorption isotherms for benzene and n-heptane with poly(styrene-co-butadiene), *Journal of Polymer Science: Polymer Physics* 16 (1978) p121-130.
32. R. W. Brotzman, B. E. Eichinger, Volume dependence of the elastic equation of state. 3. Bulk-cured poly(dimethylsiloxane), *Macromolecules* 15 (1982) p531 - 535.
33. C. Menduina, J. J. Freire, M. A. Llorente, T. Vilgis, Correctly averaged non-Gaussian theory of rubberlike elasticity. Application to the description of the behavior of poly(dimethylsiloxane) bimodal networks, *Macromolecules* 19 (1986) p1212-1217.
34. J. He, K. Horie, R. Yokota, Characterization of polyimide gels crosslinked with hexamethylene diisocyanate, *Polymer* 41 (2000) p4793-4802.
35. D. W. van Krevelen, P.J. Hoftijzer, *Properties of polymers, their estimation and correlation with chemical structure*, Elsevier, Amsterdam, 1976.
36. R. S. Harland, N. A. Peppas, Hydrophilic/hydrophobic, block and graft copolymeric hydrogels: synthesis, characterization, and solute partition and penetration, *Journal of Controlled Release* 26 (1993) p157-174.
37. I. F. J. Vankelecom, B. Moermans, G. Verschueren, P. A. Jacobs, Intrusion of PDMS top layers in porous supports, *Journal of Membrane Science* 158 (1999) p289-297.
38. S. Koike, S. R., N. H., N. M., Separation of oil constituents in organic solvents using polymeric membranes, *Journal of American Oil Chemists Society* 79 (2002) p937-942.
39. H. J. Zwijnenberg, A. M. Krosse, K. Ebert, K.-V. Peinemann, F. P. Cuperus, Acetone-stable nanofiltration membranes in deacidifying vegetable oil, *Journal of American Oil Chemists Society* 76 (1999) p83-87.
40. K. Ebert, F. P. Cuperus, Solvent resistant nanofiltration membranes in edible oil processing, *Membrane Technology*, 107 (1999) p5-8.
41. L. Lin, K. C. Rhee, S. S. Koseoglu, Bench-scale membrane degumming of crude vegetable oil: process optimisation, *Journal of Membrane Science*, 134 (1997) p101-108.

42. L. P. Raman, M. Cheryan, N. Rajagopalan, Deacidification of soybean oil by membrane technology, *Journal of American Oil Chemists Society* 73 (1996) p219-224.
43. D. R. Paul, Reformulation of the solution-diffusion theory of reverse osmosis, *Journal of Membrane Science* 241 (2004) p371-386.

The permeation performance of the PAN/PDMS composite membranes at high-pressure

Abstract

The purpose of this work is to investigate the permeation performance of the poly(acrylonitrile)/poly(dimethyl siloxane) (PAN/PDMS) composite membrane at high pressure. In specific, the effect of transmembrane pressure on the oil/hexane flux and oil retention is studied. The hexane flux increases linearly with applied pressure and no membrane compaction is found up to 30 bar. The membrane stability under the pressure is confirmed by similar hexane permeability at low and high pressure. No concentration polarization is found for the studied system. The PAN/PDMS tailor-made composite membrane presents high hexane permeability (around $3.0 \text{ lm}^{-2}\text{h}^{-1}\text{bar}^{-1}$) coupled with high oil retention (about 93%). The oil permeability coefficient increases with hexane flux, due to the solvent-induced solute dragging. The results for PAN/PDMS composite membranes are compared with the GKSS membranes, showing that the GKSS membrane compacts at pressure above 20 bar. The hexane permeability of the GKSS membrane is higher than of our PAN/PDMS tailor-made composite due to the differences in cross-linking degree and pore intrusion. Their retention characteristics are, however, similar.

5.1. Introduction

Solvent resistant nanofiltration membranes (SRNF) experience increasing attention lately, as they have a vast potential for novel applications in fine chemicals, pharmaceuticals, food and petrochemical industries [1]. For example, one of the most important steps in edible oil processing is the separation of hexane from oil. Compared to traditional unit operations, the use of membranes could enable considerable energy savings [2]. So far, we reported that the tailor-made PAN/PDMS composite membrane exhibits good permeation characteristics for oil/hexane solutions, up to 7 bar [3]. However, in the industrial applications pressures higher than 7 bar are required to obtain larger permeate fluxes, to be economically feasible [4 - 6].

One major drawback of the high pressure for the NF membrane may be the decline in flux due to the compaction and/or concentration polarization [4 - 13]. The membrane compaction is a mechanical deformation of the selective top layer and/or of the support membrane and, as a result, the flux through the composite decreases at high pressure. However, the compaction phenomenon is rather complex since may be reversible [7, 8] or irreversible [9] (depending on the membrane) and for the same membrane, at similar pressure, compaction may occur or not, depending on the permeating species [10]. Vankelecom et al. [11] suggested that the swelling of the membrane may have an important role for the compaction phenomenon: for the rigid polymers in non-swelling conditions, compaction at high pressures might be negligible while it may become important for the swollen networks. The authors studied the compaction of the dense PDMS membrane swollen with butanol and tetradecane. They concluded that the more swollen the membrane, the more important the compaction becomes. However, the opposite effect was observed by Machado et al. [10]. They reported a non-linear flux of alcohols through the MPF-50, which is a silicone composite membrane and, therefore, low interaction with alcohols was expected. Vankelecom et al. [11] suggested that this difference might be due to the role of the support of the MPF-50 composite membrane. On contrary, a series of papers

reported a good linearity of the flux of various solvents through the MPF-50 membrane with the applied pressure up to 55 bar [13, 14].

Concentration polarization can significantly affect the permeation performances of a SRNF membrane, at high solute concentration and high pressure. Peeva et al. [15] reported the existence of concentration polarization for tetraoctylammoniumbromide (TOABr)/toluene at 0.05-0.3 M (2.9 and 20 % w/w, respectively) and pressure up to 40 bar. Interestingly, no concentration polarization was found for the same membrane and docosane/toluene solution at concentration of 0.33 and 0.67 M (corresponding to 9.9 and 20 % w/w, respectively). The difference was attributed to the higher diffusion coefficient of docosane in toluene compared to TOABr and to the higher membrane retention towards TOABr compared with docosane. In Chapter 2 and 3, no significant effect of the stirring rate was found in the range of 100 -700 rpm for PAN/PDMS composite membrane and (oil, poly(isobutylene))/hexane solutions (above 700 rpm, the vortex occurred as discussed in Appendix I). However, the study of the hydrodynamics of the system would be useful especially at high pressure where concentration polarization may become important due to the higher permeate flux. This study investigates the transport of oil/hexane solution through the PAN/PDMS composite membrane, at pressure up to 30 bar. The stability of the membrane is studied by comparing the hexane permeability of the composite membrane at low and high pressure range. The effect of flow velocity on the permeate flux is studied in a permeation set up with cross flow configuration. The separation performances are compared with those of the semi-commercially GKSS membrane.

5.2. The effect of approximations in the solution-diffusion model at high pressure and large penetrants

The solution-diffusion model [16, 17] has already been discussed in detail in Chapter 2 and 3 of this thesis. Here, we will briefly remind the main equations and

their limitations at high pressure. The flux of a solvent species i through a non porous, dense membrane is given by:

$$J_i = \frac{D_i K_i c_{if}}{l} \left[1 - \exp\left(\frac{-\nu_i (\Delta p - \Delta \pi)}{R_g T}\right) \right] \quad \text{Equation 1a}$$

where D_i is the diffusion coefficient of i through the membrane, K_i is the sorption coefficient, c_{if} is the feed concentration of species i , respectively, ν_i is the partial molar volume of species i , Δp and $\Delta \pi$ is the difference in applied and osmotic pressure across the membrane. It has already been pointed out [14, 15, 18] one particularity of this model that needs attention: for aqueous systems, the model makes the approximation that the exponential term is small (low pressure range and small partial molar volume of water). Then, the *Equation 1* can be written as:

$$J_i = \frac{D_i K_i c_{if} \nu_i}{\ell R_g T} (\Delta p - \Delta \pi) \quad \text{Equation 1b}$$

where the solvent permeability term $P_{\text{solvent}} = \frac{D_i K_i c_{if} \nu_i}{\ell R_g T}$, is considered constant.

However, the above approximation may not be valid for organic solvents with larger partial molar volumes compared to water, especially at high-pressure, as we will show later. Similarly, the flux of the solute j is:

$$J_j = \frac{D_j K_j}{\ell} \left[c_{jf} - c_{jp} \exp\left(\frac{-\nu_j (p_f - p_p)}{R_g T}\right) \right] \quad \text{Equation 2a}$$

or, assuming that the exponential term is small

$$J_j = B(c_{jf} - c_{jp}) \quad \text{Equation 2b}$$

where B is usually constant and is called the solute permeability.

Table 1 gives an estimation of the errors that occur due to the approximation for the pure permeating components used in our study, hexane and sunflower oil, at 30 bar and 25 °C.

Table 1. Contribution of the exponential term in solution-diffusion model at 30 bar and 25 °C.

Liquid	Molar volume ($\text{cm}^3\text{mol}^{-1}$)	$\frac{v_i \Delta p}{R_g T}$	$1 - \exp\left(\frac{-v_i \Delta p}{R_g T}\right)$	Deviation (%)
Hexane	132	0.159	0.147	8.2
Oil	980	1.188	0.695	70.8

For large permeating components, like sunflower oil, the error can be quite significant (70.8%). So in the following discussion we use the extended equations (*Equations 1a* and *2a*) which take into account the influence of the transmembrane pressure and of the molar volume on the $J_{i,j}$.

5.3. Experimental

5.3.1. Materials

The PAN support membrane with MWCO of 30 kDa was provided by GKSS - Germany. The membrane was delivered in dry state and used without further treatment. The selective top layer of the composite was PDMS (RTV 615 type, kindly supplied by General Electric, The Netherlands), prepared at pre-polymer/cross-linker ratio of 10/1. The PAN/PDMS tailor-made composite membranes were prepared in a two-step coating procedure as described in Chapter 2.

The n-hexane (Merck, The Netherlands) and the sunflower oil (Fluka, The Netherlands) were used as supplied, without further purification. The refined

sunflower oil (purchased from Fluka – The Netherlands) consisted of a mixture of triglycerides (mostly C₁₈ with traces of C₁₆-C₂₀ fatty acids), of molecular weight of around 900. Linoleic acid was the major component of unsaturated chains. The PIB, Glissopal[®] of MW 1300 and 2300 were kindly provided by BASF - Germany and of MW 350, by Janex S.A.–Switzerland. The MW is given by the producer, with a degree of polydispersity (defined as the ratio of M_w to M_n, determined by GPC) in the range 1.8-3.6.

The GKSS membranes were radiation cross-linked PDMS-PAN composites supplied by GKSS Forschungszentrum, Germany [19]. The GKSS membranes were delivered in dry state and used without further treatment.

5.3.2. Permeation set-ups

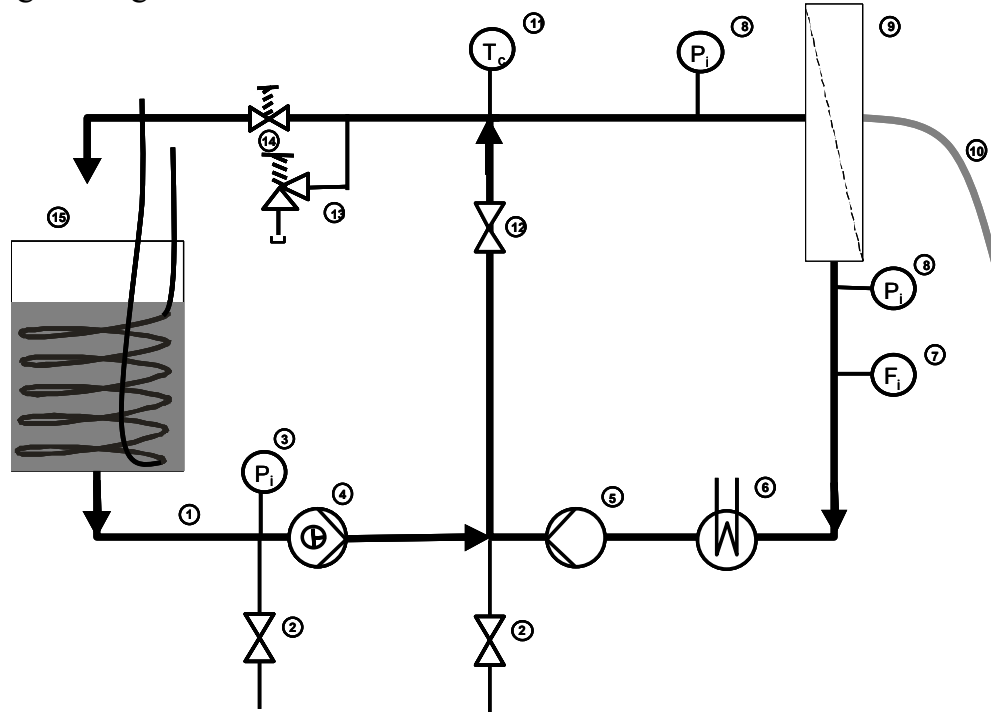
Dead end configuration

The permeation experiments in the batch mode were performed in a dead end filtration set-up described in details in Chapter 2. Helium gas was used to apply pressure up to 30 bar. The liquid permeation experiments were performed at room temperature (24 ± 3 °C), following the protocol: the membranes were placed in the test cells and a pre-conditioning step with pure hexane at 30 bar for 1 h was performed. Then, the system was slowly depressurized, the hexane was removed, the oil/hexane solution was placed in the reservoir and new pressure was applied. After each measurement, the system was slowly depressurized, the permeate was collected and analyzed and then returned to the feed reservoir.

Cross flow configuration

The liquid permeation experiments in the continuous mode were performed in a cross flow configuration set up (*Figure 1*). From the feed vessel (with a capacity of 15 l), the feed solution is pumped into the membrane cell with an effective membrane area of 250.2 cm². The permeate could either be circulated back to the

reservoir or collected separately for subsequent sample analysis. The retentate solution is recycled to the feed vessel, temperature controlled at 25°C with a heating/cooling coil.



1=feed line, 2=drain, 3=vacuum pressure meter, 4=frequency controlled pressure pump, 5=frequency controlled circulation pump, 6=heat exchanger, 7=flow meter, 8=pressure meters, 9=membrane module, 10=permeate tubing, 11=temperature controller, 12=ball valve, 13=pressure relief valve, 14=backpressure valve, 15=feed vessel.

Figure 1: Schematic drawing of the permeation set up.

Prior to an experiment, the membrane was placed in the test cell and a pre-conditioning step with pure hexane at 25 bar for 1 h was performed. Then, the system was slowly depressurized, the hexane was removed, the oil/hexane solution was placed in the feed vessel and new pressure was applied. With the pressure and cross flow set to the desired values, the permeate was circulated back to the feed vessel for an hour. The permeate was then collected in a separate vessel and used to determine de flux and oil concentration.

5.3.3. Analytical methods

The flux through the membrane was calculated by dividing the permeate volume (in l) to the membrane area (in m²) and collecting time (h). The permeate volume was determined by dividing the collected weight to the permeate density (kgm⁻³, measured by a Digital Density Meter, model DMA 50).

The sunflower oil concentration in the feed (c_{jf} , in mole fraction) and the permeate (c_{jp} , in mole fraction) solution was analyzed by refractive index measurements at 25 °C using a Abbe-3 refractometre, from Carl Zeiss, Germany. The sunflower oil retention was calculated using the equation:

$$R = \left(1 - \frac{c_{jp}}{c_{jf}} \right) \times 100 \quad \text{Equation 3}$$

For the batch mode, values and error bars reported in the tables and figures are based on at least three different samples. For the continuous mode, a single membrane was used and values and error bars reported in the figures are based on at least three different measurements.

5.4. Results and Discussion

5.4.1. Permeation experiments with the PAN/PDMS composite membrane

In order to develop membranes for industrial application, the stability of the membrane under the permeation conditions is very important. *Figure 2* shows the hexane flux through PAN/PDMS composite membrane during 15 h permeation

experiments, at 30 bar (the experiment was performed for 8 h per day. Overnight, the membranes were kept in hexane and the experiment continued the next day). The hexane flux is constant, showing that the morphology of the PAN/PDMS composite membrane does not change under the employed conditions.

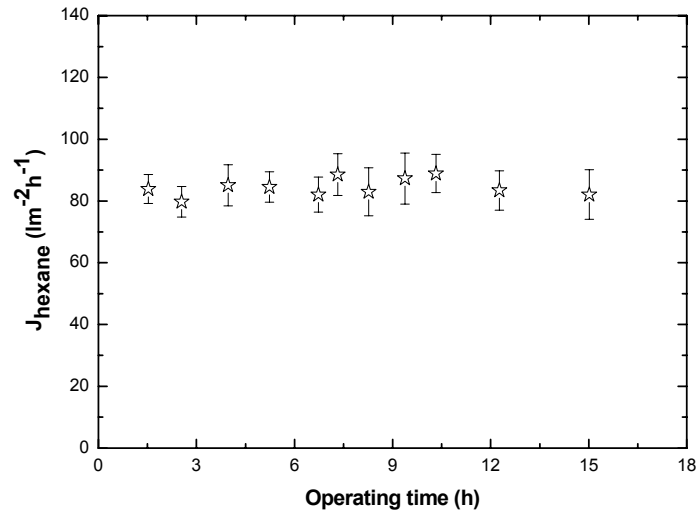


Figure 2: Hexane flux through PAN/PDMS membrane as a function of operating time, at 30 bar and 24 ± 3 °C.

In order to investigate if the membrane morphology is stable at various pressure histories, we performed a series of experiments with hexane at different pressures. After 1 h of pre-compaction with hexane at maximum applied pressure (7, 20 or 30 bar, respectively), the system was slowly de-pressurized and the hexane flux versus pressure was measured. *Figure 3* shows that the hexane flux is constant, independent on the history of the permeation experiments.

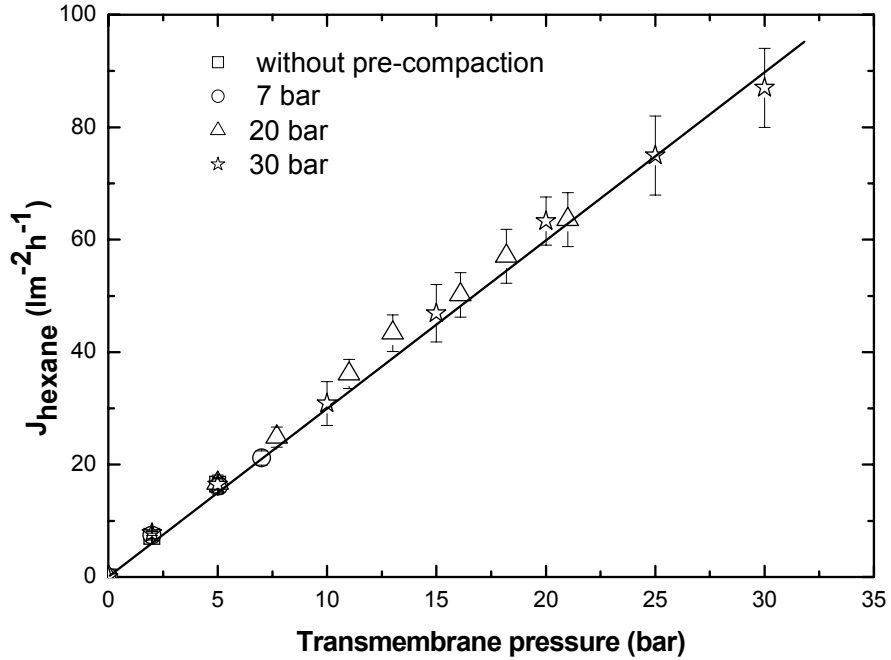


Figure 3: Hexane flux as a function of transmembrane pressure after various pre-compaction pressures, at 24 ± 3 °C.

Figure 4 shows the comparison between the hexane flux through a new, virgin PAN/PDMS composite membrane and through the same membrane after continuous permeation of about 1 month. In both cases, the hexane flux is similar, indicating the stability of the membrane under employed conditions.

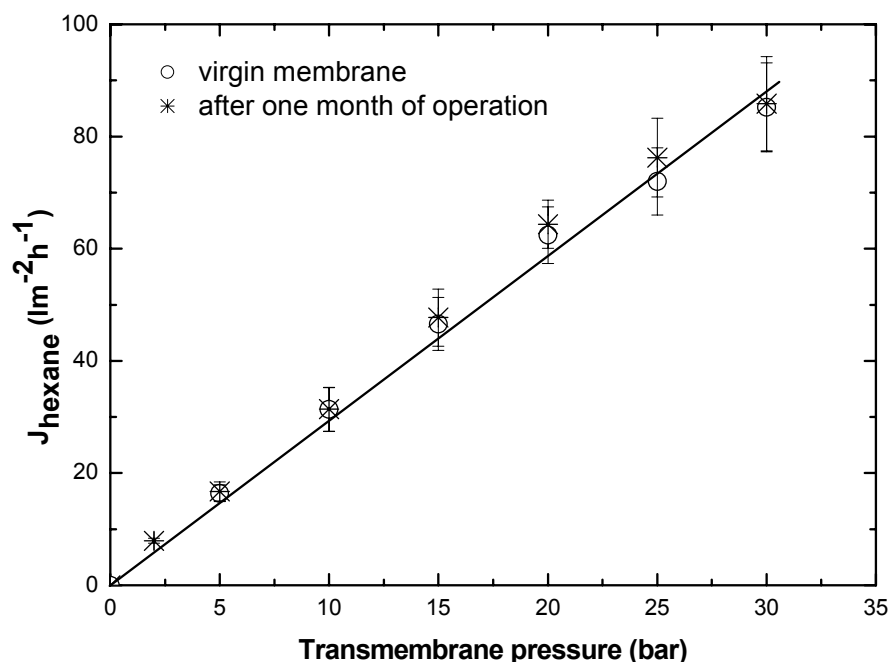


Figure 4: Hexane flux as a function of transmembrane pressure through a PAN/PDMS virgin membrane and through one and the same membrane after about 1 month of oil/hexane permeation experiments, at 24 ± 3 °C.

Figure 3 and 4 show that the hexane flux increases linearly with applied pressure, indicating no membrane compaction (for the data of pre-compaction at 20 and 30 bar, the linear correlation between hexane flux and applied pressure has the least squares regression of 0.99). Therefore, Equation 1b can be used to describe the hexane transport through the PAN/PDMS at high pressure, as well. Although the importance of the exponential term approximation has been shown (see 5.2), the approximation (see Equation 1b) still gives a reasonable prediction of the hexane flux, due to the relative low molar volume of hexane. The hexane permeability is $P_{\text{hexane}} = 3.0 \pm 0.3 \text{ lm}^{-2}\text{h}^{-1}\text{bar}^{-1}$, in agreement with that at low pressure reported in Chapters 2 and 3.

The linear increase of the solvent flux with applied pressure is consistent with results reported in other studies [9, 13]. On contrary, Paul et al. [20 - 22] reported that the flux of various solvents through lightly cross-linked, freestanding natural

rubber membrane increased linearly at low pressures (up to 6 bar) and levels off at higher pressures (limiting flux). The authors attributed the limiting flux to the solvent concentration gradient within membrane. This membrane was highly swollen by the organic solvents and, under the applied pressure, large concentration gradients developed through the membrane even at relatively low pressures. The concentration in the membrane on the permeate side drops to zero and the flux through the membrane reaches a limiting value as feed pressure increases. The decrease in the slope of the curve at the higher concentration difference reflects a decrease in diffusion coefficient as the swelling of the membrane decreases, according to the solution-diffusion model. The difference between the experimental results reported by Paul et al. and our data is probably due to the membrane thickness. They used thick, free-standing natural rubber membrane of 275 μm , whereas we used a PAN/PDMS composite membrane with a selective PDMS layer of about 1-2 μm where such a significant gradient in hexane concentration is not probable. To study the effect of the membrane thickness on the concentration gradient, we also performed permeation experiments with the dense, free-standing PDMS membrane. First, the PDMS membrane was swollen in hexane and then placed in the test cells, directly on the PAN support, and low pressure (1 bar) was applied. A significant highly hexane flux than expected for a dense PDMS membrane was obtained. By examining the membrane after the permeation measurement, large cracks in the PDMS membrane could be observed, indicating that the measured hexane flux corresponds to the PAN support rather than to the dense silicone membrane. The same procedure was performed for a dry dense PDMS but again the same phenomenon occurred, probably because the used dense, free-standing PDMS membrane did not have mechanical resistance to stand the applied pressure. For oil/hexane solution, we performed permeation experiments in the concentration range of 0.008-0.039 mol fraction (corresponding to 8-30 % w/w), investigating the effect of high pressure on the permeation characteristics of the PAN/PDMS composite membranes.

Figure 5 shows that the total flux (oil and hexane) decreases with increase in permeation time, at transmembrane pressure of 15 and 30 bar, respectively.

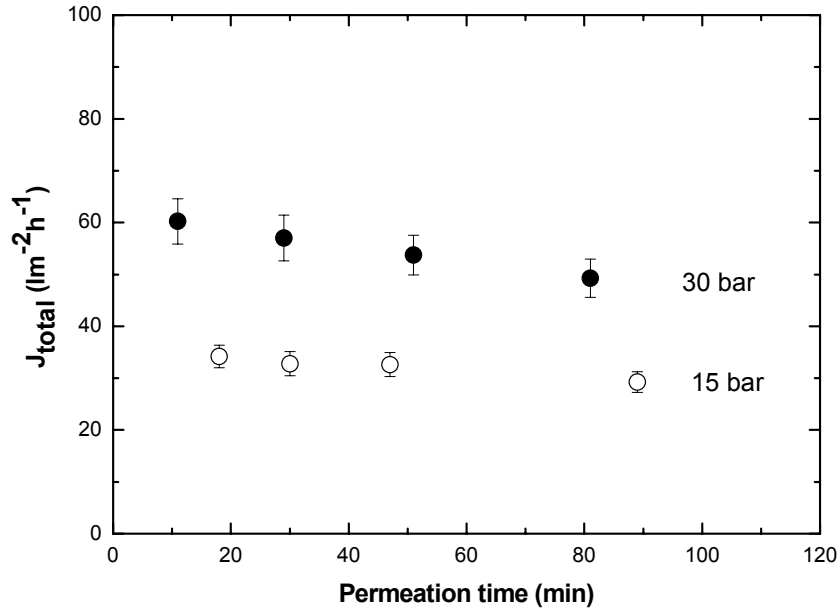


Figure 5: Total flux through PAN/PDMS membranes as a function of permeation time, at 0.008 mol fraction oil/hexane and 24 ± 3 °C.

One possible cause for this behavior could be the increase in concentration of the feed solution during the batch mode permeation experiment. This effect is more important at low feed concentration and high transmembrane pressure (larger permeate flux). For example, for oil/hexane feed solution of 0.008 mol fraction, at 30 bar transmembrane pressure, the concentration of the feed increases to 0.012 mol fraction in 1 h. So the viscosity of the solution inside the membrane ($\eta_{apparent}$), the membrane swelling (SD) and the osmotic pressure difference ($\Delta\pi$) will change as well. Those parameters are found to be responsible for the mass transport in Chapter 3. For the PAN/PDMS composite membrane at a given cross-linking degree, the normalized hexane permeability $\frac{P_{hexane} \times \eta_{apparent}}{SD}$ is similar at various oil/hexane concentrations. To be able to know the hexane flux at the

starting feed concentration, we use the normalization $\frac{P_{\text{hexane}} \times \eta_{\text{apparent}}}{SD}$ at the

beginning of permeation experiment and at the end of permeation experiment. Therefore, the J_{hexane} can be corrected, eliminating the concentration mode.

Figure 6 shows the measured and corrected J_{hexane} versus transmembrane pressure of a 0.008 mol fraction oil/hexane feed solution.

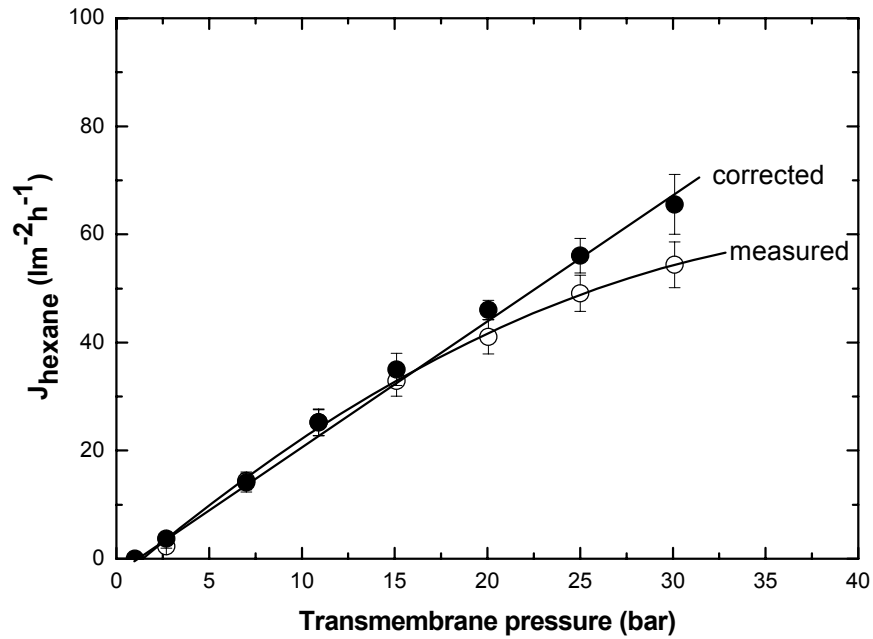


Figure 6: Hexane flux as a function of transmembrane pressure: measured and corrected data for the concentration mode. Experimental conditions: 0.008 mol fraction oil/hexane feed, at 24 ± 3 °C.

It seems that the curvature of the J_{hexane} can be eliminated by the applied correction and the hexane flux through the PAN/PDMS membranes becomes linear with the transmembrane pressure.

Figure 7 presents the corrected hexane flux versus transmembrane pressure at various oil/hexane concentrations.

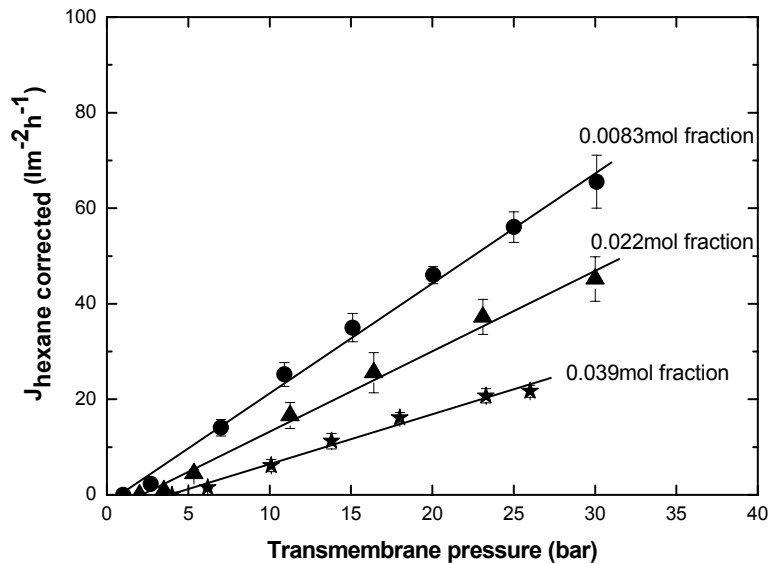


Figure 7: The hexane flux through PAN/PDMS membrane as a function of transmembrane pressure, at various oil/hexane concentrations and 24 ± 3 °C.

The hexane permeability (defined as the slope of J_{hexane} versus pressure) decreases with increase in oil concentration of the feed solution due to the increase of feed viscosity. The decrease of flux through the membrane with increase of the solute concentration is consistent with previously published data [6, 9, 14].

A second permeation set up was also available (on a limited basis), allowing to perform permeation experiments through the PAN/PDMS composite membrane in cross flow mode, up to 25 bar and cross flow rate up to 2.4 l/min. The aim of this study is to investigate if concentration polarization phenomenon is important in this system. First, the permeation of oil/hexane concentrations of 0.008 and 0.022 mol fraction were performed at various pressures and flow rates. The mass transfer limitation caused by concentration polarization is expected to be more important at higher oil concentration.

Figure 8 shows the hexane flux through the PAN/PDMS membrane as a function of transmembrane pressure, at 0.022 mol fraction concentration. Similar results were obtained at 0.008 mol fraction concentration (not shown here).

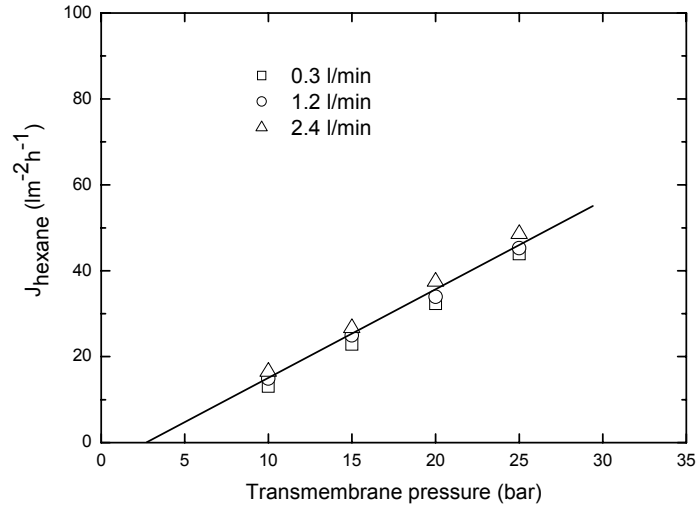


Figure 8: Hexane flux through the PAN/PDMS membrane as a function of transmembrane pressure, at various flow rates. Experimental conditions: concentration of 0.022 mol fraction, 25 °C.

The cross flow rate does not have a significant effect on the hexane flux, over the tested range, indicating the absence of concentration polarization under the studied conditions. Peeva et al. [15] did not find any influence of the flow rates on the flux for docosane/toluene solution at concentration of 0.05 and 0.09 mole fraction while the flow rate influence was significant for TOABr/toluene at 0.006-0.04 mole fraction. The difference was attributed to the higher diffusion coefficient of docosane in toluene compared to TOABr and to the higher membrane retention towards TOABr compared with docosane.

Figure 9 shows the effect of operating pressure on the hexane flux for the 0.008 and 0.022 mole fraction oil/hexane feed solutions. In both cases, the linearity with applied pressure indicates that no concentration polarization occurs in the system. The hexane permeabilities (calculated from the slope of the graphs of Figure 9) are similar with the values found in batch mode (Table 2).

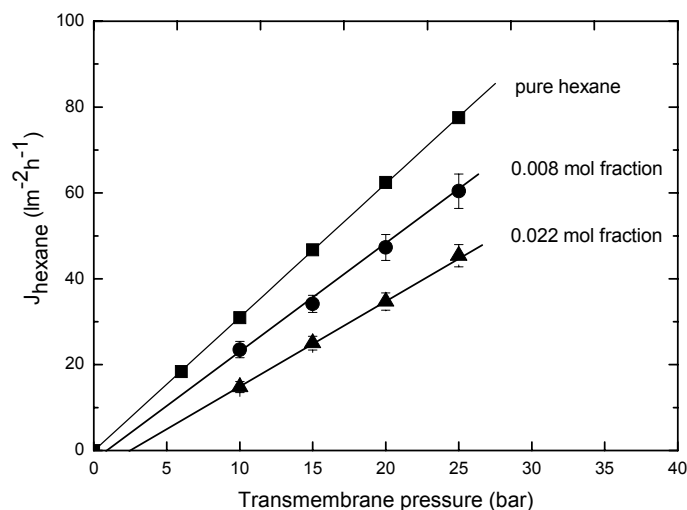


Figure 9: Hexane flux through the PAN/PDMS membrane as a function of transmembrane pressure, at various oil/hexane concentrations and 25 °C.

It is worth to mention that the hexane permeabilities are similar to the values reported at low-pressure range (Chapter 3). *Table 2* shows the comparison between the hexane permeability of the PAN/PDMS composite membrane, at low and high pressure, in batch and continuous mode.

Table 2: Comparison between the P_{hexane} at low and high pressure for PAN/PDMS membrane, at various oil/hexane concentrations.

Oil concentration (mole fraction)	$P_{low\ pressure}$ ($lm^{-2}h^{-1}bar^{-1}$)	$P_{high\ pressure}^a$ ($lm^{-2}h^{-1}bar^{-1}$)	$P_{high\ pressure}^b$ ($lm^{-2}h^{-1}bar^{-1}$)
0	3.1 ± 0.4	3.0 ± 0.3	3.1
0.008	2.4 ± 0.3	2.3 ± 0.2	2.5 ± 0.1
0.022	1.8 ± 0.4	1.7 ± 0.3	2 ± 0.1
0.039	1.1 ± 0.3	1.1 ± 0.2	n.m.

a values measured in batch mode

b values measured in continuous mode

n.m not measured

There is no significant difference between the membrane performances at high and low pressure, indicating the stability of PAN/PDMS membrane under employed conditions.

Figure 10 presents the oil retention by the membrane versus transmembrane pressure at various oil/hexane concentrations. For the calculation of R_{oil} , the average of the concentration of the initial feed and the retentate was used as concentration of feed.

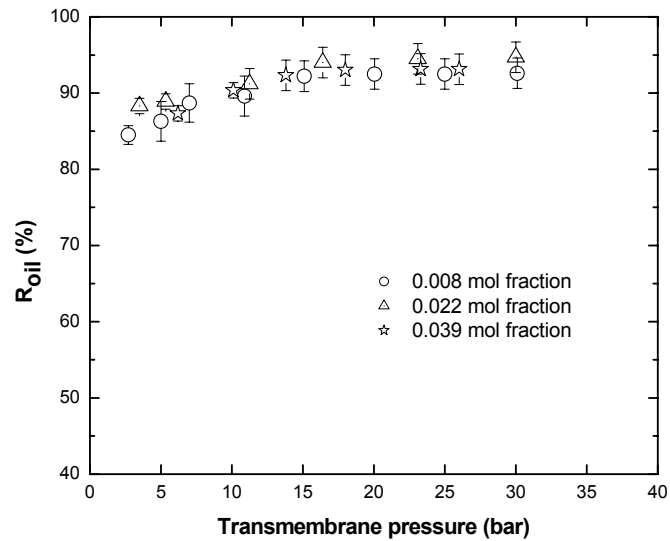


Figure 10: Oil retention by PAN/PDMS membrane as a function of transmembrane pressure, at various oil/hexane concentrations and 24 ± 3 °C.

At low pressures, the retention increases with the transmembrane pressure. When the pressure increases, the increase of hexane flux is much higher than the relative increase of the oil flux leading to increase of retention at high pressure (*Figures 11 and 12*).

Oil rejection by PAN/PDMS was also studied at different cross flow rates and oil concentrations. No significant influence of the flow rate was found at 0.008 and 0.022 mol fraction, indicating the lack of concentration polarization under the employed conditions.

Figure 11 shows the effect of hexane flux upon the oil permeability (B) at various oil/hexane feed concentrations.

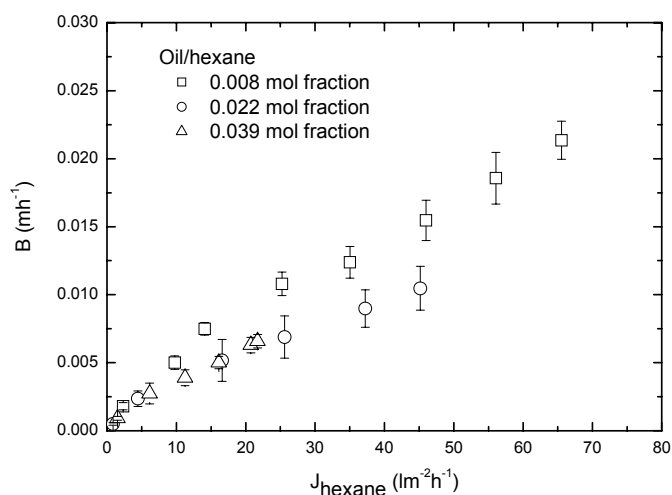


Figure 11: Effect of the hexane flux upon oil permeability coefficient, at various oil/hexane concentrations.

To calculate B the *Equation 2a* was used, since the approximation (*Equation 2 b*) introduces a large error (see 5.2). The oil permeability coefficient increases significantly with hexane flux. The results of *Figure 11* confirm the data obtained at low pressure range (1-7 bar) where the dragging effect is found to be dependent on the molecular weight and on the concentration of the solute in feed (*Figure 12*).

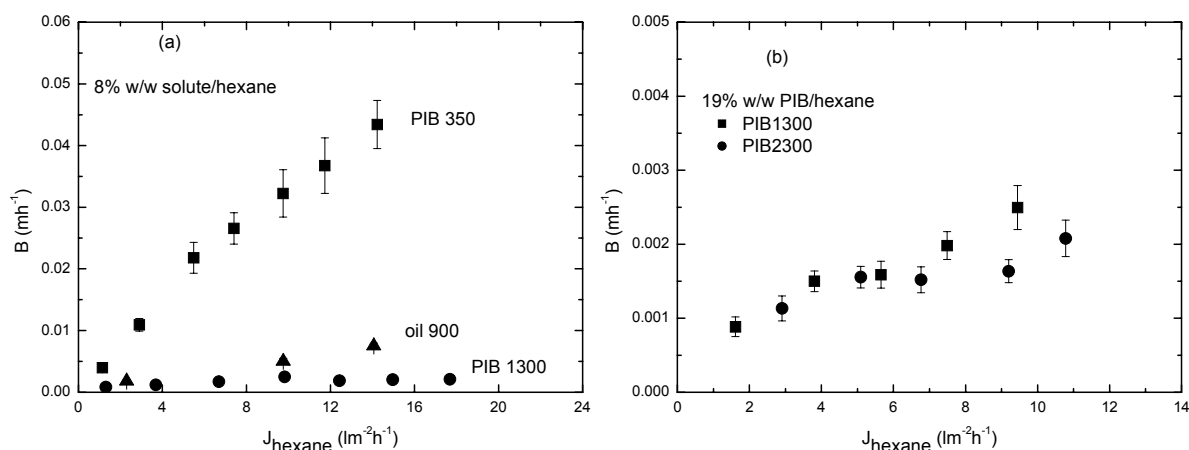


Figure 12: Effect of molecular weight at (a) low feed concentration and (b) at high feed concentration upon oil permeability.

Probably, at high solute concentrations where the swelling of the membrane is lower and the “apparent” viscosity inside the membrane is higher, the dragging effect on the solute transport is restricted, as already discussed in [3].

5.4.2. Permeation experiments with the GKSS membrane

The GKSS membrane was also characterized in order to compare its separation performance at high pressure with that of the PAN/PDMS tailor-made membrane. The GKSS membrane used in the current study is a radiation cross-linked PAN/PDMS composite [19]. The gas permeation experiments show that the membrane selectivity α_{CO_2/N_2} is 10.3 ± 0.4 , indicating a PDMS selective top-layer. We performed permeation experiments with oil/hexane solution in the concentration range of 0-0.039 mol fraction (corresponding to 0-30 % w/w). *Figure 13* presents the effect of the transmembrane pressure on the flux of pure hexane.

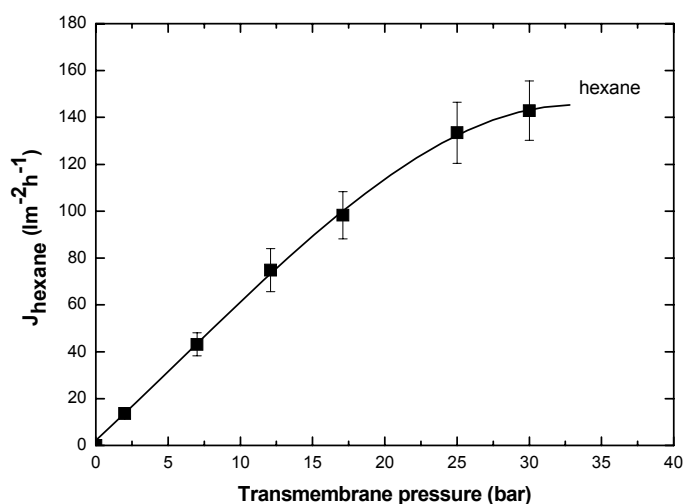


Figure 13: Hexane flux through the GKSS membrane as a function of transmembrane pressure at 24 ± 3 °C.

Unlike the PAN/PDMS tailor-made membrane, hexane flux through the GKSS membrane is not linear with transmembrane pressure, suggesting that the membrane is compacted at pressure higher than 20 bar. One possible cause may be the compaction of the support membrane, phenomenon already reported for other composite membrane (MPF-50) [11]. In Chapter 2, we reported the permeation performance of GKSS at low pressure, too. The hexane flux increased linearly with the applied pressure up to 7 bar, indicating that no compaction occurred. Interestingly, Robinson et al. [23] reported a non-linear correlation between the hexane flux through a GKSS membrane and the applied pressure (up to 9 bar). Based on this finding, they proposed two distinct mechanisms for the hexane transport through a GKSS membrane, pore-flow and solution-diffusion model, the inflexion point being the transition between the models.

The hexane permeability, P_{hexane} , of the GKSS membrane is calculated from the slope of the linear part of J_{hexane} versus transmembrane pressure. P_{hexane} of GKSS membrane is about two times higher than of PAN/PDMS (5.9 and 3.0 $\text{lm}^{-2}\text{h}^{-1}\text{bar}^{-1}$, respectively). The difference might be due to the difference in the cross-linking degree of the PDMS network and/or in the pore intrusion of PDMS. Note that the

PAN/PDMS composite membrane used in this study is prepared at pre-polymer/cross-linker ratio of 10/1. In Chapter 4, we reported the hexane flux for the PAN/PDMS prepared at various pre-polymer/cross-linker ratios and pore intrusions. *Table 3* compares the PDMS thickness visualized by SEM and the effective thickness of the PDMS calculated from CO₂ permeability measurements, assuming that the gas transport is completely determined by the PDMS for our PAN/PDMS tailor-made membranes and for the GKSS membrane.

Table 3: Effective and visualized PDMS thickness, and hexane permeability of the PAN/PDMS membranes prepared at pre-polymer/cross-linker of various ratios and of the GKSS membrane.

Pre-polymer/cross-linker ratio	$l_{\text{eff}}(\text{CO}_2)$ (μm)	l_{SEM} (μm)	P_{hexane} ($\text{lm}^{-2}\text{h}^{-1}\text{bar}^{-1}$) ¹
10/0.7	1.9 ± 0.2	0.9 ± 0.2	4.5 ± 0.5
10/1	2.0 ± 0.2	1.0 ± 0.2	3.1 ± 0.4
10/2	2.2 ± 0.3	1.8 ± 0.3	4.1 ± 0.5
GKSS membrane	2.2 ± 0.2	2.0 ± 0.2	5.9 ± 0.8

For the PAN/PDMS composite membranes prepared at pre-polymer/cross-linker ratios of 10/0.7 and 10/1, the difference between the effective and visualized thickness is about 1 μm . In between the PAN support and the top layer an intermediate layer probably exists where the PDMS penetrates into the pores of the support. The difference in hexane permeability is due to the difference in membrane swelling (260 and 200 % w/w, as reported in Chapter 4). For the composite membrane prepared at pre-polymer/cross-linker ratio of 10/2, however, the difference between the effective and visualized thickness is not as much, indicating that the pore intrusion in this membrane is less than for the other two composites. This might be the reason for the relatively high hexane permeability observed for this membrane, even though the membrane swelling is less than for

the other two membranes (about 100 %w/w, as reported in Chapter 4). A pore confinement restricts the swelling of the PDMS network immobilized inside the pores due to the rigidity of the support matrix.

For the GKSS membrane, the degree of cross-linking is not known. However, a lower cross-linking degree (as for the PAN/PDMS prepared at 10/7) combined with less pore intrusion (as for the PAN/PDMS prepared at 10/2) would lead to a PDMS composite membrane with higher hexane permeability than our tailor-made composites. Koike et al. [24] and Robinson et al. [23] reported also various hexane permeabilities ($4.7 \text{ lm}^{-2}\text{h}^{-1}\text{bar}$, effective thickness not revealed and $10 \text{ lm}^{-2}\text{h}^{-1}\text{bar}$, for $2\mu\text{m}$) through dense PDMS-based NF composite membranes. The gas selectivity of both membranes was reported to be the intrinsic PDMS gas selectivity, suggesting that the differences in hexane permeability might be given by the various cross-linking degree of the silicone network or pore penetration.

For the permeation of oil/hexane solution through the GKSS membrane, the concentration mode influences the permeate flux too, as for our PAN/PDMS composite. For the GKSS membrane, the rigorous correction with the concentration mode can not be done because the membrane swelling is not known (we do not have dense, free-standing GKSS membrane to perform swelling and partition experiments). However, for comparison, we consider the results of swelling degree with the PAN/PDMS composite membrane prepared at pre-polymer/cross-linker ratio of 10/0.7 (that has the highest hexane permeability). We apply the same procedure as for the PAN/PDMS composites to correct J_{hexane} for the concentration mode. *Figure 14* presents the effect of the transmembrane pressure on the corrected J_{hexane} through the GKSS membrane, at various oil/hexane concentrations.

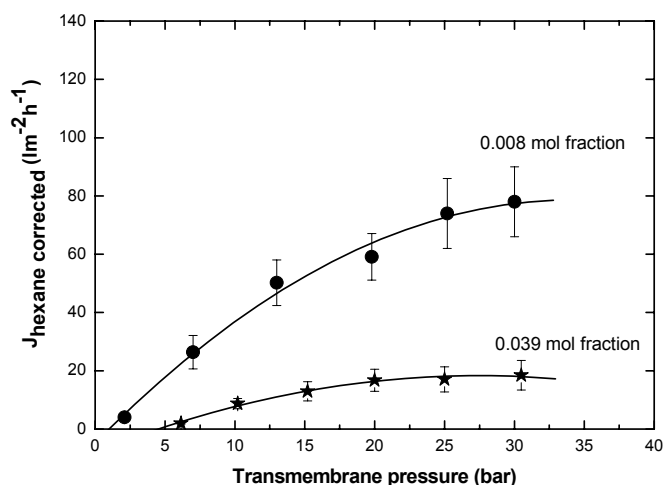


Figure 14: The hexane flux through GKSS membrane as a function of transmembrane pressure, at various oil/hexane concentrations and 24 ± 3 °C.

Unlike the PAN/PDMS tailor-made membrane, the curvature of hexane flux with the applied pressure still occurs, probably due to the membrane compaction. The x-intercepts (at $J_{\text{hexane}} = 0$) at each concentration correspond well to the osmotic pressure, $\Delta\pi$, calculated from the van't Hoff equation, as discussed in details in Chapter 3.

Figure 15 shows the oil retention of the GKSS membrane as a function of transmembrane pressure, at various oil/hexane concentrations. For the calculation of R_{oil} , the average of the concentration of the initial feed and the retentate was used as the feed concentration.

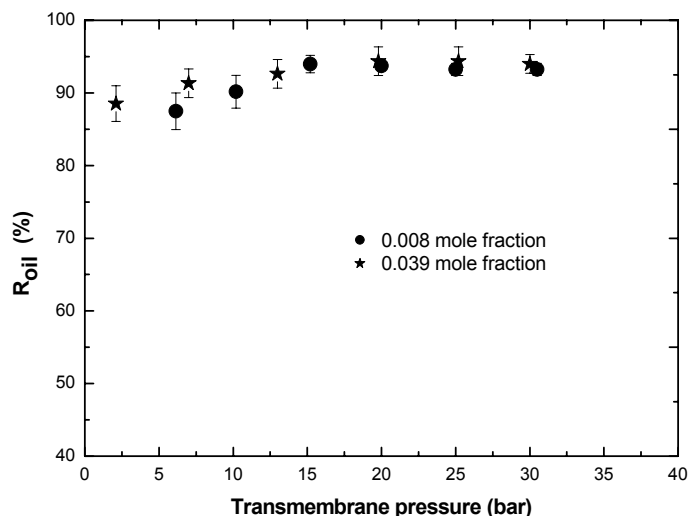


Figure 15: Oil retention for the GKSS membrane as a function of transmembrane pressure, at various oil/hexane feed concentration, at 24 ± 3 °C.

The retention of GKSS membrane is comparable with the PAN/PDMS tailor-made membrane. In addition, in Chapter 4 we reported similar retention for the PAN/PDMS composites prepared at various pre-polymer/cross-linker ratios. It seems that the differences in cross-linking degree and/or pore intrusion have no significant effect on the oil retention. Similar experimental findings are reported by Vankelecom et al. [25] studying the effect of intrusion of PDMS in Zirfon[®] (polysulfone filled zirconium oxide) support layers for pervaporation of the water-ethanol mixtures. For different pore intrusion depth, it was reported that the fluxes through the composite membranes varied, while the selectivity remained the same.

5.5. Conclusions

In this work, the tailor-made PAN/PDMS composite membrane is characterized for the separation of oil/hexane solution at high-pressure range. Our main findings are:

- Hexane flux increases linearly with the transmembrane pressure. No membrane compaction occurs up to 30 bar. The separation performances at high pressure are consistent with the low-pressure range data, indicating the stability of the PAN/PDMS composite membranes under high pressure.
- Comparison of the results from the continuous and batch mode indicates that no concentration polarization occurs in the system.
- The GKSS membrane shows a compaction at pressure above 20 bar which might be due to the support membrane. The hexane permeability of the GKSS membrane is higher than of our PAN/PDMS tailor-made composite due to the differences in cross-linking degree and pore intrusion. Their retention characteristics are, however, similar.

5.6. List of symbols

B	Solute permeability (m/h)
c_{jf}	Concentration of species j in the feed side (mole fraction)
c_{jp}	Concentration of species j in the permeate side (mole fraction)
D_{ij}	Diffusion coefficient through the membrane
J_i	flux of i through the membrane
K_j	Solute partition coefficient
$l_{eff.(CO_2)}$	Effective membrane thickness (μm)
l_{SEM}	Membrane thickness determined by SEM (μm)
MW	Molecular weight of the solute (gmol^{-1})
P	Hexane permeability through the membrane ($\text{lm}^{-2}\text{h}^{-1}\text{bar}^{-1}$)
Δp	Transmembrane pressure (bar)
R	Membrane retention (%)
α_{CO_2/N_2}	Gas selectivity of membrane for CO_2 over N_2
$\Delta\pi$	Osmotic pressure across the membrane (bar)
v	Molar volume ($\text{cm}^3\text{mol}^{-1}$)

5.7. References

1. D. Bhanushali, D. Bhattacharyya, Advances in solvent-resistant nanofiltration membranes - Experimental observations and applications, *Advanced Membrane Technology Annals of the New York Academy of Sciences* 984 (2003) p159-177.
2. S. S. Koseoglu, D. E. Engelgau, Membrane applications and research in the edible oil industry: an assessment, *Journal of American Oil Chemists Society* 67 (1990) p239-249.
3. N. Stafie, D. F. Stamatialis, M. Wessling, Insight into the transport of hexane-solute systems through tailor-made composite membranes, *Journal of Membrane Science* 228 (2004) p103-116.
4. K. K. Reddy, R. Subramanian, T. Kawakatsu, N. M., Decolorization of vegetable oils by membrane processing, *European Food Research Technology* 213 (2001) p212-218.
5. H. Zwijnenberg, A. Krosse, K. Ebert, K. Peinemann, C. FP, Acetone-stable nanofiltration membranes in deacidifying vegetable oil, *Journal of American Oil Chemists Society* 76 (1999) p83-87.
6. L.P. Raman, M. Cheryan, N. Rajagopalan, Solvent recovery and partial deacidification of vegetable oils by membrane technology, *Fett/Lipid* 98 (1996) p10-14.
7. J. P. Sheth, Y. Qin, K. K. Sirkar, B. C. Baltzis, Nanofiltration-based diafiltration process for solvent exchange in pharmaceutical manufacturing, *Journal of Membrane Science* 211 (2003) p251-261.
8. E. Gibbins, M. D' Antonio, D. Nair, L. S. White, L. M. Freitas dos Santos, I. F. J. Vankelecom, A. G. Livingston, Observations on solvent flux and solute rejection across solvent resistant nanofiltration membranes, *Desalination* 147 (2002) p307-313.

9. J. Whu, B. Baltzis, K. Sirkar, Nanofiltration studies of larger organic microsolute in methanol solutions, *Journal of Membrane Science* 170 (2000) p159-172.
10. D. R. Machado, D. Hasson, R. Semiat, Effect of solvent properties on permeate flow through nanofiltration membranes. Part I: investigation of parameters affecting solvent flux, *Journal of Membrane Science* 163 (1999) p93-102.
11. I. F. J. Vankelecom, K. De Smet, L. E. M. Gevers, A. Livingston, D. Nair, S. Aerts, S. Kuypers, P. A. Jacobs, Physico-chemical interpretation of the SRNF transport mechanism for solvents through dense silicone membranes, *Journal of Membrane Science* 231 (2004) p99-108.
12. L. White, Transport properties of a polyimide solvent resistant nanofiltration membrane, *Journal of Membrane Science* 205 (2002) p191-202.
13. D. Bhanushali, S. Kloos, C. Kurth, D. Bhattacharyya, Performance of solvent-resistant membranes for non-aqueous systems: solvent permeation results and modeling, *Journal of Membrane Science* 189 (2001) p1-21.
14. D. Bhanushali, S. Kloos, D. Bhattacharyya, Solute transport in solvent-resistant nanofiltration membranes for non-aqueous systems: experimental results and the role of solute-solvent coupling, *Journal of Membrane Science* 208 (2002) p343-359.
15. L. G. Peeva, E. Gibbins, S. S. Luthra, L. S. White, R. P. Stateva, A. G. Livingston, Effect of concentration polarisation and osmotic pressure on flux in organic solvent nanofiltration, *Journal of Membrane Science* 236 (2004) p121-136.
16. H. Lonsdale, U. Merten, R. Riley, Transport of cellulose acetate osmotic membranes, *Journal of Applied Polymer Science*, 9 (1965) 1341.
17. J. G. Wijmans, R. W. Baker, The solution-diffusion model: a review, *Journal of Membrane Science* 107 (1995) 1-21.
18. J. G. Wijmans, The role of permeant molar volume in the solution-diffusion model transport equations, *Journal of Membrane Science* 237 (2004) p39-50.

19. M. Schmidt, K.-V. Peinemann, N. Scharnagl, K. Friese, R. Schubert, Patent DE 19507584 C2, 1995
20. D. R. Paul, O. M. Ebra-Lima, Pressure-induced diffusion of organic liquids through highly swollen polymer membranes, *Journal of Applied Polymer Science* 14 (1970) p2201-2224.
21. D. R. Paul, J. D. Paciotti, O. M. Ebra-Lima, Hydraulic permeation of liquids through swollen polymeric networks. II. Liquid mixtures, *Journal of Applied Polymer Science* 19 (1975) p1837-1845.
22. D. R. Paul, J. D. Paciotti, Driving force for hydraulic and pervaporative transport in homogeneous membranes, *Journal of Applied Polymer Science* 13(1975) p1201-1214
23. J. P. Robinson, E. S. Tarleton, C. R. Millington, A. Nijmeijer, Solvent flux through dense polymeric nanofiltration membranes, *Journal of Membrane Science* 230 (2004) p29-37.
24. S. Koike, S. R., N. H., N. M., Separation of oil constituents in organic solvents using polymeric membranes, *Journal of the American Oil Chemists Society* 79 (2002) p937-942.
25. F. J. Vankelecom, B. Moermans, G. Verschueren, P. A. Jacobs, Intrusion of PDMS top layers in porous supports, *Journal of Membrane Science* 158 (1999) p289-297.

Effect of solvent and solute type on the mass transport through the PAN/PDMS composite membrane

Abstract

This work studies the influence of the solvent and solute type on the mass transport through the poly(acrylonitrile) (PAN)/poly(dimethylsiloxane) PDMS composite membranes. First, the role of the solvent (toluene and hexane) in the transport of sunflower oil is investigated. The flux of toluene through the PAN/PDMS membrane is lower than of hexane due to the higher viscosity of toluene compared to hexane. For the oil/toluene and oil/hexane solutions, the main parameters of the toluene/hexane transport through the PAN/PDMS tailor-made membranes are the “apparent” viscosity inside the membrane and the membrane swelling degree. The flux coupling for oil/toluene seems to be stronger than for oil/hexane probably due to the higher friction of toluene. The membrane retention of oil in toluene is lower than in hexane due to the lower toluene flux and smaller radius of gyration of oil in toluene. Osmotic phenomena are observed for oil/hexane and oil/toluene solution and can be interpreted using the van't Hoff equation, indicating that they behave as ideal systems.

For tetraoctylammonium bromide (TOABr)/toluene solution, the toluene flux is not linear with the applied pressure probably due to the concentration polarization phenomenon. The membrane retention is found to be 100 % and (almost) no osmotic effect was depicted, indicating the non-ideality of this system. This is probably due to ion-pairs clustering of TOABr in toluene and the thermodynamic non-ideality of the system.

6. 1. Introduction

The effect of the solvent and solute type on the mass transport through the nanofiltration (NF) membrane is an important issue for many processes of technological and scientific interests. The membrane-solvent-solute interaction is rather a complex aspect due to the wide range of polarity, viscosity and surface tensions for the solvents [1]. Moreover, the solvent-solute system complicates the interaction among solvent-solute-membrane. We reported [2] that the hexane transport through tailor-made PAN/PDMS membrane is influenced by an “apparent” viscosity of the solution inside the membrane and the membrane swelling. Vankelecom et al. [1] reported that the flux of various solvents (polar and non-polar) was influenced by the solvent viscosity and its affinity for a laboratory-made PAN-poly(ester) (PE)/PDMS membrane.

Koops et al. [3] performed permeation experiments of several solutes in ethanol and n-hexane through a laboratory-made cellulose acetate membrane. They concluded that the competition between solute-membrane-solvent interactions is important for the mass transport. A similar conclusion was drawn by Bhanushali et al. [4] permeating organic dyes and triglycerides in polar and non-polar solvents through a polyamide and a silicone type NF membrane. For the solvent/solute transport mechanism through the same membrane (STARMEM™ polyimide NF membrane), Scarpello et al. [5] suggested that other effects besides sieving may be important as the same solute is rejected to various extents in the presence of different solvents.

This work studies the influence of the solvent and solute type on the mass transport through the PAN/PDMS composite membrane. In particular, the influence on the separation performance of the membrane (flux and retention), on the solute-solvent coupling effect and on the osmotic pressure is explored. First, the role of the solvent (toluene and hexane) in the transport of sunflower oil is investigated. Then the role of solute (sunflower oil and TAOBr) in toluene is studied.

6.2. Experimental

6.2.1. Materials

The PAN support membrane with MWCO of 30 kDa was provided by GKSS - Germany. The membrane was delivered in dry state and used without further treatment. Its specifications are given in Chapter 2. The selective top layer of the composite was PDMS (RTV 615 type, kindly supplied by General Electric, The Netherlands), prepared at pre-polymer/ cross-linker ratio of 10/1. The PAN/PDMS tailor-made composite membranes were prepared in a two-step coating procedure as described in Chapter 2.

The toluene (Merck, The Netherlands), tetraoctylammonium bromide (TOABr, Aldrich, The Netherlands) and the sunflower oil (Fluka, The Netherlands) were used as supplied, without further purification. The refined sunflower oil consisted of a mixture of triglycerides (mostly C₁₈ with traces of C₁₆-C₂₀ fatty acids), of molecular weight of around 900. Linoleic acid was the major component of unsaturated chains. *Figure 1* shows the structures of the sunflower oil and TOABr.

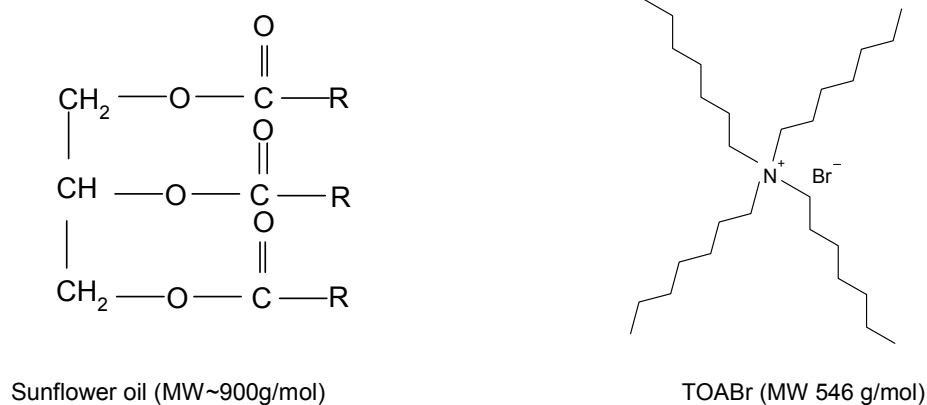


Figure 1: Structure of the sunflower oil and TOABr.

6.2.2. Permeation set-up and analytical methods

All the liquid permeation experiments were performed in a dead-end filtration set-up described in detail in Chapter 2. The permeation experiments were performed at room temperature (24 ± 3 °C), following the protocol: the membranes were placed in the test cells and a pre-conditioning step with pure toluene at 30 bar for 1 h was performed. Then, the system was slowly depressurized, the toluene was removed, the solute (oil or TOABr)/toluene solution was placed in the reservoir and new pressure was applied. The flux through the membrane was calculated by dividing the permeate volume (in l) by the membrane area (m^2) and the collecting time (h). After each measurement, the system was slowly depressurized, the permeate was collected and analyzed and then returned to the feed reservoir.

The sunflower oil concentration in the feed and the permeate solutions was analyzed by UV spectroscopy (Varian, Carry 300) at a wavelength of 295 nm. The absorbance was measured without dilution, using a 1cm cuvette with toluene as blank.

The concentration of TOABr was determined by gas chromatography (Shimadzu GC-2010 using a flame ionization detector and a Megabore column of diameter $\phi=0.32$ mm and length $l=25$ m).

Each permeation experiment was performed at least in triplicate. Values and error bars reported in the *Tables* and *Figures* are based on at least three different membranes.

The viscosities of the solutions were measured using Ubbelohde viscometer (model OC with an instrument coefficient of 0.0143 cSt/s) obtained from Tomson, The Netherlands. The densities of the solutions were measured using Digital Density Meter DMA 50, purchased from Anton Paar, The Netherlands.

6.2.3. Swelling experiments

For the swelling experiments, freestanding, thick PDMS membranes were used. They were prepared from 75 % (w/w) PDMS/hexane solution at room temperature by mixing the RTV A and RTV B components in 10:1 ratio. The details concerning the membrane preparation and swelling experiments are presented in Chapter 3. In the end of the swelling experiments, the samples were removed from the liquid solutions and dried. From the difference between the initial and final dry weight, the concentration of the

solute in the membrane ($c_{j,membrane}$) was measured and the solute partition coefficient K_j was calculated as presented in Chapter 3.

6.3. Results and discussion

6.3.1. Viscosity of the feed solutions

Figure 2 presents the kinematic viscosities of the various solutions.

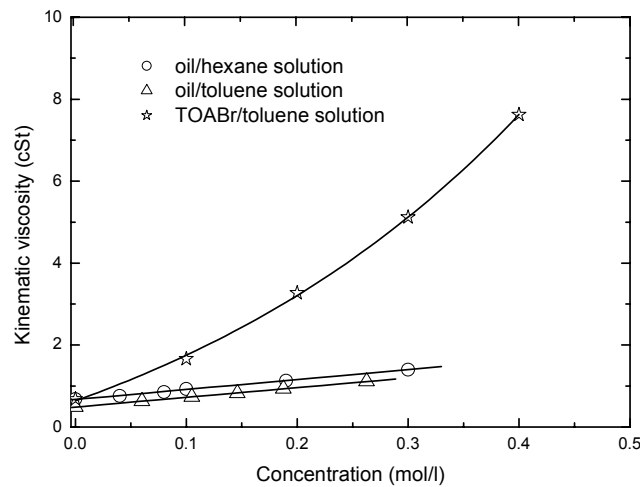


Figure 2: Kinematic viscosity of the feed solutions used in this study.

The viscosity of the oil/toluene and oil/hexane solution increases slightly with the oil concentration. However, the viscosity of TOABr/toluene solution increases significantly with the TOABr concentration. This behavior was already reported by Peeva et al. [6], suggesting that mass transfer limitations in the hydrodynamic boundary layer may be expected in this system due to the increased viscosity. The significant increase of solution viscosity with the TOABr concentration may be due to the self-association of TOABr in ion-pair clusters reported in the literature [7, 8] as will be discussed later.

6.3.2. The influence of the solvent on separation performance

6.3.2.1. Swelling measurements with dense PDMS membrane

The swelling degree of the PDMS dense membrane in various oil/toluene and oil/hexane solutions is an experimental measure of the affinity of silicone membrane-toluene/hexane-oil system. *Figure 3* presents typical results of the membrane swelling degree (SD) and of the solvent fraction (ϕ_{solvent}), at various oil/toluene concentrations. For comparison, the data obtained in Chapter 3 for the oil/hexane system are presented, too. The solvent fraction might be a better way to compare the swelling results of both oil solutions due to the difference in their density (note that $\rho_{\text{toluene}} = 0.87$ and $\rho_{\text{hexane}} = 0.66 \text{ gcm}^{-3}$, respectively [9]).

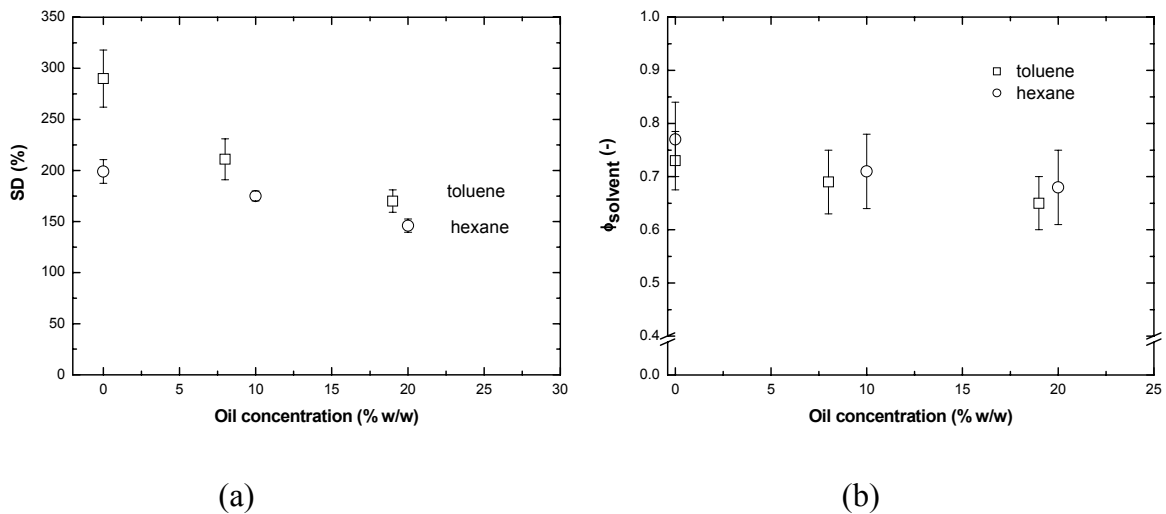


Figure 3: Typical results of the effect of the oil concentration upon (a) swelling degree of PDMS dense membranes and (b) solvent fraction, at various oil concentrations.

The membrane swelling in pure toluene is high, as expected from their similar solubility parameters ($\delta_{\text{toluene}} = 18.2$ and $\delta_{\text{PDMS}} = 14.9 - 15.6 \text{ MPa}^{1/2}$ [9]). The membrane swelling decreases with the increase of oil concentration, being very low in pure oil (about 5 % as reported in Chapter 3).

According to the Flory-Huggins solution theory, the χ interaction parameter of PDMS–toluene is calculated (the details concerning calculation of χ are presented in Chapter 3). *Table 1* summarizes the results for toluene, hexane and oil.

Table 1: Flory-Huggins interaction parameter (χ) calculated from the SD experiments [2].

	Toluene	Hexane	Oil
$\chi_{\text{PDMS-penetrant}}$	0.61 ± 0.02	0.58 ± 0.03	2.11 ± 0.02

For pure toluene-hexane, the $\chi_{\text{PDMS-solvent}}$ value of about 0.6 indicates a high membrane-toluene/hexane interaction whereas the χ_{oil} value of 2.11 shows a small interaction between membrane-oil. This indicates that the sorption of toluene-hexane in PDMS is thermodynamically more favorable than of oil in PDMS. When toluene and hexane are compared, the interaction parameter between PDMS-solvent is similar. *Table 2* presents the concentration of oil in the swollen PDMS membrane and the partition coefficients calculated for oil/toluene at various concentrations. For comparison, the data reported in Chapter 3 for the oil/hexane system, at similar oil concentrations are presented, too.

Table 2: Concentration inside the membrane and oil partition coefficient for the dense PDMS membrane and oil/toluene and oil/hexane systems, at 22 °C.

Solution	Oil conc. (% (w/w))	c_{membrane} (% (w/w))	K_{oil} (-)
Oil/toluene	8	2.0 ± 0.2	0.25 ± 0.02
	19	8.3 ± 1.0	0.44 ± 0.06
Oil/hexane	8	4.7 ± 0.3	0.59 ± 0.02
	19	8.1 ± 0.6	0.43 ± 0.04

For the 8 % w/w solution, the oil concentration inside the membrane is lower for toluene solution than for hexane solution. This indicates a decrease of oil affinity for PDMS membrane when toluene solution is used. Interestingly, for the 19% w/w feed solution, the oil concentration inside the membrane is similar for both oil/toluene and oil/hexane solutions.

In the end of the swelling experiments, when the swollen PDMS samples are rinsed with toluene and dried in the vacuum oven, the weight of the membrane does not differ from its initial dry weight. This result shows the stability of the dense PDMS membrane under the employed conditions.

6.3.2.2. Permeation performance

The filtration performance of the PAN/PDMS composite membrane in oil/toluene solutions at concentration of 0 - 19 %(w/w) was systematically investigated, including the influence of feed concentration and the effect of the transmembrane pressure upon the separation characteristics. For comparison, some of the results of oil/hexane system are included, too.

First, the behavior of the PAN/PDMS composite membrane at high pressure and longer permeation time was investigated. *Figure 4* shows the toluene flux through the membrane during permeation experiments at 30 bar.

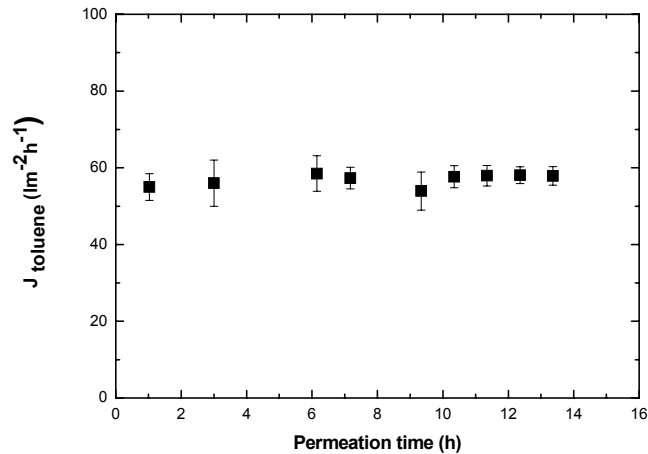


Figure 4: Toluene flux through PAN/PDMS composite membrane as a function of permeating time, at 30 bar and $24 \pm 3 \text{ }^\circ\text{C}$.

The flux of pure toluene through the PAN/PDMS membrane stays constant for 14 h of filtrations under pressure, indicating no compaction in time. In addition, no flux hysteresis with the applied pressure was found, showing that the applied pressure does not affect the membrane morphology. *Figure 5* presents the effect of the operating pressure on the toluene flux at various transmembrane pressures. For comparison, the hexane flux is given as well.

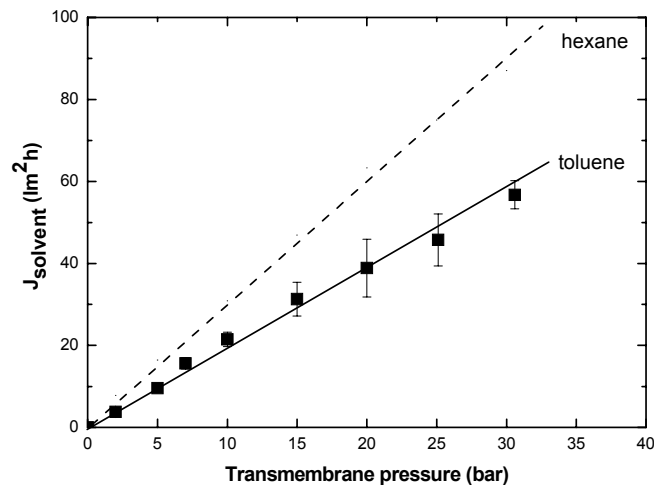


Figure 5: Toluene and hexane flux through PAN/PDMS composite membrane as a function of transmembrane pressure, at $24 \pm 3 \text{ }^\circ\text{C}$.

In both cases, the linearity of J_{solvent} with the applied pressure indicates that no compaction of the membrane occurs over the applied pressure range. The solvent permeability coefficient, P , (calculated from the slope of the plot of J_{solvent} versus Δp) is found to be $2.0 \pm 0.3 \text{ lm}^{-2}\text{h}^{-1}\text{bar}^{-1}$ for toluene while for hexane is $3.0 \pm 0.4 \text{ lm}^{-2}\text{h}^{-1}\text{bar}^{-1}$. The mass transport through the dense PDMS membrane can be described with the solution-diffusion model [1, 2, 6], presented in detail in Chapter 2. Shortly, the permeability of the penetrant through the membrane can be described by:

$$\text{Permeability} = \text{Solubility} \times \text{Diffusivity} \qquad \text{Equation 1}$$

Solubility is a thermodynamic parameter, corresponding to the amount of the penetrant sorbed by the membrane under equilibrium conditions. *Figure 3* shows that the affinity of toluene and hexane towards the dense PDMS is similar. However, the diffusivity of toluene through the PDMS is lower than of hexane (*Table 3* shows that η_{toluene} is higher than η_{hexane} and the Stokes-Einstein equation correlates the diffusion coefficient of the solvent to its viscosity). This experimental finding indicates that the diffusion coefficient is more important than the sorption for the transport of toluene-hexane through the PAN/PDMS composite membrane.

The toluene permeability reported for other silicone type NF composite are: $1.2 \text{ lm}^{-2}\text{h}^{-1}\text{bar}^{-1}$ for PAN-PE/PDMS membrane [1] and $1.3 \text{ lm}^{-2}\text{h}^{-1}\text{bar}^{-1}$ for the MPF-50 membrane (“silicone” based composite) [10]. For comparison, the toluene permeability of some non-silicone NF membranes: $0.6 \text{ lm}^{-2}\text{h}^{-1}\text{bar}^{-1}$ for a polyamide type membrane (Desal 5, Osmonics) [4] and $1.8 \text{ lm}^{-2}\text{h}^{-1}\text{bar}^{-1}$ for a polyimide membrane (STARMEM™ 122, W.R. Grace&Co.) [6] (in Chapter 3 the values of P_{hexane} reported in literature were given).

Figure 6 presents the effect of the transmembrane pressure on the solvent flux, corrected for the increase in concentration of the feed solution during the batch mode permeation experiment. The correction procedure is presented in detail in Chapter 5. Shortly, the solvent flux is corrected for the changes in feed viscosity, membrane swelling and osmotic pressure.

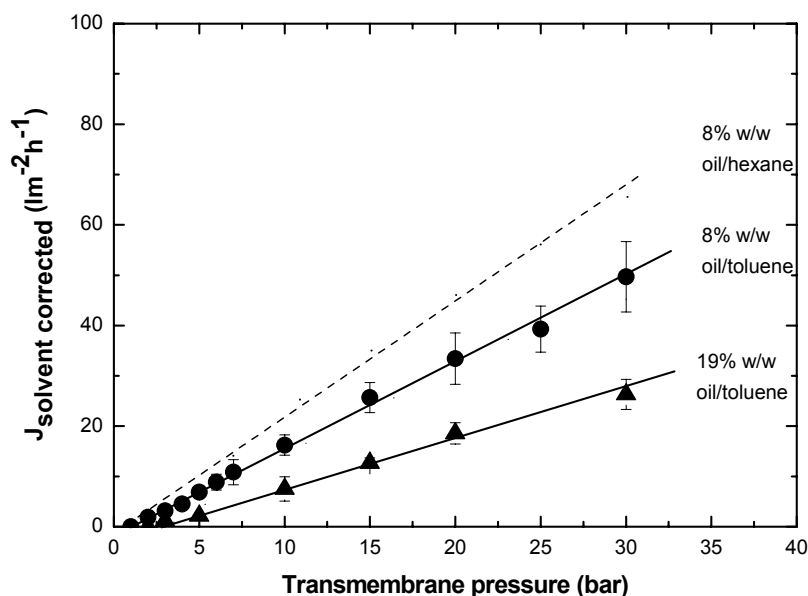


Figure 6: Corrected solvent flux through PAN/PDMS composite membrane as a function of transmembrane pressure for various oil/solvent concentrations, at 24 ± 3 °C.

Osmotic phenomena similar to those reported for oil and PIB/hexane solutions in Chapter 3 are found. *Figure 6* allows the quantification of the x -intercepts (at $J_{\text{solvent}} = 0$) for each oil/solvent concentration which can be compared with the osmotic pressures, $\Delta\pi$, calculated using the van't Hoff equation:

$$\Delta\pi = \frac{R_g T \Delta c}{M} \quad \text{Equation 2}$$

Δc is the solute concentration difference across the membrane and M is the solute molecular weight. The x -intercepts are again in very good agreement, within experimental error, with those of $\Delta\pi$ of *Equation 2* (x -intercept/calculated $\Delta\pi$ value: for 8% w/w, 1.1 bar/1.3 bar, for 19% w/w, 2.5 bar/2.7 bar). The van't Hoff equation is applicable in oil/toluene solutions due to the relative low feed concentrations (0.08-0.18 mol/l). Therefore, it looks as the oil/toluene and oil/hexane solutions behave as ideal systems concerning the osmotic phenomena.

The toluene permeability coefficient at various feed concentrations (calculated from the slopes of the graphs of *Figures 5 and 6*) decreases with the increase of oil concentration (see *Table 3*). This is due to the increased viscosity of the feed solution with oil concentration.

For oil/hexane solutions, we reported that the main parameters affecting the hexane permeability through the PAN/PDMS are an “apparent” viscosity and membrane swelling [2]. It remains open whether the toluene permeability can be normalized for these parameters, too.

Table 3: Parameters concerning the transport of oil / solvent solutions through the PAN/PDMS composite membranes, at 24 ± 3 °C.

Solvent	Oil conc. (% (w/w))	η_{apparent}^a (cSt)	P_{solvent} ($\text{lm}^2\text{h}^{-1}\text{bar}^{-1}$)	ϕ_{solvent} (-)	$P \eta_{\text{apparent}} / \phi_{\text{solvent}}$ ($\text{l cSt m}^2\text{h}^{-1}\text{bar}^{-1}$)
Toluene	0	0.61 ± 0.02	2.0 ± 0.3	0.73 ± 0.07	1.7 ± 0.2
	8	0.72 ± 0.01	1.6 ± 0.2	0.70 ± 0.06	1.6 ± 0.2
	19	0.89 ± 0.01	1.1 ± 0.2	0.64 ± 0.07	1.5 ± 0.2
Hexane	0	0.48 ± 0.02	3.0 ± 0.4	0.77 ± 0.08	1.8 ± 0.3
	8	0.57 ± 0.01	2.3 ± 0.3	0.73 ± 0.06	1.8 ± 0.3
	19	0.63 ± 0.01	1.7 ± 0.4	0.69 ± 0.07	1.6 ± 0.2

^a kinematic viscosity measured at 24 ± 3 °C (with Ubbelohde viscometer, from Tamson, The Netherlands).

^b calculated from the swelling experiments, assuming $\phi_{\text{solvent}} + \phi_{\text{PDMS}} = 1$.

The “apparent” viscosity inside the membrane is estimated from the concentration of oil in a hypothetical solvent/oil phase inside the membrane for the dense PDMS membranes (results of partition experiments of *Table 2*) and the plots of viscosity versus oil/toluene and oil/hexane concentration (data of *Figure 2*). For the swelling degree, the results of *Figure 3* concerning the dense PDMS membranes are used.

Table 3 shows that for various oil/solvent concentrations, the normalized P_{solvent} values do not differ significantly. If we assume the solution-diffusion model to hold for this

system, then we can interpret the solvent viscosity as a measure for the diffusion coefficient of solvent inside the silicone network and swelling as a measure for the solubility. However, the solvent/solute flux equations used in solution-diffusion model (described in details in Chapter 2) disregard the interaction between the solvent and solute. The effect of flux coupling of solvent-solute was experimentally depicted when permeating the oil and PIB solutions in hexane, at low and high applied pressure. The dragging effect was found to be influenced by the membrane swelling, the solute size, the concentration of feed solution (Chapter 3 and 5), and the cross-linking degree of PDMS network (Chapter 4). It would be interesting to study the influence of solvent on the permeability coefficient of oil too. *Figure 7* shows the effect of J_{solvent} on the J_{oil} at feed concentration of 8 % w/w oil/solvent solution.

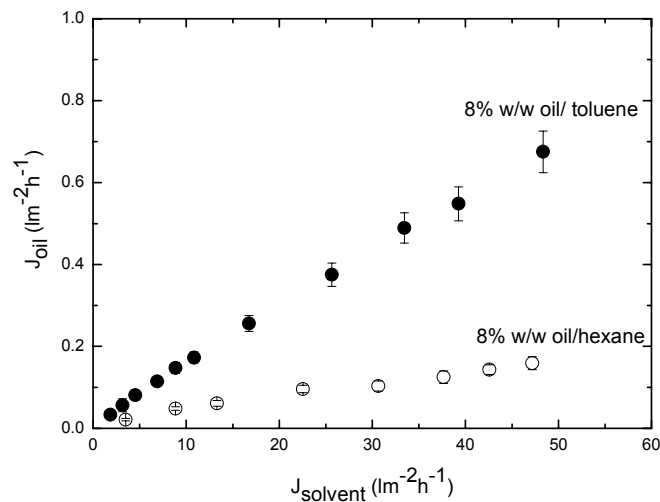


Figure 7: Oil flux as a function of the solvent flux at feed concentration of 8 % w/w.

For the same toluene/hexane-oil solution concentration, the oil flux increases with the solvent flux, indicating a flux coupling of solvent-oil system (solvent induced solute dragging). Interestingly, the coupling (dragging) seems to be more significant for the toluene-oil than for the hexane-oil system although the concentration of oil inside the membrane is lower for the toluene than for the hexane solution (*Table 2*). For the solute/solvent-membrane system, the dragging effect depends on the membrane swelling, the concentration of the solute, size of the solute, the solute-solvent affinity

and the viscosity of the solvent. The solubility of toluene and hexane in the dense PDMS membrane seems to be, however, similar when the results of the swelling experiments are compared (*Figure 3*). A good parameter to describe the solute size is the Stokes radius [3]. However, the Stokes radiuses of oil in toluene and of oil in hexane are similar, 1.72 and 1.98×10^{-10} m, respectively (calculated by using the Stokes Einstein equation). The dragging of solute by solvent would be larger when solute (oil) and solvent have a high affinity (similar solubility parameters). However, the difference in solubility parameter between oil ($\delta_{\text{oil}}=16.0 \text{ MPa}^{1/2}$, calculated with the group contribution method [11], considering linoleic acid as the main component of the oil) and hexane ($\delta_{\text{hexane}}=14.9 \text{ MPa}^{1/2}$ [9]) is lower than between oil and toluene ($\delta_{\text{toluene}}=18.2 \text{ MPa}^{1/2}$ [9]). This indicates a higher affinity of oil towards hexane compared to toluene. So the membrane swelling, the size of the oil and the oil-solvent affinity can not explain the experimental findings of *Figure 7*.

The difference in the solvent viscosity might be a probable cause for the larger dragging of oil by toluene. For toluene, the viscosity is 0.61 cSt and for hexane, 0.48 cSt. The larger viscosity for toluene implies a higher friction between the toluene molecules. Therefore, toluene might drag along more oil molecules than hexane.

Figure 8 shows the effect of solvent on the oil permeability coefficient for 8% w/w oil/solvent solution.

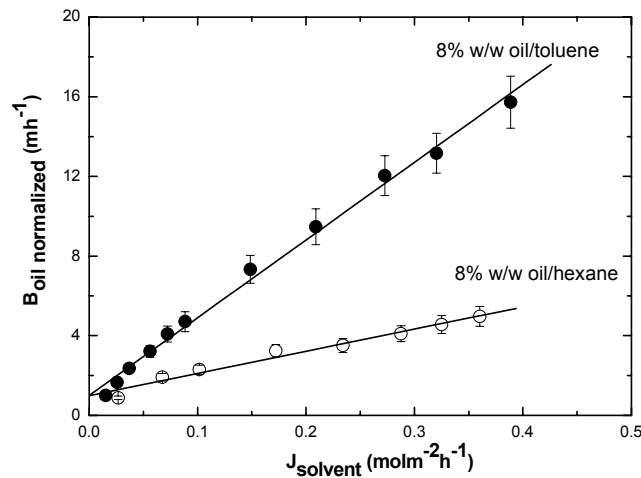


Figure 8: Effect of J_{solvent} upon normalized oil permeability coefficient, for 8% w/w oil/toluene and oil/hexane concentration.

The oil coefficient, B_{oil} , was calculated by using the solution-diffusion equation that describes the flux of oil, J_{oil} , through the membrane (presented in Chapter 5). We already showed that using the approximation to calculate B_{oil} generates large error, especially at high pressure. Therefore, we used the extended equation that takes into account the influence of the transmembrane pressure and of the solute molar volume on J_{oil} through the membrane. The B_{oil} normalized was calculated by extrapolating the B_{oil} -value to zero solvent flux, B_0 (intercept with the y-axis). Then the B_{oil} -value for toluene and hexane systems was divided by B_0 . So we can study directly the effect of the solvent on the solvent-induced solute dragging.

The B_{oil} normalized for the 8 % w/w oil/toluene solution is higher than for the 8 % w/w oil/hexane solution, as expected from the results of *Figure 7*. This indicates a stronger flux coupling between oil/toluene compared to oil/hexane. The presence of toluene or hexane might influence the permeability coefficient of oil through the PDMS membrane due to the change in the overall friction in the system. This overall friction results from frictional forces between solvent and oil, between solvent and membrane, and between oil and membrane. The resulting flux coupling of oil/toluene might be influenced stronger by this overall friction than that of oil/hexane because $\eta_{toluene}$ is higher than η_{hexane} . *Figure 9* shows the effect of transmembrane pressure on the oil retention at the 8 % and 19 % (w/w) oil/toluene solutions. For comparison, the results of oil/hexane are plotted, too.

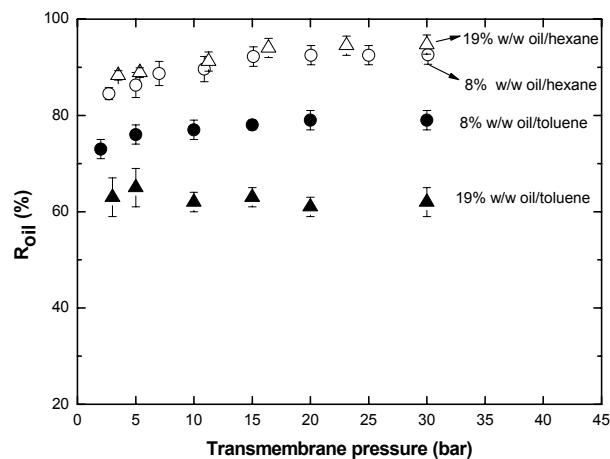


Figure 9: Oil retention by the PAN/PDMS composite membrane as a function of transmembrane pressure, for 8 and 19% (w/w) oil/toluene and oil/hexane solutions.

For 8 % w/w oil/toluene solution, the membrane retention increases slightly with the applied pressure (from 73 until 79%). When the pressure increases, the increase of toluene flux is much higher than the relative increase of oil flux leading to increase of retention (*Figure 7*). Similar results were reported in literature for various solute/solvent systems [2-5]. Interestingly, at 19 % w/w oil/toluene solution, the membrane retention is significantly lower compared to the membrane retention at 8% w/w feed. At 19 % w/w oil/toluene solution, a slight effect of concentration polarization may be expected since the calculated Reynolds number (*Figure 12*, details about the calculations of Re number are given later) indicates that the flow is in the transition regime of flow from laminar to turbulent. However, it does not have a significant effect on the J_{toluene} (*Figure 6*).

The membrane retention is lower for the oil/toluene solutions than for the oil/hexane solutions. Possible causes for this behavior may be the difference in the membrane swelling, the physico-chemical characteristics of oil in toluene and hexane, the viscosity of solvents and the dragging effect. However, the membrane is equally swollen in toluene and hexane and the Stokes radiuses of the oil in toluene and hexane are rather similar, 5.99 and 6.65×10^{-10} m. A smaller radius of gyration for oil molecules is expected in hexane compared to toluene due to the larger difference in the solubility parameters between oil/toluene and oil/hexane (as discussed above). This may decrease the membrane retention for the oil/toluene system. The larger viscosity of toluene implies a lower diffusivity of toluene molecules through the PDMS than for hexane, decreasing the membrane retention as well. In addition, it seems that the flux coupling is stronger for oil-toluene than for oil-hexane (*Figure 7*). All the above parameters may lower the membrane retention for the oil/toluene system compared to the oil/hexane system.

The results mentioned above show clearly that the solvent has a strong effect on the permeation characteristics of the PAN/PDMS composite membrane.

6.3.3. The influence of the solute on separation performance

For the TOABr-toluene, the viscosity of solution increases significantly with concentration (*Figure 2*) and the existence of mass transfer limitation might be, therefore, expected [6]. *Figure 10* shows the effect of transmembrane pressure on J_{toluene} through the PAN/PDMS composite membrane, at various TOABr/toluene concentrations. For comparison, the J_{toluene} of oil/toluene solution at 8 % w/w is given too.

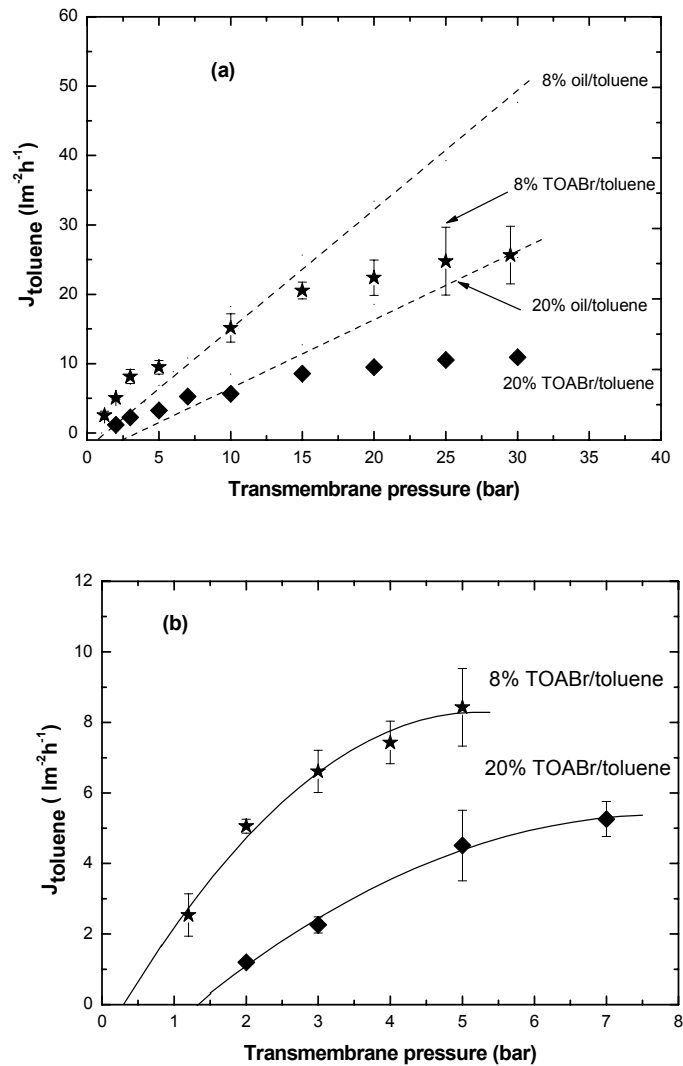


Figure 10: (a) Toluene flux as a function of transmembrane pressure at various TOABr/toluene concentrations, at 24 ± 3 °C, and (b) zooming in at low-pressure range.

Figure 10 shows that the toluene flux through the PAN/PDMS composite increases significantly with pressure at low-pressure range and then a plateau is reached.

This behavior is markedly different from that observed for oil/toluene solution where the toluene flux increases linearly with the applied pressure. In addition, *Figure 11* shows that the membrane retention for TOABr is 100%, at all the applied pressures and feed concentrations.

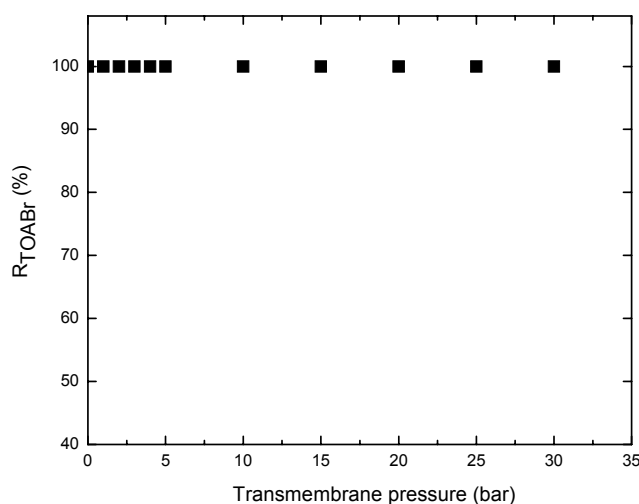


Figure 11: TOABr retention by the PAN/PDMS composite membrane as a function of transmembrane pressure, for 8 and 20% w/w TOABr/toluene solutions.

The solubility parameter of TOABr is significantly different than that of oil, toluene and PDMS ($\delta_{TOABr} = 22.0$, $\delta_{oil} = 16.0$, $\delta_{toluene} = 18.2$ and $\delta_{PDMS} = 14.9 - 15.6$ MPa^{1/2}, respectively) [9, 11, 12]. Unfavorable interactions exist between TOABr-toluene and TOABr-PDMS when compared to oil-toluene and oil-PDMS. Interestingly, by the end of the partition experiments, a deposition of TOABr was observed on the PDMS dense membrane that appears to stick to the membrane surface, generating large errors in the measurement (note that the concentration of TOABr is below the solubility limit of TOABr in toluene [13]). In addition, TOABr may associate in dimeric or polymeric ion-pairs species in toluene due to its specific chemical structure (*Figure 1*). The polymerization of tetraalkylammonium salts in various organic solvents (including toluene) was already reported in literature [7, 8]. The authors stated that no

dissociation of ion pairs was observed because of the low relative permittivity of toluene.

The non-linearity of toluene flux with pressure could be also attributed to the concentration polarization at higher pressure. The membrane retention for TOABr is 100%, which increases the build up of the solute in the boundary layer during permeation experiments. For the stirred batch cell, the Reynolds number (Re) can be estimated by [3, 14]:

$$\text{Re} = \frac{\omega r^2}{\eta} \quad \text{Equation 3}$$

where ω is the stirrer speed (rad/s), r is the radius of the stirred batch cell (m) and η is the kinematic viscosity of the solution (m^2/s). The value of Re indicates the flow regime. Reddy et al. [14] reported a turbulent flow for $32000 < \text{Re} < 82000$, transition from laminar to turbulent flow for $8000 < \text{Re} < 32000$ and laminar flow for $\text{Re} < 8000$. *Figure 12* shows the variation of Reynolds number with solute concentration, for various initial feed solutions used in this study.

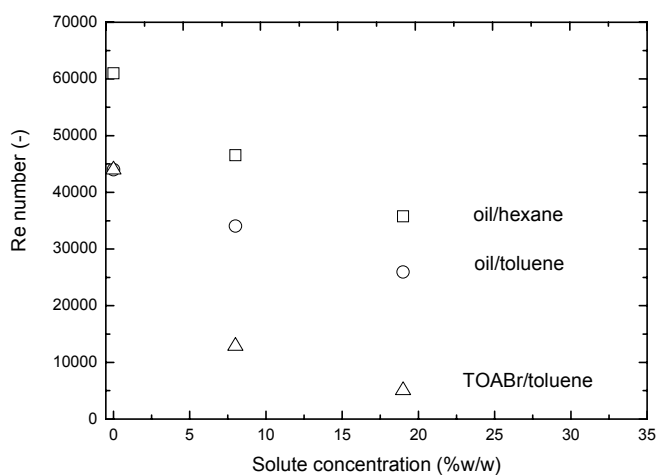


Figure 12: Variation of Reynolds number with solute concentration, for various solute/solvent systems used in this study.

For TOABr/toluene solutions, the Re number indicates a hydrodynamic condition located in the transition regime (at 8% w/w TOABr/toluene feed solution) and laminar (at 20 % w/w TOABr/toluene feed solution), respectively and, hence, the concentration polarization phenomena may be important in these systems.

Interestingly, when J_{toluene} versus pressure is zoomed in at low-pressure range (*Figure 10 b*), almost no osmotic pressure effect can be observed. *Table 4* presents the comparison between the calculated osmotic pressure by *Equation 2* and the the x -intercepts of the plots of J_{toluene} versus transmembrane pressure of *Figure 10b*.

Table 4: Comparison between the $\Delta\pi$ calculated by the van't Hoff equation and the x -intercepts of the plots of J_{toluene} versus transmembrane pressure of *Figure 10b*.

TOABr conc. (% w/w)	$\Delta\pi_{\text{calculated}}$ (bar)	x -intercept (bar)
8	3.0	0.3
19	8.0	1.3

Table 4 shows that the x -intercepts are significantly lower than the calculated osmotic pressures. TOABr may associate in dimeric or polymeric species in toluene due to its ion-pairs structure [7, 8]. Therefore, the “effective” concentration of the associated species decreases and the molecular weight increases, both decreasing the osmotic pressure value as predicted by *Equation 2*. This hypothesis may be supported by the significant increase of the viscosity of TOABr/toluene solutions with concentration (*Figure 2*). In addition, the fact that the osmotic pressure is significantly lower than expected from the van't Hoff equation may be attributed to the non-ideality of the TOABr/toluene system [6, 15]. The authors reported very high membrane retention for TOABr (~99%) using polyimide membranes, too. It is interesting to compare our values for the membrane permeabilities with those reported by Peeva et al. (the P_{permeate} is calculated from the linear part of the plot of *Figure 10*) using STARMEM™ 122, a polyimide nanofiltration membrane and a cross flow permeation set up.

Table 5: Comparison of P_{permeate} measured in this study with a PAN/PDMS composite membrane with P_{permeate} reported in [6] with a polyimide membrane.

TOABr conc. (mol/l)	P_{permeate} ($\text{lm}^{-2}\text{h}^{-1}\text{bar}^{-1}$)	
	This study	Peeva et al.[6]
0	2.0 ± 0.2	1.8
0.3	0.8 ± 0.1	1.7

The values are similar for toluene, but they differ significantly for the 0.3 mol/l TOABr/toluene solution. This could be attributed to difference in the type of membrane and experimental set up.

6.4. Conclusions

Studying the influence of the solvent and solute on the mass transport through the tailor-made PAN/PDMS membranes the following conclusions can be drawn:

- Toluene and hexane flux increases linearly with the applied pressure, showing that no compaction effect occurs within the studied pressure range. Toluene flux is lower than hexane flux through the PAN/PDMS membrane due to the higher viscosity of toluene compared to hexane.
- For the oil/toluene and oil/hexane solutions, the solvent permeability decreases with the concentration of feed due to the increase of the feed viscosity and osmotic pressure.
- An “apparent” viscosity inside the membrane and the membrane swelling are the most important parameters governing the solvent (toluene and hexane) transport through the PAN/PDMS composite membrane.
- The flux coupling for oil-toluene is stronger than for oil-hexane probably due to the higher friction of toluene with the oil molecules.
- The membrane retention of oil in toluene is lower than in hexane due to the lower toluene flux and smaller radius of gyration of oil in toluene. TOABr retention is 100% for all the applied pressure.
- Osmotic phenomena are observed for oil/hexane and oil/toluene solution and can be interpreted using the van't Hoff equation, indicating that they behave as ideal systems. For TOABr/toluene, the osmotic pressure found is significantly lower than estimated by the van't Hoff equation. This is probably due to ion-pairs clustering of TOABr in toluene and the non-ideality of the system.
- For TOABr/toluene and the PAN/PDMS membrane, the toluene flux is not linear with the applied pressure, probably due to the concentration polarization phenomenon.

6.5. List of symbols

B_{oil}	Oil permeability coefficient (m/h)
c_j	Concentration of species j (% w/w)
D	Diffusion coefficient (m ² /h)
J_i	Flux of species i through membrane (lm ⁻² h ⁻¹)
k	The Boltzmann coefficient (J/K)
K	Partition coefficient
MW	Molecular weight of the solute
P	Solvent permeability through the membrane (lm ⁻² h ⁻¹ bar ⁻¹)
R	Membrane retention
r_s	the Stokes radius (m)
SD	membrane swelling degree (%)
t	Time (h)
T	Temperature (K)
V	Molar volume (m ³ /mol)

Greek symbols

χ	Interaction parameter
$\phi_{solvent}$	The solvent volume fraction(-)
δ	Solubility parameter (MPa ^{1/2})
Δp	Transmembrane pressure (bar)
$\Delta\pi$	Osmotic pressure difference across the membrane (bar)
η	Viscosity (cSt)

6.6. References

1. I. F. J. Vankelecom, K. De Smet, L. E. M. Gevers, A. Livingston, D. Nair, S. Aerts, S. Kuypers, P. A. Jacobs, Physico-chemical interpretation of the SRNF transport mechanism for solvents through dense silicone membranes, *Journal of Membrane Science* 231 (2004) p99-108.
2. N. Stafie, D. F. Stamatialis, M. Wessling, Insight into the transport of hexane-solute systems through tailor-made composite membranes, *Journal of Membrane Science* 228 (2004) p103-116.
3. G. H. Koops, S. Yamada, S.-I. Nakao, Separation of linear hydrocarbons and carboxylic acids from ethanol and hexane solutions by reverse osmosis, *Journal of Membrane Science* 189 (2001) 241-254.
4. D. Bhanushali, S. Kloos, D. Bhattacharyya, Solute transport in solvent-resistant nanofiltration membranes for non-aqueous systems: experimental results and the role of solute-solvent coupling, *Journal of Membrane Science* 208 (2002) p 343-359.
5. J.T. Scarpello, D. Nair., L.M. Freitas dos Santos, L.S. White, A.G. Livingston, The separation of homogeneous organometallic catalysts using solvent resistant nanofiltration, *Journal of Membrane Science* 203 (2002) p71-85.
6. L.G. Peeva, E. Gibbins, S.S. Luthra, L.S. White, R.P. Stateva, A.G. Livingston, Effect of concentration polarisation and osmotic pressure on flux in organic solvent nanofiltration, *Journal of Membrane Science* 236 (2004) p121-136.
7. K. Sawada, E. Takahashi, T. Horie, K. Satoh, Solvent effects on ion-pair distribution and dimerization of tetraalkylammonium salts, *Monatshefte fur Chemie* 132 (2001) p1439-1450.
8. C. Klofutar, S. Paljk, Aggregation of tri-n-octylammonium chloride (TOACHCl), tri-n-octylammonium bromide (TOAHBr) and tri-n-octylammonium iodide (TOAHI) in benzene solutions, *Inorganica Chimica Acta*, 40(1980) pX167
9. J. Brandrup, E.H. Immergut, *Polymer Handbook*, Wiley Interscience, second edition, 1975.

10. X.J. Yang, A. G. Livingston, L.M. Freitas dos Santos, Experimental observations of nanofiltration with organic solvents, *Journal of Membrane Science* 190 (2001) p45-55.
11. D. W. van Krevelen, P.J. Hoftijzer, *Properties of polymers, their estimation and correlation with chemical structure*, Elsevier, Amsterdam, 1976.
12. A.F.M. Barton, *Handbook of solubility parameters and other cohesion parameters*, CRC: Boca Raton, 1983
13. A. Livingston, L. Peeva, S. Han, D. Nair, S.S. Luthra, L.S. White, L. M. Freitas dos Santos, Solvent nanofiltration in liquid phase organic synthesis reactions, *Advanced membrane technology annals of the New York Academy of sciences* 984 (2003) p123-141.
14. K. K. Reddy, T. Kawakatsu, J. Snape, M. Nakajima, Membrane concentration and separation of L-aspartic acid and L-phenylalanine derivatives in organic solvents, *Separation Science and Technology* 31 (1996) p1161-1178.
15. E. Gibbins, M. D' Antonio, D. Nair, L. S. White, L. M. Freitas dos Santos, I. F. J. Vankelecom, A. G. Livingston, Observations on solvent flux and solute rejection across solvent resistant nanofiltration membranes, *Desalination* 147 (2002) p307-313.

Preparation and characterization of a composite membrane with PEO-PDMS-PEO as selective layer

Abstract

Nanofiltration (NF) membranes are prepared by dip coating of a cross-linkable polyethylene oxide (PEO)-poly(dimethyl siloxane) (PDMS) triblock copolymer on a polyacrylonitrile (PAN) support. The selective top layer of the composite is a UV-cured α,ω dimethacryloyl PEO-PDMS-PEO block copolymer. The chemical composition of the copolymer is studied by Fourier transform infrared spectroscopy (FTIR) and its molecular weight is determined by Gel permeation chromatography (GPC). Swelling and contact angle measurements confirm the hydrophilic character of the PEO-PDMS-PEO membrane compared to the PDMS membrane. The fluxes of gases and solvent through the PAN/PEO-PDMS-PEO composite membrane are found to be lower compared to PAN/PDMS composite membrane, probably due to the lower molecular weight (MW) of PDMS segment of the polymer chain and/or the quality of composite (pore intrusion). A linear correlation between the fluxes of 5 solvents through the hydrophilic and hydrophobic PDMS-based NF composite membrane and membrane swelling/solvent viscosity is found.

7.1. Introduction

Siloxane-based NF membranes are high performance materials with good chemical and thermal stability, exhibiting high fluxes for the non-polar liquid, however, having low fluxes for the polar solvents [1-5]. To overcome this disadvantage, the preparation of block copolymers containing a polar PEO segment and a non-polar PDMS segment would be a good approach to tune the solvent flux through the membrane. Various degrees of hydrophilicity of the PEO-PDMS-PEO copolymer can be obtained by changing the MW of segments, and/or the PEO/PDMS ratio and/or the polymer topology (block or graft copolymers) [6]. Metz et al. [7] already pointed out the importance of some of these parameters for PEO/poly(butylenes terephthalate) (PBT) block copolymer used for gas and water vapor permeation. So far, the correlation between the morphology of high MW PEO-PDMS copolymer and their gas permeation was studied [8]. However, no systematic study with respect to the liquid permeation under pressure is yet done. Recently, the transport mechanism of the organic solutions through the NF membranes has received a lot of attention [1-3,9-12]. Three main transport models have been used in the NF literature: the solution-diffusion model [4, 9, 10, 13], Spiegler-Kedem model [1, 11] and the pore flow model [3, 12]. The solution-diffusion model assumes that the transport through the dense, non-porous PDMS takes place by penetrant solvation into the membrane and its diffusion through the membrane. The separation is achieved due to the differences in solubility and/or diffusivity of the penetrants. In contrary, the pore model considers that the membrane contains “pores” or free volume elements of Angstrom-dimension which cause the transport of the species through PDMS, with solution viscosity and membrane thickness being the parameters controlling the mass transport. The Spiegler-Kedem model assumes that the solute flux is a combination of diffusion and convection. Bhanushali et al. [3] reported that parameters such as the molar volume of the solvent, surface energy and sorption determine the mass transport of various solvents through a silicone and a polyamide type of membrane. However, Machado et al. [2] found no correlation between the solvent flux and molecular

volume of various organic solvents (polar and non-polar) for the MPF-50, a commercially available silicone membrane. Only solvent viscosity and surface tension of membrane determined solvent permeation. Other studies [4, 13] reported on the dependence of the solvent flux on the membrane swelling and on the solvent viscosity. In spite of the performed studies, the exact transport mechanism is still a big point of discussion. Its unified approach is rather complex since organic solvents have a wide range of polarity, viscosity and surface tensions [4]. In addition, the solvent-solute-membrane interactions are very complex, too [1, 11]. Unfortunately, most of the existing membranes have been performed on the commercially available membranes, the exact physico-chemical properties of which are not completely known. In a different approach, we prefer to start from a well-known, thoroughly characterized, tailor-made composite membrane. We reported [Chapter 3, 5, and 6] that the solution-diffusion model might describe the transport of hexane and toluene through the PAN/PDMS composite membranes of various cross-linking degree if the model allows for a solvent flux-dependent solute permeability (solvent induced solute dragging). Within the current study we outline the correlation between the material/penetrant properties and permeation performance for two PDMS-based NF membranes.

We focus our study on the PDMS-based NF membrane with two complimentary aims:

- To prepare and characterize a PAN/PEO-PDMS-PEO composite membrane. The characterization of the PEO-PDMS-PEO membrane by FTIR, DSC, swelling, gas and solvent permeation experiments with special emphasis on the comparison of its features with the ones of the PAN/PDMS composite membrane.
- To check whether the solvent viscosity and membrane swelling are responsible for the solvent flux through the PDMS-based NF membranes.

7.2. Experimental

7.2.1. Materials

The α,ω -dihydroxy PEO-PDMS-PEO block copolymer (ABA type, Q 3669, with PEO/PDMS content of 52/48 % w/w) was kindly supplied by Dow Corning, UK. Methacrylic anhydride (94%) was obtained from Aldrich, The Netherlands. 4-Dimethylaminopyridine (DMAP, 99%) was purchased from Fluka, The Netherlands. The photoinitiator, Darocur 4265, was obtained from Ciba, The Netherlands. The PAN support membrane with a MWCO of 30 kDa was provided by GKSS Forschungszentrum, Germany. The membrane was delivered in dry state and used without further treatment. The selective top layer of the composite was a UV-cured α,ω -dimethacryloyl PEO-PDMS-PEO block copolymer film. Tetrahydrofuran (THF), *n*-hexane, *n*-heptane, toluene, isopropanol, ethanol and methyl ethyl ketone (MEK) (Merck) were used as supplied, without further purification.

7.2.2. Acylation of PEO-PDMS-PEO

Figure 1 shows the structure of a commercially available α,ω -dihydroxy PEO-PDMS-PEO triblock copolymer used in this study. Because we would like to prepare PEO-PDMS-PEO membrane, the copolymer needs to have cross-linkable functionality. We chose to introduce methacrylate (MA) functional groups, which are specifically suitable for UV curing. Therefore, the following acylation reaction was performed to convert the OH-terminated PEO-PDMS-PEO copolymer into the MA-terminated copolymer. *Figure 1* shows the acylation reaction steps.

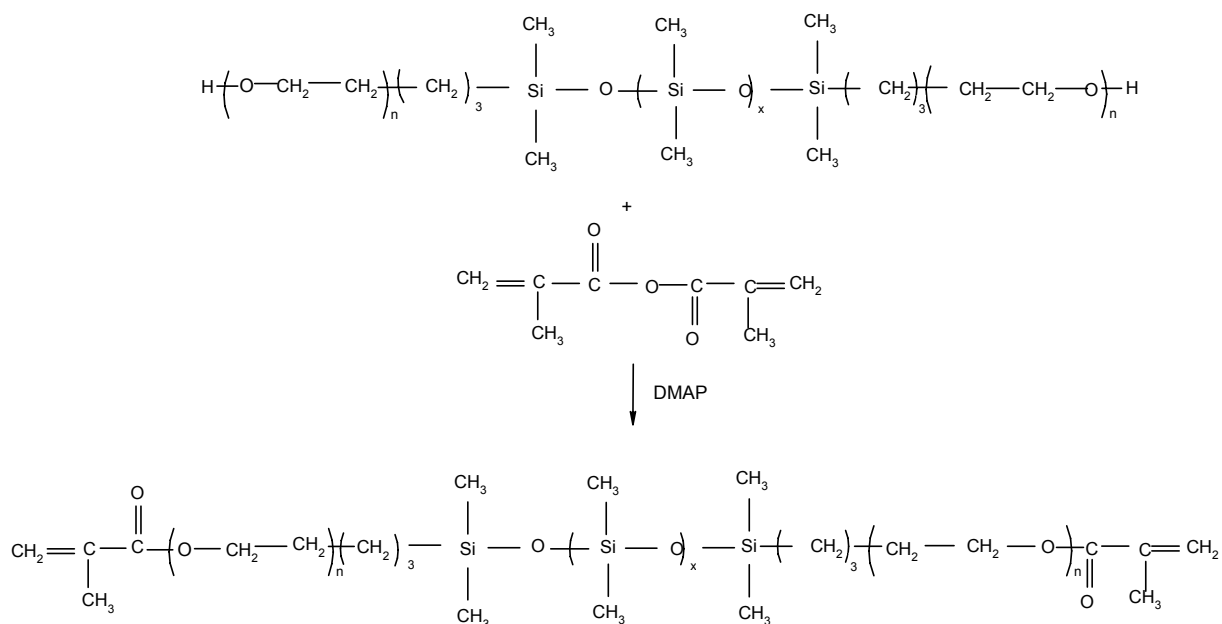


Figure 1: Synthesis of a UV-curable PEO-PDMS-PEO copolymer.

The acylation reaction of α,ω -dihydroxy PEO-PDMS-PEO with methacrylic anhydride was conducted according to [14]. The PEO-PDMS copolymer (18 g or $1 \cdot 10^{-2}$ mol OH estimated) was stirred in a mixture of THF (90 ml) and DMAP (0.6 g or $4.9 \cdot 10^{-3}$ mol) with an excess of methacrylic anhydride (6.4 g or $4 \cdot 10^{-2}$ mol). The mixture was stirred for 72 h to assure complete conversion. The reaction mixture was concentrated on a rotary evaporator and precipitated in *n*-heptane (400 ml). Traces of *n*-heptane were removed under vacuum.

7.2.3. Membrane preparation

The free-standing, thick PEO-PDMS-PEO membrane was prepared by casting a mixture of α,ω -dimethacryloyl PEO-PDMS-PEO block copolymer and photoinitiator on a glass plate, at room temperature (the photoinitiator is activated by UV light to form radicals which start the polymerization reaction). The glass plate was then placed in a UV-exposure chamber equipped with two Philips TLD 15/05 lamps (15W, wave length of 366 nm). The chamber was first flushed with N_2 for 1 h (to remove oxygen) and then UV irradiation was performed for 2 h.

The PAN/PEO-PDMS-PEO tailor-made composite membranes were prepared via dip-coating. The PAN support was glued on a glass plate with PVC tape and briefly immersed in a vessel containing *n*-hexane to fill the pores. This was done to avoid pore intrusion of the PEO-PDMS-PEO during the dip coating process (more details concerning the prevention of pore intrusion are presented in Chapter 2). Afterwards, the excess of hexane from the PAN surface was removed with a roller. Then, the hexane impregnated PAN support was dipped in a vessel containing the PEO-PDMS-PEO/methanol solution with concentration of 20 % w/w and the photoinitiator. The composite membrane was then placed in a UV-exposure chamber and a similar UV-treatment as for the dense PEO-PDMS-PEO membrane was applied.

7.2.4. Membrane characterization

The characterization of chemical composition of the PEO-PDMS-PEO membranes was performed on an FTIR (Bio-Rad FS60). A GPC (Waters 515, using THF as solvent) was used to determine MW of the copolymer before and after the acylation reaction. For differential scanning calorimetry (DSC) measurements (Perkin-Elmer DSC 2 apparatus) the samples (1 mg) were scanned from -140 to 30 °C by a heating rate of 30 °C/min. Scanning Electron Microscopy (SEM, Jeol JSM-5600LV, at 5 kV) was used for the investigation of morphology of the PAN/PEO-PDMS-PEO composite membrane, following the procedure described elsewhere (Chapter 2).

The measurement of the swelling degree of the dense PEO-PDMS-PEO membrane was performed following the procedure described in Chapter 2. The membrane swelling is expressed as the volume fraction of solvent in the swollen polymer:

$$\phi_{solvent} = 1 - \frac{\frac{1 - w_{solvent}}{\rho_{polymer}}}{\frac{w_{solvent}}{\rho_{solvent}} + \frac{1 - w_{solvent}}{\rho_{polymer}}} \quad \text{Equation 1}$$

where $w_{solvent}$ is the mass fraction of solvent in the swollen polymer, $\rho_{polymer}$ is the density of the PEO-PDMS-PEO (1.05 gcm⁻³ [15]) and $\rho_{solvent}$ is the density of the solvent taken from [16].

The contact angle of the composite membrane was measured by placing a small drop of water on the membrane with a syringe (Dataphysics Contact Angle System OCA 15 plus). A video camera recorded the drop, while the tangent at the point where the drop contacted the solid surface was calculated with SCA 20 software. Five drops of water were measured for each surface, and the average value was calculated.

The quality of the composite membrane was assessed by performing single gas permeation measurements with N₂ and CO₂, using the set-up and procedure described in Chapter 2.

The transport of various solvents through the PAN/PEO-PDMS-PEO composite membranes was studied at room temperature (22 ± 3 °C), with the set-up and protocol described in Chapter 2.

7.3. Results and discussion

7.3.1. Characterization of the PEO-PDMS-PEO dense membrane

FTIR analysis was used to determine the extend of acylation reaction. *Figure 2* shows a comparison of the spectra of PEO-PDMS-PEO copolymer, before and after the acylation reaction.

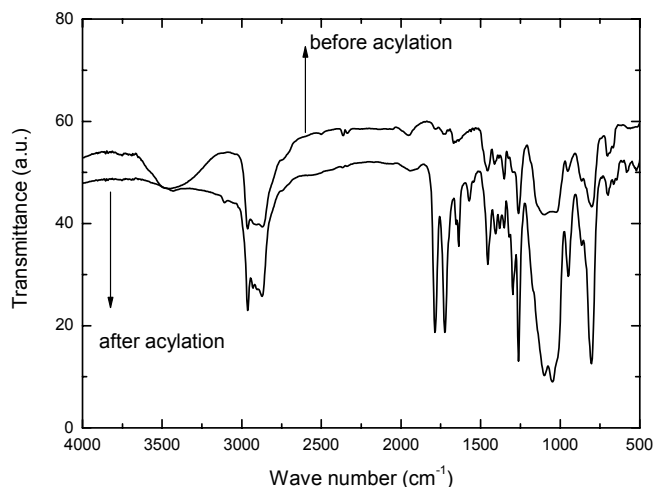


Figure 2: FTIR spectra of the PEO-PDMS-PEO copolymer before and after acylation.

Both spectra show similar peaks with the exceptions of the characteristic peak of the OH group at 3500 cm^{-1} (before acylation) and of the characteristic peak of the C=O group at $1720\text{-}1780\text{ cm}^{-1}$ (after acylation). The absence of the OH peak after acylation indicates the completeness of the acylation reaction.

Figure 3 shows the FTIR spectra of the dense, freestanding PEO-PDMS-PEO membrane. For comparison, the spectra of the dense PDMS are presented too.

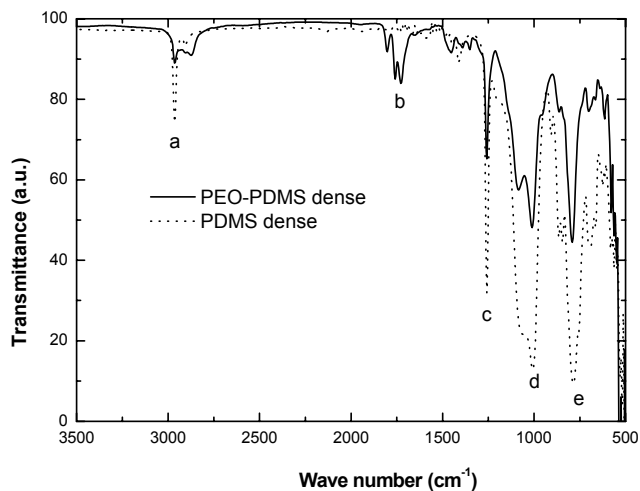


Figure 3: FTIR spectra of the dense PEO-PDMS-PEO and PDMS membranes.

Both FTIR spectra show the typical peaks of a silicone polymer: the peak (a) corresponding to the -CH_3 stretch at 2965 cm^{-1} , the peaks (c, e) corresponding to the Si-CH_3 bond at 1260 and $750\text{-}865\text{ cm}^{-1}$, the peak (d) corresponding to the broad polymer backbone band Si-O-Si between $1130\text{--}1000\text{ cm}^{-1}$. The main difference between the spectra of the PDMS membrane and the spectra of the PEO-PDMS-PEO membrane is the peak (b) corresponding to the C=O signal due to the incorporation of MA group. The peak of C-O bond from PEO contribution at 1260 cm^{-1} might be masked by the higher intensity of the Si-CH_3 peak.

Figure 4 presents a typical result of the GPC analysis for the PEO-PDMS-PEO copolymer before and after the acylation reaction. The similar results for the copolymer obtained before and after the acylation reaction indicate that the acylation reaction does not influence the MW of copolymer.

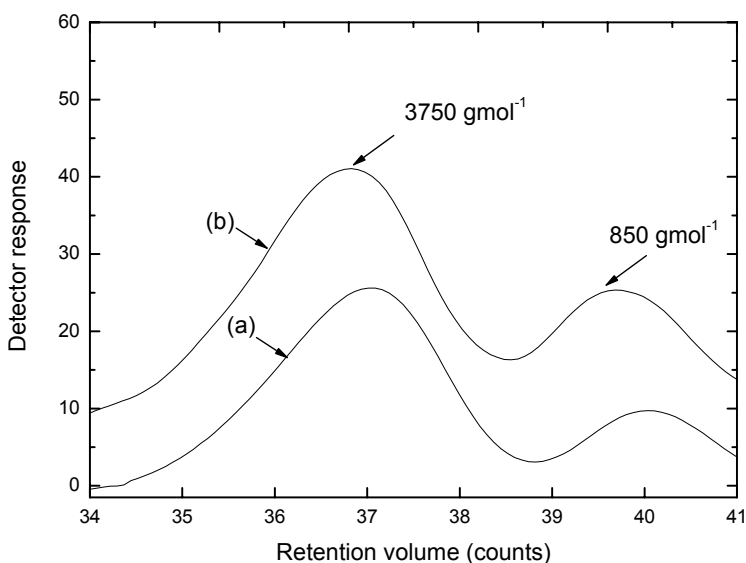


Figure 4: MW of the PEO-PDMS-PEO copolymer determined by GPC (a) before and (b) after acylation.

The GPC spectrum shows a peak of 3750 gmol^{-1} corresponding to the PEO-PDMS-PEO block copolymer and a peak of 850 gmol^{-1} , indicating, probably, some traces of low molecular weight polymer. From the GPC results and the composition of copolymer given by the supplier (PEO/PDMS content of 52/48 % w/w), an estimation of MW of PEO of about 975 gmol^{-1} and of PDMS of about 1800 gmol^{-1} is obtained. This indicates that the PEO phase may be in the non-crystalline phase due to its low molecular weight.

The DSC data were collected from the first heating of the PEO-PDMS-PEO dense membrane. A typical DSC thermogram (*Figure 5*) shows the following thermal transitions: a glass transition temperature (T_g) located at about $-80 \text{ }^\circ\text{C}$ which might correspond to the copolymer phase (note that T_g of PDMS is -123°C and of PEO is between (-115) - $(-40) \text{ }^\circ\text{C}$, depending on the MW [15-19]) and a melting temperature (T_m) at $-50 \text{ }^\circ\text{C}$ of the PDMS crystallites. The T_m of PDMS is rather close to the value reported in literature (range of $(-55) - (-45) \text{ }^\circ\text{C}$ respectively) [16].

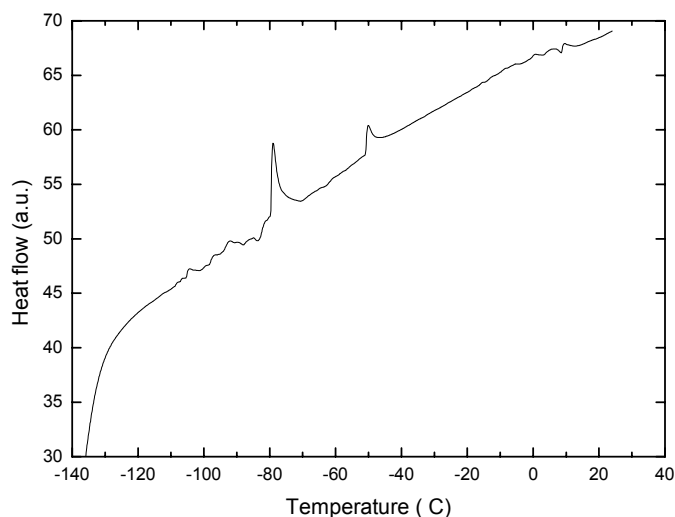


Figure 5: Heating curve of a dense PEO-PDMS-PEO membrane.

Swelling experiments of the dense membranes were performed in hexane, toluene, MEK, isopropanol, and ethanol. The solvents were chosen in order to study the influence of various physical properties of the solvent on the membrane-solvent interaction. The membrane-solvent interaction was reported to vary with changes

in solvent properties such as dielectric constant or viscosity [1-3, 13]. *Table 1* summarizes some of the relevant physical properties of various solvents used in this study.

Table 1: *Relevant physical properties of various solvents used in this study [16].*

Solvent	Dielectric constant (-)	Kinematic viscosity (cSt)
Hexane	1.9	0.49
Toluene	2.4	0.66
MEK	15.4	0.53
Isopropanol	18.3	2.56
Ethanol	24.3	1.37

Table 2 shows the results of the swelling experiments of the dense PEO-PDMS-PEO membrane in various solvents. Because the solvents have various densities, a better way to express the swelling degree is the solvent volume fraction. For comparison, the data of swelling of the dense PDMS membrane in similar solvents is given, too.

Table 2: *Swelling degree of the dense PEO-PDMS-PEO and PDMS membrane in various solvents.*

Membrane	$\phi_{solvent}$ (-)				
	Hexane	Toluene	Isopropanol	MEK	Ethanol
PEO-PDMS-PEO	0.17 ± 0.02	0.20 ± 0.02	0.44 ± 0.03	0.51 ± 0.06	0.79 ± 0.06
PDMS	0.77 ± 0.07	0.73 ± 0.08	0.30 ± 0.03	0.39 ± 0.04	0.11 ± 0.01

For PEO-PDMS-PEO dense membrane, the solvent fraction increases significantly with the polarity of the solvent, being the highest for ethanol (100%), indicating a

higher affinity towards the polar solvents. In contrast, dense PDMS membranes show the highest volume fraction in hexane, confirming its high affinity for the non-polar solvents as already reported in literature [16]. These results imply that the new PEO-PDMS-PEO membrane is more hydrophilic than the PDMS membrane only.

In the end of the swelling experiments, when the swollen samples are dried in the vacuum oven, the weight of the membrane does not differ from its initial weight, giving evidence of membrane stability under the employed conditions.

Table 3 shows the contact angle values (θ) of the PAN/PEO-PDMS-PEO composite membrane. For comparison the contact angle values obtained with the PAN/PDMS composite membrane are given, too.

Table 3: Contact angle for water of the PDMS-based composites.

	PAN/PEO-PDMS-PEO	PAN/PDMS
$\theta, (^{\circ})$	70 ± 10	105 ± 8

The results show that the top layer of the PAN/PEO-PDMS-PEO composite membrane becomes more hydrophilic than of the PAN/PDMS composite membrane when PEO segments are present. It is worth mentioning that the measured PDMS value is in agreement with data already reported (range of 95-113 $^{\circ}$) [16].

7.3.2. Gas permeation properties of the PAN/PEO-PDMS-PEO composite membrane

The SEM pictures for different membranes confirm the composite morphology of the PAN/PEO-PDMS-PEO membrane, with a very thin PDMS-PEO-PDMS top layer (of about 0.4 μm). Note that the effective thickness of the PAN/PDMS composite membrane is about 2 μm (Chapter 3).

Table 4 shows the effect of the PEO segment on the gas transport properties, (P/l) of N₂ and CO₂ and the selectivity of CO₂/N₂ (α_{CO_2/N_2}) of PAN/PEO-PDMS-PEO and PAN/PDMS composite membrane.

Table 4: Gas transport properties, P/l, and α_{CO_2/N_2} of PAN/PEO-PDMS-PEO and PAN/PDMS composite membrane.

Membrane	(P/l) _{N₂}	(P/l) _{CO₂}	α_{CO_2/N_2}
	10 ⁻⁶ cm ³ (STP)(cm) ⁻² s ⁻¹ (cmHg) ⁻¹	10 ⁻⁶ cm ³ (STP)(cm) ⁻² s ⁻¹ (cmHg) ⁻¹	(-)
PAN/ PEO-PDMS-PEO	0.3 ± 0.1	4.1 ± 0.7	13.7 ± 1.9
PAN/PDMS	16.0 ± 2.3	171.0 ± 24.0	9.8 ± 1.4

For the PAN/PEO-PDMS-PEO composite membrane, the (P/l) of N₂ is 53 times lower than through the PAN/PDMS, while the (P/l) of CO₂ is 42 times lower. It seems that the addition of PEO segment to the PDMS segment led to a severe decrease of (P/l) value of both gases. The gas transport through a dense membrane depends on the solubility of gas in the membrane material and its diffusivity within the membrane. For PDMS homopolymer, the high intrinsic permeability of CO₂ ($3200 \times 10^{-10} \text{cm}^3(\text{STP})\text{cm}(\text{cm})^{-2}\text{s}^{-1}(\text{cmHg})^{-1}$) [16] is a consequence of its high solubility and of the high flexibility of the PDMS chains. The PEO-PDMS-PEO block copolymer consists of both segments, PEO and PDMS. Nevertheless, the intrinsic permeability of CO₂ of the PEO homopolymer ($143 \times 10^{-10} \text{cm}^3(\text{STP})\text{cm}(\text{cm})^{-2}\text{s}^{-1}(\text{cmHg})^{-1}$, estimated at 35°C) [17] is much lower than of the PDMS homopolymer. Therefore, a lower permeability of CO₂ is expected for the PEO-PDMS-PEO copolymer than for the PDMS homopolymer. In addition, the morphology of the polymer is important as well. For the PEO-PDMS-PEO copolymer, the molecular weight of the siloxane segment is around 1800 gmol⁻¹ (GPC data and the PEO/PDMS ratio given by the supplier). For the dense PDMS membrane, the average molecular weight is 35500 (GPC data reported in Chapter

4). This difference implies a decrease in the flexibility of the polymer chains, hence, decreasing the gas flux through the polymer. Similar findings were reported in other studies [20, 21] involving pervaporation with the dense PDMS of various molecular weights.

For the PAN/PEO-PDMS composites, the CO₂ selectivity over N₂ is higher than the intrinsic PDMS selectivity probably due to the higher affinity towards CO₂ (PEO-PDMS-PEO copolymer has a more polar character than the PDMS homopolymer due to the presence of the PEO segment) [17].

7.3.3. Solvent permeation characteristics of the PAN/PEO-PDMS and PAN/PDMS composites

The flux of hexane, toluene, MEK, isopropanol and ethanol through the PAN/PEO-PDMS-PEO composite membrane was measured at transmembrane pressure of 30 bar. For comparison, the flux of these solvents through the PAN/PDMS composite membrane was measured as well. In Chapters 3-6, we reported that the swelling degree and the viscosity were the most important parameters affecting the mass transport of hexane and toluene through the PAN/PDMS tailor-made membrane of various cross-linking degrees. It would be interesting to see if the solvent flux through the PAN/PEO-PDMS-PEO composite membrane can be normalized, too. *Figure 6* shows the effect of membrane swelling and solvent viscosity on solvent permeability (obtained by dividing the solvent flux through the composite membrane over the applied pressure) for both composite membranes, PAN/PEO-PDMS-PEO and PAN/PDMS membrane. For the normalization, data of *Table 1* and of *Table 2* are used.

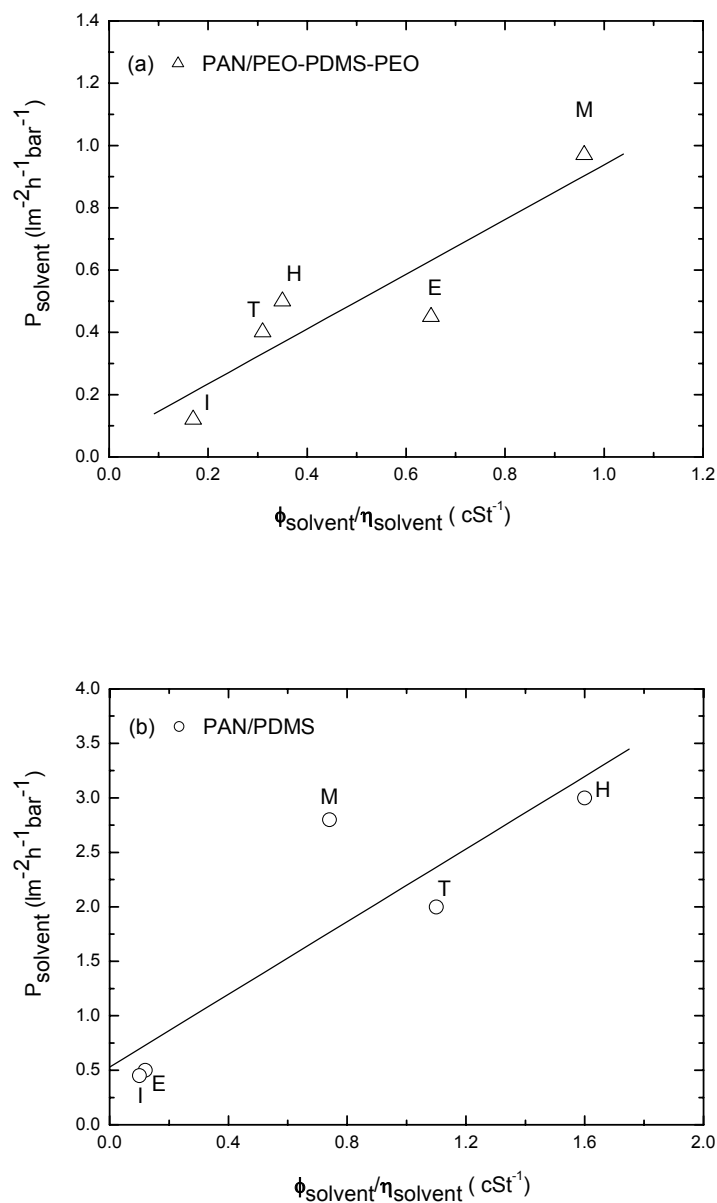


Figure 6: Solvent permeability measured at 30 bar through (a) PAN/PEO-PDMS-PEO and (b) PAN/PDMS membrane as a function of membrane swelling (ϕ_{solvent}) and solvent viscosity (η_{solvent}). I, E, M, T, H stands for isopropanol, ethanol, MEK, toluene, and hexane, respectively.

For the PAN/PEO-PDMS-PEO and PAN/PDMS composite membranes, a reasonable linear correlation (R^2 of 0.90 and 0.86) exists between the solvent flux

and swelling degree versus solvent viscosity. For PAN/PDMS membrane, the P_{solvent} correlates better ($R^2=0.99$) with the $\phi_{\text{solvent}}/\eta_{\text{solvent}}$ if we consider MEK as an outlier (it is not known why MEK appears to have a special behavior). This is an important finding of our research, showing that the normalization of the P_{solvent} with the membrane swelling and solvent viscosity can be applied reasonably for a more hydrophilic selective layer, too. If we assume the solution-diffusion model to hold for this system, then we can interpret the swelling as a measure for the solubility and the viscosity as a measure for the diffusion coefficient of the solvent inside the polymer network. Interestingly, Vankelecom et al. [4] also reported a good linearity between the fluxes of various solvents (polar and non-polar) through a thin film composite consisting of PDMS as the selective layer and PAN/polyester (PE) as the support. The authors suggested that the viscosity could be regarded as a property that reflects the mutual interaction between the diffusing molecules and their interactions with the membrane. However, Bhanushali et al. [1] corroborated the dependence of solvent permeability on its viscosity with the viscous (convective) flow. Robinson et al. [12] suggested that the PDMS membrane might contain pores of Angstrom-dimension which cause the transport of the species, with feed viscosity and membrane thickness being the parameters controlling the mass transport.

The PAN/PDMS composite membrane has silicone only as the selective layer, therefore the flux of non-polar solvents (hexane, toluene) is significantly higher than of the polar solvents (ethanol, isopropanol). Similar results have been reported for other silicone-based nanofiltration membranes [1-5]. Interestingly, the P_{solvent} of the PAN/PEO-PDMS-PEO membrane is lower compared to the PAN/PDMS composite membrane, independent on the polarity of the solvent, although higher fluxes for polar solvents were expected due to the hydrophilicity of the top-layer (data of contact angle and swelling experiments). The lower flux obtained through the PAN/PEO-PDMS-PEO composite membrane than through the PAN/PDMS is consistent with the gas permeation results. It may be that the PEO-PDMS-PEO copolymer chains are less flexible than of the PDMS homopolymer due to the low molecular weight segments of PDMS of the PEO-PDMS-PEO copolymer (1800 compared to 35500 gmol^{-1}). Therefore, the

diffusion of components through the PEO-PDMS-PEO membrane is lower compared to the dense PDMS only. Similar findings were reported in other study [20] concerning pervaporation of ethanol/water through silicone membranes of various PDMS chain lengths: the ethanol permeability was found to be double when the PDMS length increased from 1000 to 15000 g mol^{-1} . Bennett et al. [21] concluded that the use of PDMS with at least MW of 18000 was found to have a beneficial effect for phenol/water pervaporation. In addition, the quality of composite (pore intrusion) may be responsible for the low flux through the PEO-PDMS-PEO composite as well. In Chapter 4, we reported for the PAN/PDMS that the pore intrusion restricted the swelling of the PDMS layer, lowering the flux of the membrane.

7.4. Conclusions

The following conclusions can be drawn from this study:

- PAN/PEO-PDMS-PEO composite membrane is reproducibly prepared via dip coating.
- The contact angle and swelling experiments reveal an increased hydrophilicity of the PAN/PEO-PDMS compared to the PAN/PDMS membrane.
- The gas and the solvent fluxes through the PAN/PEO-PDMS-PEO membrane is lower compared to PAN/PDMS composite membrane
- A linear correlation between the fluxes of various solvents (polar and non polar) through the hydrophilic and hydrophobic PDMS-based NF composite membrane and membrane swelling/solvent viscosity is found.

7.5. List of symbols

MW	Molecular weight (gmol^{-1})
P_{solvent}	Permeability of hexane through the membrane
w_{solvent}	Weight fraction of PDMS at swelling equilibrium
$\alpha_{\text{CO}_2/\text{N}_2}$	Gas selectivity of membrane for CO_2 over N_2
η	Viscosity (cSt)
ρ	Density (gcm^{-3})
ϕ_{solvent}	Penetrant volume fraction

7.6. Acknowledgements

M.A. Hempenius and C. Padberg (Materials Science and Technology of Polymers Group, University of Twente, The Netherlands) are acknowledged for their assistance in the PEO-PDMS-PEO synthesis and in performing GPC and DSC analysis, as well as for the fruitful discussions.

7.7. References

1. K. S. Bhanushali D, Bhattacharyya D, Solute transport in solvent-resistant nanofiltration membranes for non-aqueous systems: experimental results and the role of solute-solvent coupling, *Journal of Membrane Science* 208 (2002) p343-359.
2. D. R. Machado, D. Hasson, R. Semiat, Effect of solvent properties on permeate flow through nanofiltration membranes. Part I: investigation of parameters affecting solvent flux, *Journal of Membrane Science* 163 (1999) p93-102.
3. K. S. Bhanushali D, Kurth C, Bhattacharyya D, Performance of solvent-resistant membranes for non-aqueous systems: solvent permeation results and modeling, *Journal of Membrane Science* 189 (2001) p1-21.
4. I. F. J. Vankelecom, K. De Smet, L. E. M. Gevers, A. Livingston, D. Nair, S. Aerts, S. Kuypers, P. A. Jacobs, Physico-chemical interpretation of the SRNF transport mechanism for solvents through dense silicone membranes, *Journal of Membrane Science* 231 (2004) p99-108.
5. X.J. Yang, A. G. Livingston, L. F. d. Santos, Experimental observations of nanofiltration with organic solvents, *Journal of Membrane Science* 190 (2001) p45-55.
6. A. Jonquieres, R. Clement, P. Lochon, Permeability of block copolymers to vapors and liquids, *Progress in Polymer Science* 27 (2002) p1803-1877.
7. S. J. Metz, J. Potreck, M. H. V. Mulder, M. Wessling, Water vapor and gas transport through a poly(butylene terephthalate) poly(ethylene oxide) block copolymer, *Desalination* 148 (2002) p303-307.
8. H. B. Park, C. K. Kim, Y. M. Lee, Gas separation properties of polysiloxane/polyether mixed soft segment urethane urea membranes, *Journal of Membrane Science* 204 (2002) p257-269.
9. L. G. Peeva, E. Gibbins, S. S. Luthra, L. S. White, R. P. Stateva, A. G. Livingston, Effect of concentration polarisation and osmotic pressure on

- flux in organic solvent nanofiltration, *Journal of Membrane Science* 236 (2004) p121-136.
10. L. White, Transport properties of a polyimide solvent resistant nanofiltration membrane, *Journal of Membrane Science* 205 (2002) p191-202.
 11. G. H. Koops, S. Yamada, S.-I. Nakao, Separation of linear hydrocarbons and carboxylic acids from ethanol and hexane solutions by reverse osmosis, *Journal of Membrane Science* 189 (2001) 241-254.
 12. J. P. Robinson, E. S. Tarleton, C. R. Millington, A. Nijmeijer, Solvent flux through dense polymeric nanofiltration membranes, *Journal of Membrane Science* 230 (2004) p29-37.
 13. N. Stafie, D. F. Stamatialis, M. Wessling, Insight into the transport of hexane-solute systems through tailor-made composite membranes, *Journal of Membrane Science* 228 (2004) p103-116.
 14. G. Höfle, W. Steglich, H. Vorbruggen, 4-Dialkylaminopyridine als hochwirksame Acylierungskatalysatoren, *Angew. Chem.* 90 (1978) p602-615.
 15. Z.-R. Zhang, M. Gottlieb, Amphiphilic poly(ethylene oxide) / poly(dimethylsiloxane) polymers 1. Synthesis and characterization of cross-linked hydrogels, *Thermochimica Acta* 336 (1999) p133-145.
 16. J. Brandrup, E.H. Immergut, *Polymer Handbook*, J. Wiley&Sons, second edition, 1975.
 17. H. Lin, B. D. Freeman, Gas solubility, diffusivity and permeability in poly(ethylene oxide), *Journal of Membrane Science* 239 (2004) p105-117.
 18. S. J. Clarson, J. A. Semlyen, *Siloxane Polymers*, Edition, PTR Prentice Hall, New Jersey, 1993.
 19. A. Noshay, J. E. McGrath, *Block Copolymers: overview and critical survey*, Academic Press, London, 1977.
 20. Y. T. Lee, K. Iwamoto, H. Sekimoto, M. Seno, Pervaporation of water-dioxane mixtures with poly(dimethylsiloxane-CO-siloxane) membranes prepared by a sol-gel process, *Journal of Membrane Science* 42 (1989) p169-182.

21. M. Bennett, B. J. Brisdon, R. England, R. W. Field, Performance of PDMS and organofunctionalised PDMS membranes for the pervaporative recovery of organics from aqueous streams, *Journal of Membrane Science* 137 (1997) p63-88.

Conclusions and outlook

The work described in this thesis is a systematic study performed to identify the key parameters affecting the transport through the poly (dimethyl siloxane) (PDMS)-based nanofiltration (NF) membranes. The understanding of the influence of the physicochemical interactions between solvent, solute and membrane on the transport through the NF membrane could form the foundation for a modeling approach capable of predicting the membrane performance.

Specific achievements of this research can be outlined as follows:

- Understanding the interaction between polymer-solvent-solute is crucial in developing NF membranes with suitable chemical stability, high solvent permeability and high retention towards various solutes. This is evident from the swelling experiments of Chapters 3-7, indicating that the selective top layer has to have high affinity for the solvent and low affinity for the solute. PDMS is a suitable top layer for a composite used in the separation applications involving non-polar solvents with P_{hexane} of about $3 \text{ lm}^{-2}\text{h}^{-1}\text{bar}^{-1}$ and oil retention of about 90 %.
- The flux of the hexane through the composite membrane can be regulated based on the amount of the cross-linker used for the preparation of the PDMS top layer. However, the membrane retention is similar and high (~90 %) for all composites of various cross-linking, probably due to the highly swollen state of the silicone network. This allows us to obtain PAN/PDMS composite membrane with high permeation performance by

further improving the balance between cross-linking degree and pore penetration of the PDMS.

- The flux of solvents (polar and non-polar) through the PDMS-based composite membrane is found to be dependent on the apparent viscosity and the membrane swelling. If we assume the solution-diffusion model to hold for this system, then we can interpret the solvent viscosity as a measure for the diffusion coefficient of the solvent inside the polymer network and the swelling as a measure for the solubility. But the solution-diffusion model does not consider the solute-solvent coupling (solvent-induced solute dragging) that is found experimentally. However, the increase of solvent flux with the applied pressure is much higher than the respective increase of solute flux causing an increase of the membrane retention at higher pressures. For a given solvent, the dragging effect is more important at lower molecular weight of the solute and at lower feed concentration (Chapters 3-5). For a given solute, the dragging seems to be more important for the solvent with higher viscosity (Chapter 6).
- The solute rejection of PAN/PDMS composite membrane seems to be dependent on the interaction between solvent-solute, solute-solute and solute-membrane. This is evident from the results obtained with the sunflower oil and tetraoctylammonium bromide (TOABr) presented in Chapter 6. The lower oil retention in toluene than in hexane indicates a preferential oil-toluene coupling effect. For the TOABr /toluene solutions, the high membrane retention is probably due to the low interaction between TOABr-PDMS and to the high interaction between TOABr-TOABr molecules.

- For oil/hexane and oil/toluene, osmotic phenomena similar to those reported in aqueous systems are observed and interpreted using the van't Hoff equation. For TOABr/toluene solutions, the osmotic phenomena can not be interpreted with the van't Hoff equation. This is probably due to ion-pairs clustering of TOABr in toluene and to the thermodynamic non-ideality of the system.
- The PAN/PDMS composite showed promising permeation results for the transport of non polar solvent (hexane and toluene). The permeability of the polar solvents however, is rather low (see Chapter 7). Poly (ethylene oxide) PEO-PDMS-PEO block copolymer seems to be a promising material for the preparation of composites because its composition and/or morphology could be tailored so that the hydrophilicity/hydrophobicity balance of the material matches with a large spectrum of organic solvents. Although the first composites (presented in Chapter 7) show promising results, a lot of optimization is still required. The solvent flux could potentially increase if composites with thinner top layer and/or minimized pore intrusion are prepared. The application of PEO and PDMS segments at different ratios and/or of other molecular weights could also have an impact on the solvent permeability.

Although this thesis has addressed several important aspects of the transport of various solvent/solutes through the NF membranes, however, there are still some issues to be addressed by others in the future:

- The preparation of NF membranes with tailored properties based on the investigated system will be a challenge in the future. There is certainly not a “one membrane fits all” solution for the solvent resistant NF membrane field. The first composites prepared in this thesis using block copolymers (PEO-PDMS-PEO) could be a plausible direction to follow. Still a lot of optimization is required.

- The development of a mathematical model capable to describe the transport of solvent/solute through the membrane will be a challenge (maybe the greatest), as well. This model should consider solvent/solute coupling and should be based on a thoroughly thermodynamic analysis of the solvent/solute/membrane system. It is advised to model the transport using a Maxwell-Stefan approach.

Summary

Solvent resistant nanofiltration (SRNF) membranes have a strong potential for various applications ranging from the pharmaceutical to the chemical and the food industries. However, the transport mechanism through the SRNF membranes is still under investigation.

This thesis presents a systematical experimental study performed in order to identify the key parameters that could affect the membrane transport characteristics through poly(dimethyl siloxane) (PDMS)-based SRNF membranes. A complete understanding of the solvent, solute and membrane characteristics that influence the solvent/solute flux through the membrane could form the foundation for a modeling approach capable of predicting the membrane performances.

Chapter 2 describes the preparation of a composite membrane consisting of a poly(acrylonitrile) (PAN) ultrafiltration support membrane and a PDMS selective top layer. A composite membrane with good quality of the PDMS top layer is obtained when a 7% (w/w) PDMS/hexane coating solution is applied. The results show that the PAN/PDMS composite membrane has a good permeation performance, the hexane permeability (P_{hexane}) around $3 \text{ lm}^{-2}\text{h}^{-1}\text{bar}^{-1}$ and oil retention of about 90%. An increase in the thickness of the PDMS layer decreases the hexane flux through the membrane, but has no influence on the oil retention.

Chapter 3 gives an insight into the transport of hexane-oil and hexane-poly(isobutylene) (PIB) systems through the PAN/PDMS composite membrane. Osmotic phenomena similar to those reported in aqueous systems, are observed and interpreted using the van't Hoff equation. The hexane flux increases linearly with the applied pressure and the P_{hexane} decreases with the increase of the feed concentration. The normalization of P_{hexane} by the solution viscosity inside the swollen membrane and the swelling of the membrane results in a constant value quantifying the hexane transport independent of the solute type and concentration in the feed mixture. If we assume the solution-diffusion model to hold for this

system, then we can interpret the solvent viscosity as a measure for the diffusion coefficient of hexane inside the polymer network and the swelling as a measure for the solubility. However, the solution-diffusion model does not account for the solute-solvent flux coupling found experimentally. For a given solute, the effect of flux coupling decreases with the molecular weight of the solute and the solute concentration.

Chapter 4 focuses on the effect of the cross-linking degree of PDMS on the dense membrane characteristics and on the permeation performance of the PAN/PDMS composite membrane. The swelling of the dense membrane decreases with the increase of the cross-linker amount. In addition, the partition coefficient of PIB in the membrane decreases with the increase of the cross-linker amount and the molecular weight of PIB. The P_{hexane} through the PAN/PDMS membrane prepared at pre-polymer/cross-linker ratio of 10/0.7 is higher than at 10/1 (4.5 and 3.1 $\text{lm}^{-2}\text{h}^{-1}\text{bar}^{-1}$, respectively) due to the higher membrane swelling (260 and 200%w/w). The P_{hexane} through the PAN/PDMS membrane prepared at pre-polymer/cross-linker ratio of 10/2 is higher than through the composite prepared at ratio of 10/1 (4.1 and 3.1 $\text{lm}^{-2}\text{h}^{-1}\text{bar}^{-1}$) although the membrane swells less (100 and 200 % w/w). This might be due to the a reduction of pore intrusion of PDMS for the composite membrane at ratio of 10/2 compared to 10/1 and/or due to the heterogeneous quality of the formed silicone network. The cross-linker amount has no effect on the PIB retention probably due to the highly swollen state of the silicone network. This allows us to obtain PAN/PDMS composite membranes with high permeation performance (large flux and good retention) by further improving the balance between cross-linking degree and pore penetration.

Chapter 5 investigates the permeation performance of the PAN/PDMS composite membrane with an oil/hexane solution at high pressure. Membrane compaction and concentration polarization are not observed up to 30 bar. The separation performance of the membrane is similar at low and high pressure and for the batch and continuous mode as well, indicating the membrane stability under the tested conditions. At high pressure, the coupling of solvent-solute flux is found as well,

confirming the data obtained at low pressure range where the dragging effect is found to be dependent on the molecular weight and on the concentration of the solute in the feed. The comparison with a silicone GKSS membrane shows that the P_{hexane} for the GKSS composite membrane is higher than through our PAN/PDMS (5.9 and 3.1 $\text{lm}^{-2}\text{h}^{-1}\text{bar}^{-1}$), however the GKSS membrane compacts at pressure above 20 bar.

Chapter 6 studies the influence of the solvent and solute type on the mass transport through the PAN/PDMS composite membrane. First, the role of the solvent (toluene or hexane) in the transport of sunflower oil is investigated. The flux of toluene through the PAN/PDMS membrane is lower than the flux of hexane (2.0 and 3.1 $\text{lm}^{-2}\text{h}^{-1}\text{bar}^{-1}$) due to the higher viscosity of toluene compared to hexane (0.61 and 0.48 cSt). The flux coupling for oil/toluene seems to be stronger than for oil/hexane probably due to the higher friction between toluene and oil molecules. The membrane retention for oil in toluene is lower than in hexane due to the lower toluene flux and smaller radius of gyration of oil in toluene. Osmotic phenomena are observed for oil/hexane and oil/toluene solutions and can be interpreted using the van't Hoff equation, indicating that they behave as ideal systems.

Second, the effect of solute on the membrane performance is studied, using solutions of toluene with oil or with tetraoctylammonium bromide (TOABr). For the TOABr/toluene solution, the toluene flux is not linear with the applied pressure probably due to the concentration polarization phenomenon. The membrane retention is found to be 100 % and (almost) no osmotic effect was depicted. This is probably due to ion-pairs clustering of TOABr in toluene and to the non-ideality of this system.

In Chapter 7 a new nanofiltration (NF) membrane is prepared consisting of a PAN ultrafiltration support membrane and polyethylene oxide PEO-PDMS-PEO triblock copolymer as selective top layer. Swelling and contact angle measurements confirm the hydrophilic character of the PEO-PDMS-PEO membrane compared to the PDMS membrane. The flux of gases and solvent through the PAN/PEO-PDMS-PEO composite membrane is found to be lower

compared to the PAN/PDMS composite membrane, probably due to the lower molecular weight of the PDMS segment in the polymer chain and/or the quality of the composite (pore intrusion). A linear correlation exists between the fluxes of 5 solvents through the hydrophilic and hydrophobic PDMS-based composite membranes and the membrane swelling and solvent viscosity.

Chapter 8 summarizes the main conclusions of the work described in this thesis and gives an outlook and suggestions for future work.

Samenvatting

Oplosmiddelbestendige nanofiltratiemembranen (in Engels: solvent resistant nanofiltration (SRNF) membranes) vormen een zeer aantrekkelijk alternatief voor vele verschillende toepassingen, variërend van de farmaceutische en de chemische industrie tot de voedingsmiddelenindustrie. Het precieze transportmechanisme in SNRF membranen is echter nog niet opgehelderd.

Dit proefschrift beschrijft een systematisch, experimenteel onderzoek dat als doel heeft de belangrijkste parameters te identificeren die het transport door SRNF membranen gebaseerd op PDMS bepalen. Inzicht in de eigenschappen van het oplosmiddel, de opgeloste stof en het membraan, die de flux van oplosmiddel en opgeloste stof door het membraan beïnvloeden, kan de basis vormen voor een model dat in staat is de membraanprestaties te voorspellen.

Hoofdstuk 2 beschrijft het maken van composietmembranen bestaande uit een poly(acrylonitriël (PAN)) ultrafiltratiedragermembraan en een selectieve toplaag van poly(dimethylsiloxane) (PDMS)). De beste composietmembranen worden verkregen als de toplaag op de drager wordt aangebracht met een PDMS/hexaan oplossing die 7 gew.% polymeer bevat. De resultaten tonen aan dat deze membranen goede permeatie-eigenschappen hebben: de hexaanpermeabiliteit bedraagt $3 \text{ lm}^{-2}\text{h}^{-1}\text{bar}^{-1}$ en de olieretentie is ongeveer 90%. Een toename in de dikte van de PDMS-toplaag resulteert in een afname van de hexaanflux door het membraan, maar heeft geen invloed op de olieretentie.

Hoofdstuk 3 geeft inzicht in het transportmechanisme van hexaan en olie en hexaan en poly(isobutylene) (PIB) door PAN/PDMS-composietmembranen. Osmotische verschijnselen die vergelijkbaar zijn met de verschijnselen die zijn aangetoond in waterige systemen, zijn waargenomen en geïnterpreteerd met behulp van de vergelijking van van't Hoff. De hexaanflux neemt lineair toe met de opgelegde druk en de hexaanpermeabiliteit neemt af met toenemende voedingsconcentratie. Normalisatie van de hexaanpermeabiliteit met de viscositeit

van de oplossing in het gezwollen membraan en de zwellings van het membraan, leidt tot een constante waarde die aangeeft dat het hexaantransport onafhankelijk is van het type opgeloste stof en de concentratie in het voedingsmengsel. Als aangenomen wordt dat het oplossings-diffusiemodel geldt voor dit systeem, dan kan de viscositeit van de oplossing beschouwd worden als een maat voor de diffusiecoëfficiënt van hexaan in het polymeernetwerk en kan de zwellings gezien worden als een maat voor de oplosbaarheid. Het oplossings-diffusiemodel houdt echter geen rekening met de experimenteel waargenomen koppeling tussen de flux van het oplosmiddel en de opgeloste stof. Voor een gegeven opgeloste stof, daalt het effect van die koppeling met het molecuulgewicht en de concentratie van de opgeloste stof.

Hoofdstuk 4 beschrijft de invloed die de graad van crosslinken van het dichte PDMS membraan op de membraaneigenschappen en het permeatiegedrag van de PAN/PDMS composietmembranen heeft. De zwellings van het dichte membraan neemt af met toenemende hoeveelheid crosslinker. Daarnaast neemt de verdelingscoëfficiënt van PIB in het membraan af met toenemende hoeveelheid crosslinker en toenemend molecuulgewicht van PIB. De hexaanpermeabiliteit door PAN/PDMS-membranen die gemaakt zijn met een pre-polymeer/crosslinker verhouding van 10/0.7 is hoger dan bij gebruik van een verhouding 10/1 (respectievelijk 4.5 en 3.1 $\text{lm}^{-2}\text{h}^{-1}\text{bar}^{-1}$). Dit is het gevolg van de grotere zwellings van het membraan (260 en 200 gew.%). PAN/PDMS-membranen die gemaakt zijn met een pre-polymeer/crosslinkerverhouding van 10/2 hebben een hogere hexaanpermeabiliteit dan die membranen die gemaakt zijn met een verhouding van 10/1 (4.1 en 3.1 $\text{lm}^{-2}\text{h}^{-1}\text{bar}^{-1}$), hoewel de zwellings lager is (100 en 200 gew.%). Dit wordt waarschijnlijk veroorzaakt door het feit dat bij gebruik van de verhouding 10/2 er minder polymeer in de poriën van de poreuze PAN-drager kan doordringen en/of door de heterogene kwaliteit van het polymeernetwerk. Waarschijnlijk doordat het PDMS-netwerk sterk gezwollen is, heeft de hoeveelheid crosslinker geen invloed op de PBI-retentie. Dit maakt het mogelijk om, door het verbeteren van de verhouding tussen de mate van crosslinken en

poriepenetratie, PAN/PDMS-composietmembranen te maken met zeer goede permeatieeigenschappen (hoge flux en hoge retentie).

Hoofdstuk 5 is gewijd aan het permeatiegedrag van PAN/PDMS-composietmembranen bij hoge drukken. Membraancompactie en concentratiepolarisatie zijn niet waargenomen bij drukken tot 30 bar. De scheidende eigenschappen van het membraan zijn gelijk bij zowel lage als hoge druk, als bij een batch en een continu proces. Dit toont aan dat het membraan stabiel is onder de geteste omstandigheden. Ook bij hoge drukken is de koppeling tussen de flux van het oplosmiddel en de opgeloste stof waargenomen. Dit bevestigt de data die verkregen zijn bij lage drukken, waar waargenomen is dat dit effect afhangt van het molecuulgewicht en de concentratie van de opgeloste stof in de voeding.

Vergelijking met een PDMS-composietmembraan van GKSS toont aan dat de hexaanpermeabiliteit van het GKSS-membraan hoger is dan de permeabiliteit van het PAN/PDMS-membraan (5.9 en $3.1 \text{ lm}^{-2}\text{h}^{-1}\text{bar}^{-1}$), maar ook dat er bij het GKSS-membraan compactie optreedt bij drukken hoger dan 20 bar.

In hoofdstuk 6 wordt de invloed van het oplosmiddel en het type opgeloste stof op het massatransport door PAN/PDMS-composietmembranen beschreven. In de eerste plaats wordt de rol van het oplosmiddel (tolueen en hexaan) op het transport van zonnebloemolie onderzocht. Door de hogere viscositeit van tolueen in vergelijking met hexaan (0.61 en 0.48 cSt) is de flux van tolueen door het PAN/PDMS-membraan lager dan de flux van hexaan (2.0 en $3.1 \text{ lm}^{-2}\text{h}^{-1}\text{bar}^{-1}$). Koppeling van fluxen lijkt sterker aanwezig bij het systeem olie/tolueen dan bij het systeem olie/hexaan. Waarschijnlijk is dit het gevolg van de grotere frictie tussen olie en tolueen moleculen. Door de lagere tolueenflux en de kleinere gyrationstraal van olie in tolueen is de membraanretentie voor olie in tolueen lager dan de overeenkomstige waarde voor olie/hexaan. Voor beide systemen (olie/tolueen en olie/hexaan) worden osmotische verschijnselen waargenomen. Deze kunnen beschreven worden met de vergelijking van van't Hoff, wat aantoont dat er sprake is van ideale systemen.

In de tweede plaats wordt het effect van de opgeloste stof op de membraanprestaties onderzocht. Hierbij wordt gebruik gemaakt van een oplossing van olie in toluen en een oplossing van tetraoctylammonium bromide (TOABr) in toluen. In geval van het TOABr/toluene mengsel is de flux niet lineair met de opgelegde druk. Dit wordt waarschijnlijk veroorzaakt door concentratiepolarisatieverschijnselen. De membraanretentie is 100% en een osmostisch effect is (vrijwel) niet waarneembaar. Dit komt waarschijnlijk door clustering van TOABr-ionparen in toluen en door het niet ideale gedrag van het systeem.

In hoofdstuk 7 wordt de bereiding van een nieuw type nanofiltratiemembraan beschreven dat bestaat uit een PAN ultrafiltratiedrager en een selectieve toplaag van een polyethylene oxide, PEO-PDMS-PEO triblokcopolymeer. Onderzoek naar het zwellingsgedrag en contacthoekmetingen tonen aan dat het PEO-PDMS-PEO-membraan een hydrofieler karakter heeft dan het PDMS membraan. De gas- en oplosmiddelflux door dit type membraan met een PEO-PDMS-PEO toplaag zijn iets lager dan de overeenkomstige waarden voor PAN/PDMS-composietmembranen. Dit wordt waarschijnlijk veroorzaakt door het lagere molecuulgewicht van het PDMS-segment in de polymeerketen en/of door de kwaliteit van het composietmembraan (poriepenetratie). Er blijkt een lineaire relatie te bestaan tussen de flux van vijf verschillende oplosmiddelen door zowel de hydrofiel als de hydrofobe op PDMS gebaseerde composietmembranen en de zwelling van het membraan en de viscositeit van het oplosmiddel.

Hoofdstuk 8 vat de belangrijkste conclusies van het werk dat in dit proefschrift beschreven staat, samen. Bovendien geeft het een toekomstvisie en aanbevelingen voor verder onderzoek.

Acknowledgements

Although I like referring to this work as “my thesis”, it actually belongs to many people, thanks to whom I developed myself professionally and personally.

Chronologically, I would like to express my gratitude to my first teacher, Stoica, then my math master, Jurjiu and my chemistry inspiration, Bunea. Special thanks for the trust and support I got from my driving force in the chemical academic world, Professor Burghilea. Professor Meghea is acknowledged for her guidance during my (short) Ph.D. study time in Romania. I want to thank Professor Verweij for giving me the opportunity to come to the Netherlands.

I would like to thank my promoter, Matthias, for his support and interest in the project. I am grateful to Marcel Mulder, the first supervisor of the project. To achieve this Ph.D. thesis would not have been possible without the support of Dimitris, my supervisor of the last 2 years and 6 months. We may have struggled sometimes but your continuous interest in my work and your guidance were always valuable to my project and to me personally.

I wish to acknowledge all the members of the project’s user-committee who constantly supported the work of this thesis, with special thanks to Geert-Henk and Petrus for the fruitful discussion.

I am grateful to Harmen who introduced me in the SRNF world and helped me to design and realize the experimental set-up. Thanks Marcel Boerrigter, who always solved efficiently any (computer and nano-organic related) problem. This thesis would have been less complete without the experimental contribution of Kwasi (results described in Chapter 6) and Jutta (part of the results of Chapter 5). Thanks to all the people who carefully read and corrected the chapters of this thesis: Kitty (thanks for the samenvatting and for the support in the last years), Harmen, Sybrand, Mark, Rob. Erik, thanks for the lab and safety issues support and many thanks to Greet for her help in the paperwork (and for smiling all the time). Jolanda and Arthur, you were so motivated and enthusiastic students!

I would not have completed my work of Chapters 4 and 7 without the contribution and support of Mark and Clemens (MTP), especially for the copolymer synthesis and characterization. Mark, I enjoyed a lot your passion for the polymer world, thanks for sharing it with me! Clemens, thanks for being always in a good mood.

Of course this period would not have been the same without all the nice colleagues from the MTG group. I am grateful for the last 4 years and 3 months in which I received from the MTG fellows everything I need to develop into who I am today. Thanks, I learned from all of you. I was proud being part of you.

Many thanks to all my roommates: Mercedes, Samuel, Maarten, Peter, Tao, Magda, Kitty, Sybrand, Marius, Ana (multumesc), Saiful.

I would like to thank to all my former colleagues from IMS group of 1999, especially to Fiona and Natascha for the good and fruitful time I had as a research fellow there.

Outside work I happened to find dear friends: Monse (thanks for the good “cappuccino-flat” shared moments) and Tomas, Adina and Reli, Patrice, Laura and Cas, Pascalle, Patrick, Kim and Mark, Govert, Florinda, Valerie and Marc (merci pour les lundis), doamna Heghes. Edyta (thanks for helping me to give up smoking) and Abdulah thank you for the nice Zweringweg moments. Andre and Marja, thanks for the “dancing Sundays” and kindness in organizing the promotion party.

Special thanks to Mercedes, for being such a wonderful friend: we can discuss about so many things! I am very grateful to have you as my dear friend (and paranimf).

Ik wil langs deze weg ook mijn nederlandse familie bedanken, Janny, Jan, Nineke, Rene en alle tantes en ooms voor het zorgen dat ik me thuis voel in Nederland en voor jullie steun en belangstelling in goede tijden maar ook op momenten dat het moeilijker was. Ik vond het ook geweldig om jullie in 2002 in Roemenie te mogen begroeten.

Familiei mele, atat de dragi, mereu alaturi de mine: va multumesc si va iubesc! Imi este dor de voi, dragii mei: mamica (un exemplu de tarie, curaj si gandire pozitiva), Luminita (tica I, care ne-a crescut si ne-a indrumat cand eram noi tici mici), Geta (nenumaratele noastre discutii m-au ajutat sa ajung mai repede la adevar, bucurie si dragoste. Multumesc mult, tica III, nasica si paranimfa), Stefania (tica cea mai mica, un suflet frumos), nenea Petrica (un om puternic), Paul (intotdeauna calm si de ajutor), Radu (multumesc pentru multele discutii si lectii de condus, nasule).

Apoi, multumesc altor oameni minunati ai familiei care inca mai sunt printre noi: tanti Florica, Catalin, Marilena, nenea Nicu, tanti Cica, doamna Sandulescu, Andi, Emi, Adriana, Dan, Eduard (multumim pt botezul si nunta de neuitat). Multumesc prietenilor mei dragi de care ma leaga atatea amintiri de neuitat: Cris (am impartit atatea momente si experiente!), Monica, Lili, Verona, Lumi, Vio, Aura, Catalin, Silviu, Eduardo, Florin. Imi lipsiti.

La sfarsit, as vrea sa-i multumesc lui Wim, iubit si sot minunat, partener si prieten drag, care imi daruieste atata dragoste si liniste! Tu esti mereu alaturi de mine si ma incurajezi sa merg mai departe. Iti multumesc pentru sufletul tau frumos, iubite Blond.

Nela